

**ESTIMATING FOLIAR AND WOOD LIGNIN
CONCENTRATIONS, AND LEAF AREA INDEX (LAI) OF
EUCALYPTUS CLONES IN ZULULAND USING
HYPERSPETRAL IMAGERY**

Ingrid Bongiwe Mthembu

Submitted in fulfilment of the academic requirements for the degree of
Master of Science
in Applied Environmental Sciences

School of Environmental Sciences,
Faculty of Science and Agriculture
University of KwaZulu Natal, Pietermaritzburg

December 2006

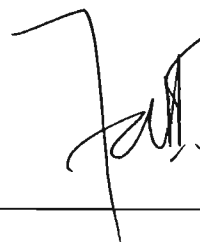
DECLARATION

The work described in this thesis was carried out at the CSIR (Council for Scientific and Industrial Research) centre in FFP (Forestry and Forest Products) while registered with the School of Applied Environmental Sciences, University of KwaZulu Natal in Pietermaritzburg. This work was done under the supervision Dr Fethi Ahmed.

I hereby certify that the research work reported in this thesis is the result of my own original investigations except where acknowledged.



Ingrid Bongwiwe Mthembu
Durban (CSIR)



Dr Fethi Ahmed (Supervisor)
University of KwaZulu Natal

ACKNOWLEDGEMENTS

I would like to thank Dr Fethi Ahmed for supervising this project. He has encouraged and showed confidence in my abilities. I would also like to thank Professor Phillip Turner for his direction.

I would like to thank CSIR for making this project happen and for the resources they provided. I would like to thank both staff and students at the CSIR with special thanks to Thulile Ntonhle Mgenge, Mark Govender, Christian Ngcobo, Thokozani Gumede, Thamsanqa Ndebele, David Drew and Mthokozisi Majozi.

I would like to thank Karen Wentzel and Minette Lubbe (CSIR – Meraka Institute) for helping with atmospheric correction. I would also like to thank the staff from the International Institute for Geo-Information Science and earth Observation (ITC - Netherlands) for also helping with atmospheric correction, Moses Azong Cho, Jelger Kooistra and Frank Van Ruitenbeek.

ABSTRACT

To produce high quality paper, lignin should be removed from the pulp. Quantification of lignin concentrations using standard wet chemistry is accurate but time consuming and costly, thus not appropriate for a large number of samples. The ability of hyperspectral remote sensing to predict foliar lignin concentrations could be utilized to estimate wood lignin concentrations if meaningful relationships between wood and foliar chemistry are established. LAI (leaf area index) is a useful parameter that is incorporated into physiological models in forest assessment. Measuring LAI over vast areas is labour intensive and expensive; therefore, LAI has been correlated to vegetation indices using remote sensing. Broadband indices use average spectral information over broad bandwidths; therefore details on the characteristics of the forest canopy are compromised and averaged. Moreover, the broadband indices are known to be highly affected by soil background at low vegetation cover. The aim of this study is to determine foliar and wood lignin concentrations of *Eucalyptus* clones using hyperspectral lignin indices, and to estimate LAI of *Eucalyptus* clones from narrowband vegetation indices in Zululand, South Africa

Twelve *Eucalyptus* compartments of ages between 6 and 9 years were selected and 5 trees were randomly sampled from each compartment. A Hyperion image was acquired within ten days of field sampling, SI and LAI measurements. Leaf samples were analyzed in the laboratory using the Klason method as per Tappi standards (Tappi, 1996-1997). Wood samples were analyzed for lignin concentrations using a NIRS (Near Infrared Spectroscopy) instrument. The results showed that there is no general model for predicting wood lignin concentrations from foliar lignin concentrations in *Eucalyptus* clones of ages between 6 and 9 years. Regression analysis performed for individual compartments and on compartments grouped according to age and SI showed that the relationship between wood and foliar lignin concentration is site and age specific. A Hyperion image was geo-referenced and atmospherically corrected using ENVI FLAASH 4.2.

The equation to calculate lignin indices for this study was: $LI_R = \frac{\lambda_{1750} + \lambda_{1680}}{(\lambda_{1750} + \lambda_{1680})^2}$.

The relationship between the lignin index and laboratory-measured foliar lignin was significant with $R^2 = 0.79$. This relationship was used to calculate image-predicted foliar lignin concentrations. Firstly, the compartment specific equations were used to calculate predicted wood lignin concentrations from predicted foliar lignin concentrations. The relationship between the laboratory-measured wood lignin concentrations and predicted wood lignin concentrations was significant with $R^2 = 0.91$. Secondly, the age and site-specific equations were used to convert foliar lignin concentration to wood lignin concentrations. The wood lignin concentrations predicted from these equations were then compared to the laboratory-measured wood lignin concentrations using linear regression and the R^2 was 0.79 with a p-value lower than 0.001.

Two bands were used to calculate nine vegetation indices; one band from the near infrared (NIR) region and the other from the short wave infrared (SWIR). Correlations between the VIs and the LAI measurements were generated and then evaluated to determine the most effective VI for estimating LAI of *Eucalyptus* plantations. All the results obtained were significant but the NLI and MNLI showed possible problems of saturation. The MNDVI*SR and SAVI*SR produced the most significant relationships with LAI with R^2 values of 0.899 and 0.897 respectively. The standard error for both correlations was very low, at 0.080, and the p-value of 0.001.

It was concluded that the *Eucalyptus* wood lignin concentrations can be predicted using hyperspectral remote sensing, hence wood and foliar lignin concentrations can be fairly accurately mapped across compartments. LAI significantly correlated to eight of the nine selected vegetation indices. Seven VIs are more suitable for LAI estimations in the *Eucalyptus* plantations in Zululand. The NLI and MNLI can only be used for LAI estimations in arid or semi-arid areas.

TABLE OF CONTENTS

Title Page	i
Declaration	ii
Acknowledgements	iii
Abstract	iv
Table of Contents	vi
List of Figures	ix
List of Tables	xii
List of Acronyms and Abbreviations	xiii
Chapter 1: General Introduction	1
1.1 Introduction.....	1
1.2 Lignin.....	2
1.3 Leaf Area Index	3
1.4 Aim and Objectives	6
1.5 Structure of the Thesis	7
Chapter 2: Literature Review	9
2.1 Introduction	9
2.2 Introduction to Foliar Chemistry	9
2.3 Lignin	10
2.3.1 Description of Lignin	10
2.3.2 Lignin in the Paper Industry	12
2.4 Laboratory Spectroscopy and Hyperspectral Remote Sensing... 17	
2.4.1 Near Infrared Technology	17
2.4.2 Hyperspectral Remote Sensing and Canopy Chemistry Analysis.....	21
2.5 Leaf Area Index	24
2.6 Introduction to Remote Sensing in Forestry	25
2.7 Vegetation Indices and Leaf Area Index	26
2.8 Vegetation Modelling Using Hyperspectral Narrow Bands	32
2.9 Summary	36
2.91 Quantification of Lignin	36

2.9.2 LAI and vegetation indices	37
Chapter 3: Description of study Area	38
3.1 Introduction	38
3.2 Study Area	38
3.3 Study Area Location and Description	39
3.3.1 Location	39
3.3.2 Topography	41
3.3.3 Climatic Factors	41
3.3.4 Geology and Soils	42
3.3.5 Hydrology	42
Chapter 4: Materials and Methods	45
4.1 Introduction	45
4.2 Estimation of Wood and Foliar Lignin Concentration Estimation in the Laboratory	45
4.2.1 Field Sampling.....	45
4.2.2 Sample Preparation	46
4.2.2.1 Preparation of Leaves	46
4.2.2.1 Preparation of Wood Strips.....	47
4.2.3 Biochemical Analysis	47
4.2.4 Stand Enumeration for Site Index Calculations	49
4.3 Image Pre-Processing Analysis and Data Extraction	49
4.3.1 Image Data	49
4.3.2 Extracting Reflectance Data from Hyperion Imagery.....	50
4.3.3 Computation of Lignin Indices	53
4.3.4 Statistical Analysis for the Estimation of Lignin Concentrations.....	53
4.4 Estimation of Leaf Area Index from Hyperion Data	54
4.4.1 Measuring LAI in the field using a LICOR	54
4.4.2 Correlation Analysis of Vegetation Indices Extracted from Hyperion Data with Field LAI measurements.....	55

Chapter 5: Results and Discussion	57
5.1 Introduction	57
5.2 Wood Lignin Estimation Using Hyperion Data	57
5.2.1 Wood and Foliar Lignin Determination in the Laboratory.....	57
5.2.2 Relationship Between Foliar lignin Concentrations from the Laboratory and Hyperspectral Lignin Indices	69
5.2.3 Prediction of Wood Lignin Concentrations	79
5.3 Leaf Area Index Determination Using Hyperion	82
 Chapter 6: Conclusions and Recommendations	 94
6.1 Conclusions	94
6.2 Recommendations	96
 References	 98
 Appendices.....	 122

LIST OF FIGURES

Figure 2.1 A generalized structure of lignin	11
Figure 2.2 A Generalized lignin biosynthesis pathway	13
Figure 2.3 Chemical component of wood	14
Figure 2.4 Hyperion Data Axes	21
Figure 3.1 Study area, the location of the compartments and the approximate Hyperion swath	40
Figure 3.2 Map of Southern part of the study area showing the selected compartments, main towns and catchments	43
Figure 3.3 Map of Northern Zululand showing the selected compartments, main towns and catchments	44
Figure 4.1 Markings on the felled tree and the diagrammatic locations of sampled discs.....	46
Figure 4.2 The NIRS by FOSS used to scan prepared wood strips	47
Figure 4.3 Hot water extraction procedure to remove inorganic compounds and starch	48
Figure 4.4 Solvent extraction procedure to remove non- volatile chemical substances	48
Figure 4.5 Products of Klason method; lignin and sugars	49
Figure 4.6 Hyperion image for Zululand, 24 July 2004 with the study compartments overlaid	51
Figure 4.7 Summary of the analysis procedures and outcomes of the study.....	56
Figure 5.1 Relationship between foliar and wood lignin concentration in all trees	57
Figure 5.2 Graphs (A-B) demonstrating the resulting age groupings that showed significant relationships between wood and foliar lignin concentrations	61
Figure 5.2 Graphs (C-D) demonstrating the resulting age groupings that showed significant relationships between wood and foliar lignin concentrations	62

Figure 5.2 Graphs (E-F) demonstrating the resulting age groupings that showed significant relationships between wood and foliar lignin concentrations63

Figure 5.2 Graphs (G) demonstrating the resulting age groupings that showed significant relationships between wood and foliar lignin concentrations64

Figure 5.3 Graphs (A-B) demonstrating the resulting SI groupings that showed significant relationships between wood and foliar lignin concentrations67

Figure 5.3 Graphs (C-D) demonstrating the resulting SI groupings that showed significant relationships between wood and foliar lignin concentrations68

Figure 5.4 Relationship between laboratory-measured foliar lignin concentrations and the reflectance-based lignin indices71

Figure 5.5 An illustration of foliar and wood lignin concentrations calculated from the lignin indices across the image.....72

Figure 5.6 An illustration of foliar lignin and wood lignin concentrations calculated from the lignin indices across each compartment (1 and 2)73

Figure 5.6 An illustration of foliar lignin and wood lignin concentrations calculated from the lignin indices across each compartment (3 and 4)74

5.6 An illustration of foliar lignin and wood lignin concentrations calculated from the lignin indices across each compartment (5 and 6).....75

Figure 5.6 An illustration of foliar lignin concentrations calculated from the lignin indices across each compartment (7 and 8)76

Figure 5.6 An illustration of foliar lignin concentrations calculated from the lignin indices across each compartment (9 and 10)77

Figure 5.6 An illustration of foliar lignin concentrations calculated from the lignin indices across each compartment (11 and 12)78

Figure 5.7 A comparison between laboratory-measured wood lignin concentrations and wood lignin concentrations derived from the hyperspectral image using mostly compartment specific equations80

Figure 5.8 A comparison between laboratory-measured wood lignin concentrations and wood lignin concentrations derived from the hyperspectral image using age and site specific equations81

Figure 5.6 (A-B) Graphs summarizing the regression analysis for all the calculated Vegetation Indices and field-measured LAI.....	83
Figure 5.9 (C-D) Graphs summarizing the regression analysis for all the calculated Vegetation Indices and field-measured LAI	84
Figure 5.9 (E-F) Graphs summarizing the regression analysis for all the calculated Vegetation Indices and field-measured LAI	85
Figure 5.9 (G-H) Graphs summarizing the regression analysis for all the calculated Vegetation Indices and field-measured LAI	86
Figure 5.10 Illustrations across a compartment of NDVI, of NDVI*SR and SAVI*SR calculated from two Hyperion bands in compartment 9 and 10	90
Figure 5.11 The LAI map for the Hyperion image	91
Figure 5.12 Illustrations of LAI variation across each compartment (3, 5, 6 and 8)	92
Figure 5.12 Illustrations of LAI variation across each compartment (9, 10 and 11)	93

LIST OF TABLES

Table 2.1: Approximate lignin content from softwood and hardwood.....	14
Table 3.1: Information on the selected compartments for the lignin concentrations and LAI study	39
Table 4.1: Absorption wavelengths for water and lignin	53
Table 5.1: A summary of regression analysis between wood lignin concentrations and foliar lignin concentration per compartment	58
Table 5.2: A summary of the correlation matrix for foliar, wood lignin, SI and Age	59
Table 5.3: the compartments grouped according to similar ages	60
Table 5.4: compartments grouped according to similar site indices	66
Table 5.5: A summary of linear regression analysis between all possible bands for the calculation of spectral lignin indices and laboratory measured foliar lignin concentrations	70
Table 5.6 Summary of results of the multiple-regression analysis	80
Table 5.7: A summary of the linear regression analysis between the selected possible bands and the field measured LAI	82
Table 5.8 A summary of the results of the regression analysis between the eight VI and LAI	88

LIST OF ACRONYMS AND ABBREVIATIONS

AfPAR	Absorbed fraction of Photosynthetically Active Radiation
AIS	Airborne Imaging Spectrometer
ASAS	Advanced Solid-State Array Spectroradiometer
AVIRIS	Airborne Visible/ Infrared Imaging Spectrometer
C	Carbon
CASI	Compact Airborne Spectral Imager
DN	Digital Number
<i>E.</i>	<i>Eucalyptus</i>
<i>E. gra</i>	<i>Eucalyptus grandis</i>
ENVI	The Environment for the Visualization of Images
ETM	Enhanced Thematic Mapper
ETM+	Enhanced Thematic Mapper Plus
EOS	Earth Observation System
FLAASH	Fast Line-of-sight Atmospheric Analysis of Spectral Hypercubes
FLIM	Forest-Light Interaction Model
GC-1	<i>E. grandis</i> x <i>E. calmadulensis</i> , clone type 1
GC-2	<i>E. grandis</i> x <i>E. calmadulensis</i> , clone type 2
GIS	Geographic Information System
GU-1	<i>E. grandis</i> x <i>E. urophylla</i> , clone type 1
GU-2	<i>E. grandis</i> x <i>E. urophylla</i> , clone type 2
GU-3	<i>E. grandis</i> x <i>E. urophylla</i> , clone type 3
GU-4	<i>E. grandis</i> x <i>E. urophylla</i> , clone type 4
GT	<i>E. grandis</i> x <i>E. tereticornis</i>
H	Hydrogen
H _γ	Hydrogen-gamma
IFOV	Instantaneous Field of View
JPL	Jet Propulsion Laboratory
IR	Infrared
LAI	Leaf Area Index
MSE	Mean Squared Error
MODIS	Moderate Resolution Imaging Spectrometer

MIR	Middle Infrared
MISR	Multi-Angle Imaging Spectrometer
MNLI	Modified Non-Linear Index
MSR	Modified Simple Ratio Vegetation Index
MSS	Multispectral Scanner
N	Nitrogen
NASA	National Aeronautics and Space Administration
NDVI	Normalized Difference Vegetation Index
NDLI	Normalized Difference Lignin Index
NLI	Non-Linear Vegetation Index
NLI_LI	Non-Linear Lignin Index
NIR	Near Infrared
NIRA	Near Infrared Absorbance spectra
NIRS	Near Infrared Spectroscopy
nm	Nanometer
O	Oxygen
λ	Wavelength
NPP	Net Primary Productivity
PVI	Perpendicular Vegetation Index
R	Red
RDVI	Renormalized Difference Vegetation Index
RMSE	Root Mean Square Error
ROI	Region of Interest
RSR	Reduced Simple Ratio
SAVI	Soil-Adjusted Vegetation Index
SE	Standard Error
SEC	Standard Errors of Calibration
SEP	Standard Errors of Prediction
SFSI	Shortwave Infrared Full Spectrum Imager
S:G	Syringyl to Guaiacyl ratio
SR	Simple Ratio
SWIR	Short Wave Infrared
SVI	Simple Vegetation Index

TM	Thematic Mapper
TSAVI	Transformed Soil Adjusted Vegetation Index
μm	Micrometer
USGS	United States Geological Survey
VHR	Very High Resolution
VI	Vegetation Index
WDVI	Weighted Difference Vegetation Index

CHAPTER 1: General Introduction

1.1 INTRODUCTION

Foliage plays an important role when monitoring the forest ecosystem. Because of the role played by the leaves in intercepting and absorbing the radiant energy, and transforming it to energy of organic substances through the complex process of photosynthesis, leaves are the most important organs for plant production in agriculture and in forestry (Wulder, 1998). Foliar chemical composition is one of the most important forest characteristics because it provides information about the ecosystem's processes and productivity (Curran, 1989). Foliar chemical composition can be observed by the use of chemical analysis in the laboratory, the use of spectroscopy that is well calibrated by laboratory data and the recent new technique of hyperspectral remote sensing (Smith and Curran, 1995). The pulp and paper industry has been exploiting the laboratory spectroscopy technique to quantify biochemicals such as cellulose, lignin and extractives. Quantifications of these biochemicals is very important in the pulp and paper industry due to the fact that paper is made of cellulose and for the production of white paper, lignin should be totally removed (Roberts, 1996). Remote sensing is providing highly rapid results for the quantification of biochemicals compared to the laboratory spectroscopy. This technique, however, still currently being researched and tested to validate its success in producing results comparable to those produced in the laboratory using the wet chemistry (Ramsey, 2005).

Canopy physical and biochemical characteristics control forests' net primary productivity (NPP) in many ways (Peterson *et al.*, 1988). Information on the biochemical content of vegetation canopies for large areas of terrain is of importance for the study of productivity, vegetation stress, nutrient cycling and for input to ecosystem simulation models. The forest canopy is the major locus for energy capture and water exchange in forest ecosystem. Large amounts of the nutrients, which play roles in plant structure and productivity including energy transduction, are allocated in the canopy (Coops *et al.*, 2001). Leaf area index is associated with variations in primary net yield and evapo-transpiration for a given area, as well as with global climatic changes.

1.2 LIGNIN

Lignin, an aromatic polymer with an extremely complex structure, comprises about 17 to 33% of the dry weight of wood (Baptista *et al.*, 2006). Lignin also acts as a component that assists in the resistance of the wood towards attack by microorganisms and decay (Ting, 1982). Lignin's complexity is increased by its large molecular weight. Lignin and carbohydrates exist in close association in the wood structure. There is strong evidence suggesting that formal covalent links exist between the lignin macromolecule and carbohydrate components of the wood structure (Roberts, 1996).

There are several processes to remove lignin. The most widely used commercial methods of more extensive lignin removal are based on aqueous, high temperature extraction procedures at acidic, neutral or alkaline pH levels (Roberts, 1996). The use of chemical analysis in determining the amount of lignin is costly and time-consuming, therefore, alternative methods, such as spectrometric measurements, are pursued. The region within the range of 400nm to 2500nm is compatible with optical remote sensing measures that are currently being studied using hyperspectral remote Sensing (Gastellu-Etchegorry *et al.*, 1995).

Lignin determination is useful for various applications. For this project the focus is on lignin because it is not desirable in the paper industry. In order to produce high quality paper with good strength properties it is necessary to remove the lignin from the wood or fibre matrix (Roberts, 1996). Lignin discolours with age and causes the sheets to become brittle. The ideal pulping process would therefore completely dissolve lignin without causing any loss or degradation to the carbohydrate component, however, the ideal process doesn't exist, the pulping process, therefore, is a compromise (Roberts, 1996). Because of the cost involved in lignin determination in a given area, remote sensing could be used as an important element in producing large-scale, spatially explicit estimates of foliar lignin (Jia *et al.*, 2006). If a significant relationship exists between foliar and wood lignin concentrations, then there is a high potential of estimating wood lignin from foliar lignin concentrations using hyperspectral Remote Sensing.

Lignin is a polymer of phenylpropanoid and the absorptions appear at 1120, 1200, 1420, 1450, 1690 and 1940. Takahashi *et al.*, (undated) estimated foliar chemical content by performing stepwise multiple linear with $\log(1/R)$, the first derivative of $\log(1/R)$ and the second derivative of $\log(1/R)$. The best estimation for lignin of non-destructive cumulated leaves and dry leaf powder resulted with the first derivative of $\log(1/R)$. Stepwise multiple linear-regression show an R^2 value of 0.89 for lignin for both leaf forms (Takahashi *et al.*, undated).

Measuring of biochemicals using hyperspectral sensors has its origins in the laboratory where spectrophotometers have successfully been used for decades to qualify and quantify chemical compositions of substances (Richardson and Reeves, 2005). Extensive work has been done by numerous researches where hyperspectral sensor reflectances were correlated to wet chemistry results. The correlations that resulted were significantly higher than those obtained from broadband sensors and therefore leading to conclusions that hyperspectral remote sensing could be effectively used to estimate the canopy biochemicals, including lignin (Huang, 2004).

There are a number of precursor biochemicals to wood lignin biosynthesis that can be effectively quantified using wet chemistry. This study will focus on investigating if foliar lignin concentrations can be used as a biochemical that can be linked to wood lignin concentrations because both wet chemistry and hyperspectral remote sensing can effectively quantify it. Work has not yet been done on correlating the concentrations of lignin in the canopy with the concentrations of lignin in wood. This study will attempt to establish that relationship with the use of statistical regression so as to correlate the spectral reflectances with the lignin concentrations in wood of *Eucalyptus* clones.

1.3 LEAF AREA INDEX (LAI)

Leaf area Index (LAI) is an important structural parameter used to quantify energy and mass exchange characteristics of terrestrial ecosystems such as photosynthesis, respiration, transpiration, carbon and nutrient cycle, and rainfall interception. LAI is used as an input parameter in models, such as the 3PG-S model, that are in place to predict growth and yield. Leaf Area Index is thus defined as the

total one-sided area of all leaves in the canopy within a defined region (m^2/m^2). A direct measure of LAI is relatively accurate but extremely labour intensive. Measuring and estimating LAI over large areas has proved to be problematic, thus, it is more practical to measure LAI only on limited experimental plots (Lee *et al.*, 2004).

Remote Sensing techniques have improved such that there are methods currently operational that correlate remotely sensed data with regional estimates of LAI and absorbed fraction of photosynthetically active radiation (AfPAR) (Schlerf and Atzberger, 2006). In the past three decades the traditional broadband vegetation indices (VI) and normalized difference vegetation indices (NDVIs) were widely used to estimate the canopy LAI (Gong *et al.*, 2003).

LAI is a crucial vegetation canopy property that is fundamental in describing biosphere processes and modelling carbon and vapour fluxes between atmosphere and land surfaces. Linear and non-linear relationships between optical satellite-derived spectral vegetation indices and LAI have been found for different vegetation types and climatic conditions. These empirical relationships are site and sampling condition dependent, sensor-specific, change in space and time and generally are unsuitable for application to large areas or in different phenological seasons (Pu *et al.*, 2005).

The most commonly used vegetation indices when studying the forest ecosystems using remote sensing are computed from simple functions based on the R band and NIR band. These wavebands are used to formulate various vegetation indices to acquire more precise indications of surface vegetation conditions. The simple ratio (NIR/R) and the NDVI are most frequently used to correlate with LAI and other canopy structure parameters from airborne and spaceborne remote sensing data. With increase in LAI, red reflectance decreases as light is absorbed by leaf pigments while the NIR signal increases due to the fact that more leaf layers are present to scatter the radiation upwards because plant cell walls, notably the lignin component, cause scattering of NIR energy, resulting in relatively high NIR transmittance and reflectance. The simple ratio VI has proved to be sensitive to optical properties of the soil background and therefore, its application is limited (Zhao *et al.*, 2005).

The broadband indices constructed with near infrared (NIR) and red (R) bands result in loss of information due to the fact that they use average spectral information. Moreover, the broadband indices are known to be highly affected by soil background at low vegetation cover (Haboudane, 2004). Narrow bands are crucial for providing additional information in quantifying biophysical characteristics of vegetation and more refined vegetation indices. TM band 3 (630 - 690nm) which is a red band and TM band 4 (760 – 900nm) can further be separated into 6 and 14 Airborne Visible/Infrared Imaging Spectrometer (AVIRIS) narrow bands respectively. The advantage of narrow bands is that by using some of them it is possible to correct the effects of the soil background (Fuentes *et al.*, 2006).

Perpendicular Vegetation Index (PVI) was once proposed in an attempt to reduce the effect of the soil background on VI. However, experimental and theoretical investigations indicated that soil background still has an effect. Brighter soils have resulted in higher index values for a given quantity of incomplete vegetation cover (Gong *et al.*, 2003). A number of other vegetation indices were developed to address the influence of the soil brightness. These vegetation indices are still being successfully used but the utilization of some vegetation indices can be highly specific to the nature of the site. Hyperspectral data have been researched for its suitability to estimate and model LAI predictions (Arsenault and Bonn, 2005).

Most of the research has focused on the airborne hyperspectral remote sensing and this research proved that hyperspectral remote sensing can address the soil background problem. The indices generated from hyperspectral data are thus proving to be superior to that of the broadband indices. These indices correlate better with the field measured LAI, and therefore robust models for growth and yield result since the estimates of LAI are more accurate (Cheng *et al.*, 2006). Airborne hyperspectral sensor data is widely used compared to the only spaceborne hyperspectral sensor: Hyperion. In a South Africa context, Hyperion is the most practical hyperspectral sensor to use in research because of its easy accessibility and cost effectiveness compared to the airborne sensors currently available in the market. It will, thus, be useful to research the utility of this sensor for the South African forest industry for future exploitations.

A lot of research on hyperspectral sensors has been conducted internationally but locally hyperspectral data has only been explored by the mining and geological sectors. This study will aim to demonstrate that narrow bands can be successfully used to predict LAI in forest plantations. Gong *et al.* (2003) investigated twelve vegetation indices using the traditional bands (NIR and R) and the optimal indices using bands in the NIR and SWIR. It was found, from this study that the optimal indices correlated better and significantly with measured LAI. The narrow band vegetation indices owe their accuracy to the fact that the soil background least affects them because the specific information on each pixel is packaged in many narrow bands. Only suitable bands that contain information about vegetation cover are chosen for vegetation indices (Muir *et al.*, 2006).

1.4 AIMS AND OBJECTIVES

There are two aims to this project:

1. The determination of wood lignin concentrations of *Eucalyptus* clones grown in Zululand using hyperspectral remote sensing.

Lignin determination is useful for various applications. For this project the focus is on lignin because it is not desirable in the paper industry. In order to produce high quality paper with good strength properties it is necessary to remove the lignin from the wood or fibre matrix (Roberts, 1996). Due to the cost involved in lignin determination for a single compartment, it is anticipated that remote sensing could be used to estimate wood lignin concentrations by using its ability to predict foliar lignin concentrations. Wood lignin concentrations could be estimated using meaningful relationships between wood lignin concentrations and foliar lignin concentrations derived in the laboratory. This project aims at demonstrating that lignin in wood can be determined through the use of narrow band indices constructed from a band corresponding to lignin concentrations and a respective lignin reference band.

2. The determination of leaf area index (LAI) of *Eucalyptus* clones using a combination of narrow bands of space-borne hyperspectral remote sensing

The popularity of the unitless parameter, LAI, stems from its use in numerous applications, such as modelling atmospheric carbon assimilation, evapotranspiration, fire fuel potential, habitat characteristics, herbivore grazing potential

and the forest ecosystem (Privette *et al.*, 2002). Direct measure of LAI is relatively accurate but extremely labour intensive and costly. Measuring and estimating LAI over large areas has proved to be problematic, thus, it is more practical to measure LAI only on limited experimental plots (Gong *et al.*, 2003). The broadband indices result in loss of information due to the fact that they use average spectral information over a broad bandwidth and are known to be highly affected by soil background at low vegetation cover (Haboudane, 2004). Narrow bands are crucial for providing additional information in quantifying biophysical characteristics of vegetation and more refined vegetation indices.

The following are the specific objectives of the study:

1. To establish a relationship between wood and foliar lignin concentrations of *Eucalyptus* clones
2. To establish a relationship between foliar lignin concentrations and canopy lignin indices from hyperspectral data
3. To predict foliar and wood lignin concentrations from the canopy lignin indices
4. To determine the relationship between ground measured LAI values and the nine narrow band vegetation indices
5. To map out foliar lignin concentrations, wood lignin concentrations and LAI values across the study compartments.

1.5 STRUCTURE OF THE THESIS

The first chapter has introduced a rationale for undertaking this study by looking at how biochemical contents in the forest canopy are quantified using known hyperspectral narrow bands corresponding to those specific biochemicals, and the advantages of hyperspectral vegetation indices constructed using narrow bands over broadband vegetation indices. This chapter firstly formed a theoretical framework of why it is necessary to quantify wood lignin concentrations using remotely sensed data. Secondly, the chapter explained why it is advantageous to construct indices from narrow bands that correlate more accurately to field measured LAI.

Chapter two reviews the literature covering aspects of wood lignin in the pulp and paper industry, lignin extraction methods in the laboratory, NIR technology and an example of cases of hyperspectral use in the determination of foliar chemistry. This chapter also introduces remote sensing in forestry, hyperspectral remote sensing, vegetation indices and Leaf Area Index. Furthermore, the chapter provides an insight into the work that has already been done in the determination of narrow band vegetation indices using hyperspectral remote sensing.

Chapter three describes the study areas in terms of climate, topography, soils and hydrology.

Chapter four discusses the sampling methods and methodology used in this study to quantify wood and foliar lignin concentrations in the laboratory. This chapter also describes the indirect method used to measure LAI in the field. Furthermore, this chapter describes the methods used to extract meaningful data from the Hyperion image.

Chapter five discusses the results obtained when establishing a model to predict wood lignin using data acquired in the laboratory and Hyperion data. Chapter six concludes the findings of the project and presents recommendations summed from this.

CHAPTER 2

Literature Review

2.1 INTRODUCTION

This chapter provides an understanding of the importance of foliar chemical analysis with the emphasis on the lignin and its significance in the pulp and paper industry. Current quantification methods of both wood and foliar lignin concentrations and current remote sensing techniques used to quantify foliar biochemicals are reviewed. Literature on leaf area index (LAI) is presented with emphasis on the benefits of LAI estimations from vegetation indices (VI) constructed from the hyperspectral narrow bands. This chapter also presents an introduction to vegetation indices and hyperspectral remote sensing.

2.2 INTRODUCTION TO FOLIAR CHEMISTRY

Photosynthetic studies have been used as a tool to probe the physiological basis of plant growth (Gindaba *et al.*, 2005). Leaves play a major role in the prediction of stand growth (Coops, 1999). Because of the role played by the leaves in intercepting and absorbing the radiant energy, and transforming it to energy of organic substances through the complex process of photosynthesis, leaves are the most important organs for the plant production in agriculture and in forestry (Curran *et al.*, 2001).

Photosynthesis is the primary metabolic process in nature such that without photosynthesis life on the planet would cease. Rates of photosynthesis are commonly expressed as carbon dioxide uptake per unit time per unit leaf area. The total leaf area of a plant is usually called the photosynthetic potential of a plant. Photosynthesis in higher plants' leaves takes place in organelles called chloroplasts (Dale and Milthorpe, 1983).

Foliar chemical composition is an important characteristic because it provides certain information about the ecosystem's processes and productivity (Curran, 1989). Plant productivity can be described by the amounts of chlorophyll and nitrogen, the rate of

litter decomposition, using litter lignin to nitrogen ratio and the cycling and availability of nutrients such as nitrogen. Biochemical content of vegetation canopies can also provide information about nutrient cycling; vegetation stress and can provide input to ecosystem simulation models. Foliar chemical composition can be observed by the use of chemical analysis in the laboratory, the use of spectroscopy which is well-calibrated by laboratory data and recently the new technique of remote sensing (Smith and Curran, 1995). The pulp and paper industry has been using both the traditional wet chemistry but has also moved towards using laboratory spectroscopy in quantifying constituents of interest to assess the state of each compartment. Lignin is one of the most researched biochemical in the pulp and paper industry due its properties.

2.3 LIGNIN

2.3.1 Description of lignin

Lignin is the second most important organic substance after cellulose. It is the most important structural substance of plants and thus is universally distributed in the plant kingdom from mosses upwards. Originally it was lignin that made possible that the plant life transfer from water to land. In tubular plants it is usually found in the xylem, the individual elements of which show cell walls incrustated with lignin (Christiernin *et al.*, 2005).

Lignin is defined as an aromatic polymer, the structure of which is extremely complex and it comprises about 17 to 33% of the dry weight of wood (Bernhard and Schwartz, 1997). It also acts as a component that assists in the resistance of the wood towards attack by micro organisms and decay (Ting, 1982). All lignins appear to be polymers of 4- hydroxycinnamyl alcohol (p-coumaryl alcohol) or its 3- and /or 3.5-methoxylated derivatives, respectively, coniferyl and sinapyl alcohol. The contribution of each of these three monomers to the lignin macromolecule differs, depending on the source of the lignin (Christiernin *et al.*, 2005). The generalized structure of lignin is shown in the following diagram Figure 2.1.

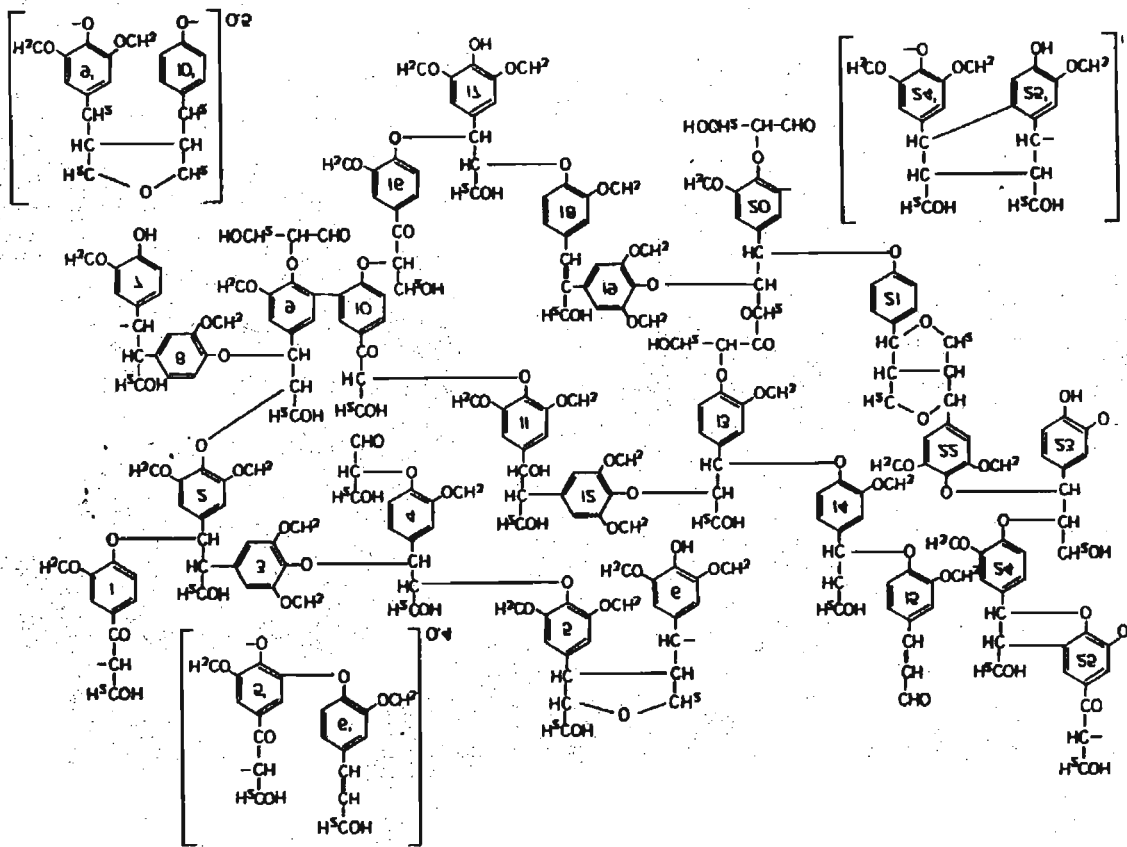


Figure 2.1 A generalized structure of lignin according to Lindberg *et al.*, 1989

In wood lignin is located in the middle lamella, from which it penetrates in gradually diminishing amounts, in to the primary and secondary layers of the cell wall (Brauns, 1952). In the true lamella of wood, lignin is the three- dimensional network polymer comprised of phenylpropane monomers linked together in different ways. In the secondary wall, lignin is a non-random two-dimensional network polymer. The chemical structure of the monomers and linkages which constitute the networks differ in different regions (i.e. the lamella vs. secondary wall), different types cell (vessels vs. fibres), and different types of wood (softwood vs. hardwood). When lignin is extracted from wood, the properties of the macromolecules made soluble will reflect the properties of the network from which they are derived (Glasser and Sarkanen, 1989).

The composition of lignin can vary, not only between plant groups but also between tissues of the same plant and even between cells of the same tissue. There is histochemical and chemical evidence that the lignin of the primary xylem in

angiosperms resembles that of gymnosperms, while lignin of the secondary xylem generally resembles that of lignin present in angiosperm (Christiernin *et al.*, 2005).

Lignin is formed from cinnamyl that are; coniferyl, sinapyl and 4-coumaryl alcohols. Various attempts were made to classify lignins according to their origin and composition, and two main classes were recognized. These classes are guaiacyl lignins and guaiacyl-syringyl lignins (del Rio *et al.*, 2005). In general guaiacyl type of lignins is present in the Gymnospermae, Pteridophyta, Cycadales; and the guaiacyl-syringyl type is present in the Angiospermae and Gnetales (Christiernin *et al.*, 2005).

The relative amounts of these monolignols found in lignin show plant specificity. Gymnosperm lignins contain mainly coniferyl alcohol; angiosperm lignins contain both coniferyl alcohol and sinapyl alcohol, whereas all three types of monolignols are found within lignins of grasses (Wardrop, 1981). Figure 2.2 shows a generalized pathway of the biosynthesis of lignin.

2.3.2 Lignin in the paper industry

The chemical composition of eucalypt wood varies within and between species and between sites. Wood chemical composition seems to be of particular importance in paper manufacture (Sandercock *et al.*, 1995). The main components of wood are cellulose, hemicellulose, extractives and trace materials, and lignin. The distribution of these in hardwood and softwood is presented in Figure 2.3.

Cellulose is the primary structural component of cell wall and of paper. Hemicelluloses are not precursors of cellulose and their function is poorly understood. Their molecular weight is too low for them to be of structural importance, however, it is widely recognized that they are beneficial to pulp and paper properties such that the tensile strength of paper generally correlates positively with the hemicellulose's content (Roberts, 1996). Resins and extractives are a small proportion of wood and they are extractable by organic solvents such as ethanol. Many of these substances are removed during the chemical pulping process but some may still be retained in the final sheet of paper (Alves *et al.*, 2006).

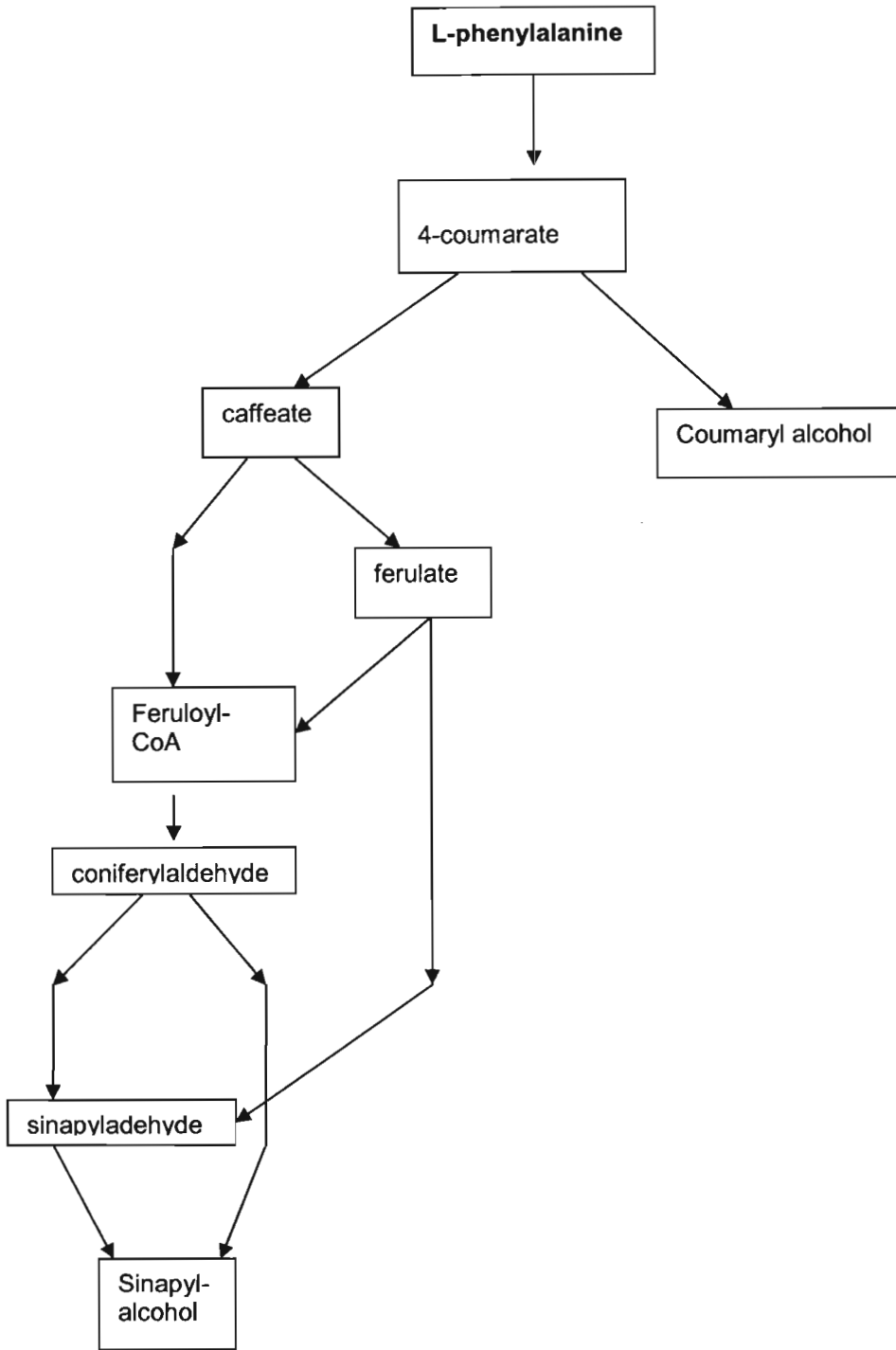


Figure 2.2 Generalized lignin biosynthesis pathway (Humphreys and Hemm, 1999)

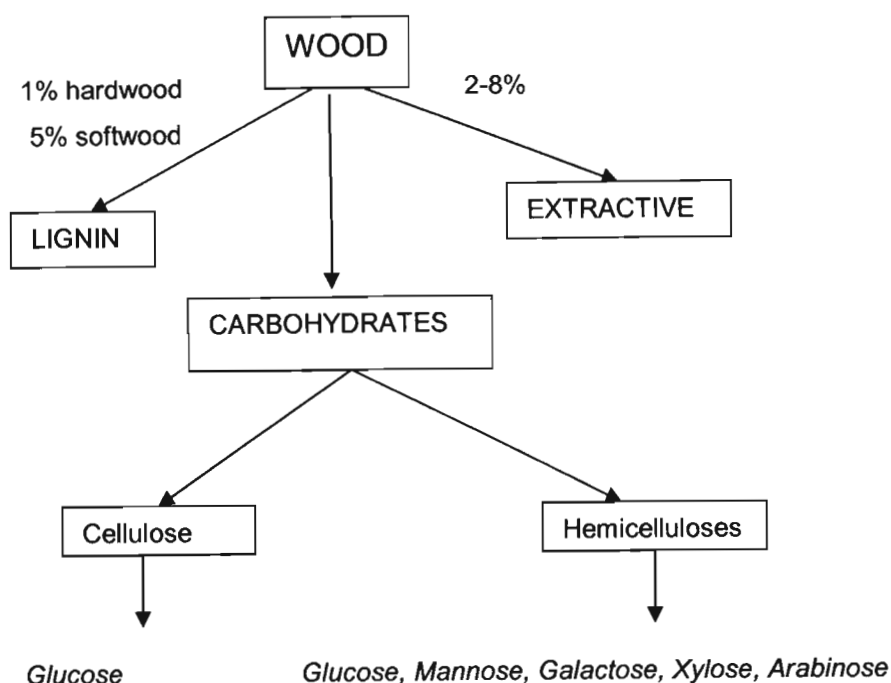


Figure 2.3 Chemical components of wood (Smook, 1992)

Lignin was initially researched in the beginning of the 19th century. From analyzing wood of various species Schulze (1865) calculated the elementary composition of lignin to be 55.6% carbon, 5.8% hydrogen and 38.6% oxygen. From this he arrived at a formula of C₁₉ H₂₄ O₁₀ (Wise and Jahn, 1952). This is not far from what was obtained in the 21st century as stated in Table 2.1.

Table 2.1: Approximate lignin content from softwood and hardwood (Christiernin et al., 2005)

Source	Carbon (%)	Hydrogen (%)	Oxygen (%)
Spruce lignin (softwood)	65.1	5.8	29.1
Beech lignin (hardwood)	62.6	5.9	31.5

Paper can be made from fibre cells in their unmodified form by mechanical pulping. Mechanical pulping is suitable only for products with a short life span because lignin is not removed. Lignin, the third component of wood, discolours in sunlight through the process of photochemical oxidation. This makes the paper to become yellow and brittle (Roberts, 1996). The use of lignin-containing fibres is only used for disposable products such as newsprint and disposable lightweight coated paper. Lignin is removed by chemical pulping for higher-quality papers that are for long-term or

lifetime use. The chemical process of delignification produces a brown pulp from residual lignin; therefore, this process is usually followed by the bleaching process (Ibarra *et al.*, 2005).

Almost all properties of lignin are undesirable for papermaking applications, hence the highest-quality paper is usually made from pulps from which most of its lignin has almost been totally removed. The ideal pulping process would completely dissolve lignin without causing any loss of the carbohydrate material. Lignin and carbohydrates exist in close association in the wood structure. There is strong evidence suggesting that formal covalent links exist between the lignin macromolecule and carbohydrate components of the wood structure (Ibarra *et al.*, 2004).

In order to make pulp for the production of paper, lignin in the wood is separated from cellulose. The chemical processes of wood at elevated pressures and temperatures can achieve this. Kraft and sulphite pulping processes are the two most widely used chemical treatments. During pulping, lignin in wood is chemically split into fragments by the cooking liquor. Unfortunately, the chemical reactions involved in the removal of lignin seem not to be selective. Substantial amounts of carbohydrates, primarily hemicelluloses and some cellulose are also chemically attached and dissolved to some extent. The hemicelluloses and some cellulose are vulnerable to acid hydrolysis, and are easily lost during acid pulping processes. The removal of either cellulose or hemicelluloses reduces the strength of the pulp and also contributes to pulp yield loss (Baptista *et al.*, 2006).

There is still some lack of knowledge of chemistry of the widely planted *Eucalyptus* species used for pulp and paper. The composition and structure determines the behaviour of wood and wood fibres during pulping, bleaching and papermaking processes. The information on chemistry of wood is crucial for the optimization of these processes and quality of pulp and paper. The chemistry of plantation eucalypt wood and the behaviour of its components during Kraft pulping and bleaching has been investigated over the past ten years by Neto *et al.* (2005) and made significant advances on the knowledge of the composition and structure of polysaccharides, lignin and extractives (Neto *et al.*, 2005).

From the study it was observed that although the relative content of lignin in wood may contribute to the different pulping performance of Eucalyptus species, the differences observed between three species that showed similar lignin content are clearly related to other factors. Extractives may contribute to the different pulping abilities negatively since they contribute to the consumption of alkali. When S:G ratio of wood and Kraft pulp lignins was plotted against the chemical charges used in the pulping and bleaching, respectively, an interesting correlation was observed confirming the effect of syringyl units in the pulping and bleaching ability (Neto *et al.*, 2005).

Constituent such as lignin require complicated laboratory procedures and are consequently costly to measure. Important lag times may occur between collections of samples and acquisition of laboratory results (Wessman, 1987). There is an amount of lignin present in leaves and this study will attempt correlate the amount of lignin present in leaves and the amount of lignin present in wood. Estimation of plant biochemical composition through high spectral resolution has its foundation in the laboratory near infrared spectroscopy (NIRS). NIRS has been used successfully to predict lignin concentrations on dried and ground foliage (Serrano *et al.*, 2002).

Foliar chemical composition and chemical analysis of plant tissue is standardised, however, the expense in time and money can severely restrict sample size (Wessman, 1987). Airborne hyperspectral remote sensing has been widely used to quantify foliar biochemical compositions since the 1980s and extensive research is still being undertaken (Curran, 1989). Measuring of biochemicals using hyperspectral sensors has its origins in the laboratory where spectrophotometers have successfully been used for decades to qualify and quantify chemical compositions of substances (Richardson and Reeves, 2005).

2.4 LABORATORY SPECTROSCOPY AND HYPERSPECTRAL REMOTE SENSING

Hyperspectral sensors or imaging spectrometers are instruments that can acquire data in many narrow contiguous spectral bands throughout the visible, near-IR, mid-IR, and thermal IR portions of the spectrum. The currently used unit for hyperspectral bands is the nanometer (nm). The use of hyperspectral remote sensing has its origins in the laboratory where chemical composition is quantified using calibrated spectrophotometers. This technology is widely known as spectroscopy, Near Infrared (NIR) technology or Near Infrared Spectroscopy (NIRS). Spectroradiometers that are used in the field also evolved from this technology (Curran, 1989).

2.4.1 Near Infrared (NIR) Technology

NIR (Near Infrared) and refers to the region of light immediately adjacent to the visible range, found between 750 and 2500nm. Near Infrared spectroscopy (NIRS) utilises the diffuse reflectance of dried, ground samples. Each constituent of a complex organic has unique absorption properties in the near-infrared (NIR) region. The absorption of NIR radiation by organic molecules is due to overtone and combination bands primarily of O-H, C-H, N-H and C=O groups whose fundamental molecular stretching and bending absorb in the mid-IR region. These overtones do not behave in a simple fashion, which makes mid-IR and NIR spectra complex and not directly interpretable as in other spectral region (Richardson and Reeves, 2005).

A measurement of a sample's diffuse reflectance, which is the sum of NIR absorption and the scattering characteristics of the sample is rapid and requires little sample preparation. The weight of the sample is not required and no chemical reagents are necessary and, moreover, the analytical time is short (Wessman, 1987). Standard wet chemistry of lignin content analyses is both time-consuming and expensive. Near infrared spectroscopy offers rapid, repeatable and accurate measurements of biochemicals or constituents (McLellan *et al.*, 1991). The NIRS standard errors of prediction are comparable to wet chemistry (Peterson *et al.*, 1988).

Four criteria have to be met for meaningful prediction when using the NIR:

1. selection of calibration samples representative of the population to be predicted,
2. accurate laboratory analysis of the calibration samples,
3. choice of the correct mathematical treatment of the NIR data for optimum information extraction and
4. choice of wavelength relevant to the total population of samples (Analytical Spectral devices, undated).

Prediction of canopy chemical compounds including lignin based on reflectance in the near- infrared has been demonstrated using hyperspectral information. The fact that many types of plant phenolics have chemical structures that are similar to lignin has been overlooked. These phenolics may have similar spectral responses to lignin's spectral responses in the near infrared. The predictive ability to determine biochemical composition of vegetation is due to the reflectance of organic compounds at different wavelengths (Foley *et al.*, 1998).

The statistical processes used in quantitative spectral analysis include multiple linear regression, classical least squares, inverse least squares and principal component regression. If the instrument is calibrated properly, it will then predict the correct amount of parameter in a sample. Validation process then follows where an instrument is set to predict scanned samples whose parameter had been measured in the lab. Correlation coefficient derived from regression between the predicted and measured values gives an indication on how well the instrument will predict the parameter of interest (Schimleck, 2003).

Spectroscopy or NIR Technology has a number of advantages that makes it a valuable tool for acquiring biochemical and chemical information. NIR technology is rapid, non-destructive, does not use chemical, or generate chemical wastes requiring disposal, simultaneously determines numerous constituents or parameters, and can be transported to nearly any environment or true portable for field work. NIR instrumentation is simple to be operated by non-chemists, and operates without fume hoods, drains, or other installations. Its accuracy is dependent on the accuracy of the reference method used for training; however the data from NIR method has better

reproducibility than the conventional method (Shenk, 1981). NIR analysis is the practical choice over mid-IR and far-IR analysis for most applications because the absorbencies/ reflectances in the NIR region are lower than in neighbouring regions and generally obey the Beer/ Lambert law, i.e., that absorbance increases linearly with concentration. This is because the NIR absorptions are generally 10-100 times weaker in intensity than the fundamental mid-IR absorption bands (Richardson and Reeves, 2005).

This technology also has a number of disadvantages associated with its use. Separate calibrations are required for each constituent and a portion of unknown samples must periodically be analyzed by the reference method to ensure that calibrations remain reliable. It may be necessary to update calibrations during the initial phases of use to incorporate outliers, until the calibration is acceptable. The information about samples in the NIR spectra can only be accessed through a sufficiently powerful computer that allowed the development of complex statistical relationship between the spectral data and the constituents determined by the conventional method. It is important to check for and remove outliers in both the training set and the validation set (Analytical Spectral devices, undated).

Similarities of lignin and cellulose features have been noted and these two compounds are often quantified together as the total amount of both lignin-cellulose. The similarity of spectral features of lignin and other phenolics in the near infrared has not yet been fully studied. If a similarity of spectral signatures of lignin and these other phenolics does exist, estimation of lignin can be affected, together with modelling the ecosystem with regards to nutrient cycling because while lignin decomposes slowly, soluble phenolics are readily leached out of the ecosystem. The experiments were conducted by Soukupova *et al.* (2000) to observe the spectral features of lignin and soluble phenolics using GER spectrophotometer and NIRS. APPENDIX 1 demonstrates characteristics of lignin when using different instruments. What was observed is that a distinctive difference between tannin and lignin was observed at shorter near infrared wavelengths between 800nm and 1300nm. In this spectral range the reflectance of lignin was observed to increase with increasing wavelength, but the reflectance of tannin over this part of the spectrum decreased with increasing wavelength. Both spectrometers recorded a significant drop in

reflectance beyond 1400nm for tannins while both instruments recorded a strong absorption feature at approximately 2140nm for tannin. The two instruments recorded a minor absorption for lignin at the same wavelength (Soukupova *et al.*, 2000).

The spectral reflectance similarity of lignin and tannin may be due to the fact that they both contain aromatic rings as well as hydroxyl groups, which have distinctive spectral characteristics in the near infrared spectral region. The use of different wavelengths for the prediction of lignin concentrations has been explained by the heterogeneity and diversity of lignin known not only within the plant kingdom but also within different tissues and developmental stages of a particular plant species. Another explanation is based on the fact that most studies use a stepwise multiple linear regression method from derivative reflectance spectra to predict leaf chemistry. This method is used to identify the best wavelengths correlated with a biochemically determined concentrations of lignin and is based on a statistical operation rather than on the understanding of biochemical composition of compounds and physical processes that govern spectral responses (Soukupova *et al.*, 2000). The table showing different wavelengths used to quantify lignin using different instruments and technologies are in APPENDIX 1.

The extracted lignin is not intact since the extraction process includes cleaving the parts of long and branched lignin molecules in order to remove them from cell walls. This study explored the spectral responses of both intact and extracted lignin molecules from wood. It was found that spectral properties of all wooden blocks showed great similarity with the extracted lignin and lignin and tannin samples, therefore the primary structure of lignin controls its spectral signature. The only exception was that the wood spectral signatures were lacking the absorption feature at 2143nm that occurred in scans of lignin and tannin powder standards (Soukupova *et al.*, 2000).

Simultaneous estimation of two or more constituents requires multiple linear regression equations. When Winch and Major in 1981 applied NIRS to predict Kjeldahl nitrogen in legumes and grasses, with standard errors of the NIRS calibration (SEC) only slightly higher than those of the laboratory (0.08 – 0.11 vs.

0.08%N) standard errors of prediction (SEP) ranged from 0.16 – 0.20%N. Shenk *et al.* (1981) reported SEP of 0.96% for crude protein, 1.13% for lignin, 1.27% for cellulose, 0.16% for calcium, 0.04% for phosphorus and 0.37% for potassium. Wessman *et al.* (1987) used multiple linear regressions, predicting wet chemistry values based on near-infrared spectra yielded correlation coefficients of 0.98 for Kjeldahl nitrogen and 0.78 for lignin, with standard errors of 0.11% for nitrogen and 2.9% for lignin. They concluded that near-infrared is very effective for rapid determination of foliar lignin and nitrogen and should be considered as routine analytical method (Wessman, 1987).

2.4.2 Hyperspectral Remote Sensing and Canopy Chemistry Analysis

Hyperspectral systems collect more than 200 bands of data, which enables the construction of a continuous reflectance spectrum curve for every pixel in the scene (Cetin, undated). The advantage of hyperspectral system is that they can discriminate among earth's surface features over narrow wavelength intervals, while these features are lost within the relatively coarse bandwidths of the various bands of conventional multispectral scanners. A hyperspectral image data set is recognized as a three-dimensional pixel array. The x-axis is the column indicator, the y-axis is the row indicator and the z-axis is the band number, which is expressed as the wavelength of that band or channel (Lillesand and Kiefer, 2000). A hyperspectral image can be visualized as shown in figure 2.4 below.

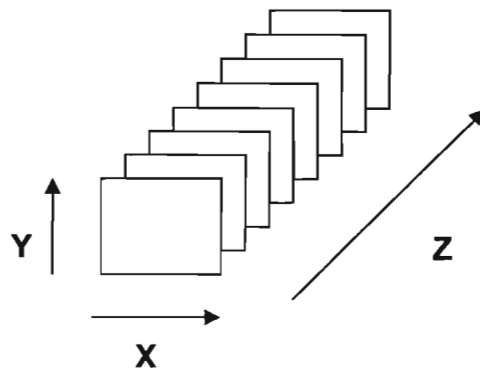


Figure 2.4 Hyperion Data Axes

When Lillesand and Kiefer (2000) compared the data produced using the Landsat TM band 7 with the data from hyperspectral sensor with regards to common minerals over the wavelength range of 2.0 to 2.5 μm , the Landsat TM sensor obtained only one data point, while a hyperspectral sensor obtained many data points over the same range (Lillesand and Kiefer, 2000). While a broadband system can only discriminate general differences among material types, a hyperspectral sensor affords the potential for detailed identification of materials and better estimates of their abundance (Jia *et al.*, 2006).

Because of the large number of narrow bands sampled, hyperspectral data enable the use of remote sensing data collection to replace data collection, which in the past, was limited to laboratory testing or expensive ground site surveys. Some application areas of hyperspectral remote sensing include determinations of surface mineralogy; water quality; bathymetry; soil type and erosion; vegetation type; plant stress; leaf water content, and canopy chemistry; crop type and condition; and snow ice properties (Plaza *et al.*, 2006).

There is not much readily available information about research done on the quantification of foliar lignin. There are a number of studies done on foliar nitrogen but only a few researchers have quantified both nitrogen and lignin using hyperspectral remote sensing. The most recent successful study of foliar lignin estimation which is accessible was done by Serrano *et al.* (2002). She utilized indices using a reference band and a band corresponding to lignin concentrations (Serrano *et al.*, 2002).

Martin and Aber (1997) used AVIRIS to determine foliar lignin and nitrogen. From the calibration equations which were developed, they obtained $R^2 = 0.87$ and 0.77 for nitrogen and lignin respectively. Calibration equations were evaluated on the basis of inter- and intra-site statistics (Martin and Aber, 1997).

Peterson *et al.* (1988) conducted a study where they presented results on reflectance spectra of forest foliage and canopies, and their relationships to chemical composition. Their research included analysis at three different stages; 1) analysis of dry, homogenous leaf samples measured in the laboratory spectrophotometer; 2)

analysis of laboratory and field spectra taken for fresh, whole leaves and 3) the analysis of AIS (Airborne Imaging Spectrometer) spectra for whole forest canopies. The first step was to perform the biochemical analysis using the wet chemistry method to determine the lignin quantities. Using the results from the wet chemistry, the spectrophotometer was calibrated. Calibration of the spectrometer allowed that the remaining sample be analyzed using the spectrometer which is a faster process of determining the lignin concentrations (Peterson *et al.*, 1988).

Regression analysis was used to determine the optimal wavelengths for predicting biochemical composition from the spectrophotometer. The regression analysis was based on raw and smoothed versions of the log (1/R) data and their respective first and second derivatives. Half to two thirds of the samples set were used to generate a calibration equation. This calibration equation was then applied to the remaining test samples to determine how well the model predicted composition from spectral reflectances. The AIS spectra were evaluated using simple correlation of canopy nutrient contents versus filtered AIS. A correlogram was generated from these data that consists of the correlation coefficient between both leaf nitrogen and lignin with NIR spectra. These laboratory techniques can predict nitrogen and lignin contents with standard errors of prediction comparable to those achieved in the wet chemistry (Peterson *et al.*, 1988).

When lignin from pine was measured in the laboratory, it had a number of absorption peaks throughout the shortwave IR and strongly absorbs in the visible region. The Oakwood lignin peaks at 1420 and 1920nm ascribed to O-H bonds, and 1696 and 2106nm ascribed to aromatic C-H bonds and phenolic hydroxyls, respectively. Spectral region between 1500 to 1700 nm is predictive of lignin content in forage grasses. For fresh leaves, the reflectance pattern is dominated by absorption of chlorophyll and accessory pigments in the visible and by water absorption in the shortwave infrared. When water content is reduced through drying, the subtler biochemical absorptions are revealed (Peterson *et al.*, 1988).

Gastellu-Etcheberry *et al.* (1995) conducted a study assessing canopy chemistry using AVIRIS. Simultaneously with AVIRIS acquisition, an atmospheric profile was carried out, and the forest vegetation was sampled for chemical analysis and laboratory spectral measurement. Predictive relations between concentrations of nitrogen, R was 97%; lignin, R was 89%; and cellulose, R was 83%, and reflectances of pre-heated pine needles were determined through stepwise analysis. A methodology was designed to assess their extrapolation to remotely acquired spectrometric data. The applications of laboratory derived relationships led to relatively large correlations for nitrogen (74%) and cellulose (79%) but poorer results were obtained for lignin (44%). Predictive equations based on laboratory measurements were applied to reflectances of pine needles that were computed through the inversion of two reflectances models. This approach improved the correlations for lignin (74%). No improvement was observed for nitrogen (70%) and cellulose (69%) (Gastellu-Etcheberry *et al.*, 1995).

2.5 LEAF AREA INDEX

Leaf area Index (LAI) is an important structural parameter used to quantify energy and mass exchange characteristics of terrestrial ecosystems such as photosynthesis, respiration, transpiration, carbon and nutrient cycle, and rainfall interception. Leaf Area Index is thus defined as the total one-sided area of all leaves in the canopy within a defined region (m^2/m^2). LAI is an important structural parameter that is used as an input into growth prediction models in forestry. Direct measure of LAI is relatively accurate but extremely labour intensive and destructive. Measuring and estimating LAI over large areas has proved to be problematic, thus, it is more practical to measure LAI only on limited experimental plots (Pu *et al.*, 2005). Remote sensing offers vast coverage of natural resources and therefore it is being exploited to estimate important forest parameters. There are models used to estimate LAI to produce LAI maps that are used as inputs to other prediction models. To produce an LAI map or prediction of a large area, a model relating field data with remote sensing data is typically developed, and the remote sensing data are then used to extrapolate that relationship to the landscape (Lee *et al.*, 2004).

2.6 INTRODUCTION TO REMOTE SENSING IN FORESTRY

Remote sensing is the science and art of obtaining information about an object, area, or phenomenon through the analysis of data acquired by a device that is not in contact with the object, area or a phenomenon under investigation. The use of remote sensing allows for the mapping of large areas efficiently, cheaply, in digital manner that allows for accuracy assessment and integration with Geographic Information System (GIS) (Benz *et al.*, 2004).

In Remote Sensing electromagnetic sensors are currently being operated from airborne and space borne platforms to assist in mapping and monitoring earth resources. The sensors acquire data on the way various earth surfaces emit and reflect electromagnetic energy. These data are analysed to provide information about the resources under investigation. Spectral responses measured by the sensors over various features often permit an assessment of the type or condition of the features. These responses are referred to as spectral signatures. Features are spectrally separable, however, the degree of separation depends on the location within the spectrum, for example water and vegetation might reflect nearly equally in visible wavelengths but separable in near Infrared wavelength (Casa and Jones, 2005).

Remote sensing instruments allow for the collection of digital data through a range of scales in a synoptic and timely manner. The use of remotely sensed images allows for mapping of large areas efficiently digitally in a manner that allows for accuracy assessment and integration with geographic information systems. The advancements in sensor technology are increasing the information content of remotely sensed data and resulting in a need for advanced analysis techniques. The advances in sensor technology are occurring concurrently with changes in forest management practices that require detailed measurements intended to enable ecosystem-level management in a sustainable manner. The review of remote sensing image analysis techniques, with reference to forest structural parameters, illustrate the dependence of spatial resolution to the level of detail of the parameters which may be extracted from remotely sensed data. As a result, the scope of a particular investigation will influence the type of imagery required and the limits to details of the parameters that should be estimated. The combinations of image

processing techniques may increase the complexity of parameters that should be extracted (Wulder, 1998).

Wavelengths have a profound effect on data collection in remote sensing. Atmospheric absorption results in the loss of energy to water vapour, carbon dioxide and ozone, etc. energy specific wavelength regions tend to be absorbed effectively by these gases, it is therefore important that the bands and spectral regions are selected with consideration to this fact. The wavelength ranges where the electromagnetic energy can be transmitted through the atmosphere are called the atmospheric windows. Therefore when selecting the sensor to be used when collecting data through remote sensing there are four things to consider; namely (a) spectral sensitivity of the sensor, (b) the presence and absence of the spectral windows in the spectral regions where one wishes to sense, (c) the source, magnitude and spectral composition of the energy available in the ranges, (d) the manner in which the energy interacts with the features under investigation. Energy is absorbed, transmitted or reflected. The amount of energy, which is reflected, transmitted or absorbed, will vary according to different earth's surfaces. These differences permit the distinguishing of different features in an image (Lillesand and Kiefer, 2000).

Foliar reflectance presents a rapid and non-destructive means to measure vegetation properties and conditions. A plant leaf has low reflectance in the visible region of the spectrum resulting from strong absorption by chlorophyll. In comparison to the visible region leaf has a higher reflectance in the near-infrared region as a result of internal leaf scattering and reduced absorption (Zhang *et al.*, 2005).

2.7 VEGETATION INDICES AND LAI

Work on spectral properties of plants began as early as 1913 when it was proved that light entering leaves is critically reflected internally at the walls where the reflective index changes from that of water (1.33) to that of air (1.00). This leads to highly efficient scattering of all wavelengths of light. Plant pigments such as chlorophyll strongly absorb light in the visible, and the liquid water in plant leaves absorbs much of the light at the wavelengths longer than 1.4 micrometers, wavelengths at which plant materials are relatively transparent. Much attention in

green vegetation is focused on the strong reflectance contrast between the visible and the near infrared (NIR) that forms a strong step in the spectrum of green vegetation where the vegetation indices are established (Lillesand and Kiefer, 2000).

Linear and non-linear relationships between optical satellite-derived spectral vegetation indices and LAI have been found for different vegetation types and climatic conditions. New methods to extract canopy properties from remote sensing data have been successfully tested. The inversion of physically based canopy reflectance models has arisen as the most promising technique for retrieving LAI. Canopy reflectance model describes the interactions of solar radiation with vegetation elements and are often coupled with leaf optical properties models that simulate the reflectance and the transmittance of a leaf as a function of its constituents. The inversion of these models allows the estimation of both leaf and canopy parameters in predictive mode, therefore overcoming the need of parameterization required for the use of regressive semi-empirical models. The accuracy of such estimations is dependent on three factors: the radiative transfer model employed, the type and quality of RS data, and the inversion procedure used (Meroni *et al.*, 2004).

The most commonly used vegetation indices when studying the forest ecosystems using remote sensing are computed from simple functions based on the R band and NIR band. These wavebands are used to formulate various vegetation indices to acquire more precise indications of surface vegetation conditions. The simple ratio (NIR/R) and the NDVI are most frequently used to correlate with LAI and other canopy structure parameters from airborne and spaceborne remote sensing data. With increase in LAI, red reflectance decreases as light is absorbed by leaf pigments while the NIR signal increases due to the fact that more leaf layers are present to scatter the radiation upwards because plant cell walls, notably the lignin component, cause scattering of NIR energy, resulting in relatively high NIR transmittance and reflectance. The simple ratio VI has proved to be sensitive to optical properties of the soil background and therefore, their application is limited (Zhao *et al.*, 2005).

NDVI provides an indication of the green leaf biomass and green leaf area. Coarse resolution induces reduction in the NDVI signal due to the fact that a pixel may not be a completely forested area because the spatial resolution covers an extensive area (Coops, *et al.*, 2001). Perpendicular Vegetation Index (PVI) was once proposed in an attempt to reduce the effect of the soil background on VIs. However, experimental and theoretical investigations indicated that soil background still has an effect. Brighter soils have resulted in higher index values for a given quantity of incomplete vegetation cover. Additional indices were formulated to address this problem. An index named weighted difference index was proposed, however it was found that it did not hold any advantage over the PVI (Gong *et al.*, 2003).

Alternative formulations that include correction factors or constants that attempt to minimize the effect of varying background reflectance on VIs followed. The soil-adjusted vegetation index (SAVI) was derived from the NDVI and the adjustment factor L was introduced to minimize soil brightness influence and to produce vegetation isolines independent of soil background. The constant L can range from zero to 1, where if L is zero then vegetation cover is very high and SAVI is equivalent to NDVI, and where L is 1 then the vegetation cover is very low. If L tends to infinity then it is equivalent to PVI. It was suggested that an adjusted factor $L = 0.5$ for intermediate vegetation amounts should be used, resulting in spectral index (SAVI) superior to the NDVI and PVI for a relatively wide range of vegetation conditions. Transformed soil adjusted vegetation index (TSAVI) was proposed to further reduce the error for a vegetation index (i.e. SAVI) for plant canopies with varying low densities (Gong *et al.*, 2003).

TSAVI is equivalent zero for bare soil and is close to 0.7 for very dense canopies. It can compensate for soil variability due to changes in solar elevation and canopy structure. The non-linear vegetation index (NLI), the renormalized difference vegetation index (RDVI) and the modified simple ratio vegetation index (MSR) were proposed to simulate non-linear relationships between VIs and the surface biophysical parameters. These indices were formulated in an attempt to linearize relationships with surface parameters that tend to be non-linear. Modifications and combining of the existing VIs brings about the improvement in the estimation of LAI. These are the following examples of the combinations of existing VIs and their

benefits:

- MNLI is a modification of NLI and it incorporates the merits of SAVI while it is more suitable for more arid areas.
- Under conditions of low LAI, where λR is relatively high and λNIR relatively low, a small change in λR produces a larger proportional change in NDVI than SR. Under conditions of high LAI where λNIR is higher and λR lower, a change in λNIR will induce a larger proportional change in SR than in the NDVI. Therefore, the NDVI*SR is expected to balance the two phenomena to increase correlation with LAI.
- SAVI*SR combines the merit of SAVI which eliminates the effect of soil background with that of SR (a wider range of VI values corresponding to narrower range of vegetation cover) (Gong *et al.*, 2003).

Sellers (1987) derived an important relationship between LAI, APAR to NDVI. Research found that under specified canopy properties, APAR was linearly related to NDVI and curvilinear related to LAI. Thus $NDVI = fAPAR = f LAI$ (Coops, *et al.*, 2001). LAI could serve as a useful indicator to characterize the condition of the forest ecosystem in the research of global change due to the fact that leaf area responds rapidly to different stress factors and changes in climatic conditions. Remote sensing provides the alternative to estimate and monitor LAI and models developed to for application to remotely sensed data rely on physically based relationships between LAI and canopy reflectances, expressed as algorithms (Lee *et al.*, 2004).

Even though there have been attempts to improve the NDVI and developing new indices to compensate for the soil background influences, so far it has not been possible to design an index that is sensitive only to the desired variable and totally insensitive to all other vegetation parameters. Therefore, different indices were defined for different purposes and each optimized to assess a process of interest. No studies have focused on retrieval of LAI without interference of chlorophyll effects (Kalacska *et al.*, 2005).

Fairly strong but site specific relationships between VIs, such as the SR, and the NDVI have been found in various studies across different vegetation types. Another problem that has been found with the NDVI is that it tends to saturate at high levels of LAI. Studies from the boreal forests have shown that NDVI is not dynamic enough to be utilized for the estimation of LAI. This can be explained by the presence of green understorey that causes a non-contrasting background reflectance in the visible area of the spectra. The inclusion of the MIR spectral band in SR based on visible and NIR reflectance has proved to provide complementary information on the optical geometrical structure of the canopy and on the optical properties of the underlying soil. The reduced simple ratio (RSR) is a MIR corrected modification of the simple ratio (SR), which was introduced to adjust for differences in canopy closure and background reflectance in the retrieval of LAI. It was found that RSR correlated better with LAI than did SR due to the fact that it reduces the effect of background reflectance and increases the sensitivity to changes in LAI (Sternberg *et al.*, 2004).

When estimating leaf area index with spectral values, caveats to consider are the presence of understorey vegetation, within-stand shadowing, bidirectional effects and stand density as well as the canopy closure. According to previous studies, it is much more difficult to estimate LAI from remotely sensed data once the foliage within the stands begins to overlap (Wulder, 1998). The openness of the overstorey and the spatial and temporal variations of the understorey vegetation can pose special challenges to the retrieval of canopy leaf area index from remotely sensed data. The research suggests that the confounding effect of the understorey vegetation is important to the interpretation of reflectance of sparse canopies. An alternate approach to retrieval of the canopy LAI is to invert a canopy reflectance (Cohen, 2003).

Rosema *et al.* (1992) introduced the forest-light interaction model (FLIM) to derive LAI and canopy coverage from TM data; Hu *et al.* (2004a) modified the FLIM and produced canopy closure maps using Compact Airborne Spectrographic Imager (CASI). A strong correlation has been found between the retrieved canopy LAI and the field measured LAI using model-based methods, where R^2 values ranged from

0.51 to 0.86. In open canopies, near infrared reflectance from understorey, particularly broad- leaved species, dominates the overall reflectance. It was suggested that simple relationships need to be replaced by canopy models in open-canopy cases especially because the understorey also changes seasonally. Images with stands that had dominating understorey generally produced poor correlations between NDVI and LAI values (Hu *et al.*, 2004b).

Another approach to the retrieval of open canopy parameters is linear spectral analysis. Linear spectral mixture analysis of multispectral and hyperspectral remote sensing data sets has been widely used and has been applied in vegetation applications. In the past decades, imaging spectrometers have been developed to acquire continuous spectra over land and water surfaces and these spectrometers include the Advanced Solid-State Array Spectroradiometer (ASAS), Airborne Visible-Infrared Imaging Spectrometer (AVIRIS), Compact Airborne Radiographic Imager (CASI) and the Shortwave Infrared Full Spectrum Imager (SFSI). Research into the development of these airborne sensors and analysis of high-resolution data has provided a background for development of spaceborne imaging spectrometers for Earth Observing System (EOS-1) (Treitz and Howarth, 1999).

Advances in imaging spectrometer technology and radiative transfer modeling have improved the possibility of accurate estimation of Leaf Area Index from spectral and angular dimensions of remotely sensed data (Mnyeni *et al.*, 2002). It is not a trivial task to find optimal vegetation indices for LAI estimation when using hyperspectral imagery because, for instance, vegetation indices derived from the red and the NIR band of the traditional TM or Multispectral Scanner (MSS) image could correspond to hundreds of equivalent counterparts in hyperspectral imagery (Zarco-Tejada *et al.*, 2005).

2.8 VEGETATION MODELLING USING HYPERSPECTRAL NARROW BANDS

Many hyperspectral vegetation studies are still based on multispectral indices that are used as reference data. Hyperspectral data can provide much more possibilities compared with multispectral data in detecting and quantifying sparse vegetation because it provides a continuous spectrum across a range in wavelengths. In past studies hyperspectral linear mixture modeling techniques have been used successfully to detect inter-annual and seasonal changes in vegetation (Frank and Menz, 2003). The high signal to noise ratio in the SWIR region allows greater discrimination of subtle spectral responses. If such subtleties are in any way related to LAI, then hyperspectral data have an advantage over broadbands (Lee *et al.*, 2004).

The possibilities of using the spectrometers have increased over the years because they have become cheaper. Selection of new wavebands in hyperspectral imaging has been performed in a number of cases, focusing on how to increase the sensitivity of the vegetation indices. These types of investigations have been conducted under controlled conditions and as a consequence of different measurement conditions; hence some level of disagreement exists in the selection of wavebands. A limited number of results have been published where hyperspectral reflectances were recorded under natural conditions in high input and high yielding crops (Hansen and Schjoerring, 2003).

However using hyperspectral data is much more complex than multispectral data in a sense that hyperspectral systems collect large volumes of data in a short time. The problems associated with large volumes of data are: data storage volume, transmission bandwidth, real-time analog to digital bandwidth and resolution, computing bottle necks in data analysis and new algorithms for data utilization (e.g. atmospheric correction is more complicated). One significant advantage of hyperspectral sensors is that they contain a substantial amount of information about atmospheric characteristics at the time of image acquisition that atmospheric models can be developed for atmospheric correction parameters (Guo *et al.*, 2006). The hyperspectral image processing considerations can be viewed in APPENDIX 2.

The problem with hyperspectral data volume and storage could best be overcome by introducing specialized sensors that will be optimized to gather data for targeted applications or employ a narrow waveband hyperspectral sensor like Hyperion from which users with different applications can extract appropriate optimal wavebands. Accuracy assessment with increasing number of wavebands would be required to determine the impact of additional bands in discriminating, quantifying, classifying and vegetation modelling (Bacjy and Groves, 2004). Recent research, which was limited to one or two species, demonstrated that the optimal information in quantitative characterization of forest canopies is present in a few specific narrowbands rendering a large number of wavebands redundant (Shettigara *et al.*, 2000).

In 400 – 2500 nm spectral range, 22 optimal wavebands were recommended that best characterizes and classifies vegetation and agricultural crops. Overall accuracies of over 90% were attained when 13 – 22 best narrowbands were used for vegetation classification. Since the data was aggregated into 10nm wide wavebands to match the first spaceborne hyperspectral sensor Hyperion, which resulted into 168 wavebands, this study rendered more than 138 of the 168 narrowbands redundant in extracting vegetation and agricultural crop (Thenkabail *et al.*, 2004a). Although some of the narrow bands can be edited due to the storage and data complexity problem, many of the advantages of the fine spectral resolution imagery may be lost and the discarded portions of data may be vital to certain remote sensing applications. Thus, a more desirable solution might be to use lossless or information preserving data compression (Thenkabail *et al.*, 2004a).

Lossless data compression is to represent the data using a minimum number of bits by reducing the statistical redundancies inherent to the data. However, this method can only provide compression ratios of about 3:1. Another alternative is lossy data compression which can provide very high compression ratios. Decompressed data is susceptible to distortion when using this method, but proper optimization of the compression system may yield distortions small enough that visual degradations are practically non-existent and classification errors are small. As a result lossy compression method is a promising solution to significantly ease the mission requirements for a hyperspectral sensor (Shettigara *et al.*, 2000).

The mean squared error (MSE) or root mean square error (RMSE) is generally used for measuring the distortion between the original and the compressed data. Data compression is usually applied at a data level digital number (DN) or radiance. Two approaches can be used to assess the how remote sensing products are affected by data compression. The first approach is to compare end product values derived from the decompressed data cube with those obtained from the original data cube. The second approach is to compare the end products derived from decompressed data cube with ground-truth and this approach is ideal, if sufficient and accurate ground-truth is available for specific applications (Hu *et al.*, 2004a). There are two assumptions that must be fulfilled if a hyperspectral sensor is to be useful in the biophysical analysis of the terrestrial ecosystem: (a) there must be a strong correlation between the canopy characteristics and the rates at which important processes occur to the biosphere. (b) These canopy characteristics will have to be data.

The study by Hu *et al.* (2004b) indicated there was a strong correlation between measured LAI and LAI estimated from hyperspectral data. Boegh *et al.* (2002) found that NIR reflectance correlated better with LAI when using the airborne multispectral data acquired by the Compact Airborne Spectral Imager (CASI) whereas Stenberg *et al.* (2004) found that band 4 of the Thematic Mapper (ETM), which corresponds to the NIR region, correlated poorly with the LAI.

Stenberg *et al.* (2004) researched the correlations between the LAI and the three SVI Spectral Vegetation Indices); the NDVI, SR and RSR (the reduced simple ratio). They found that the LAI correlated better with RSR than it did with the NDVI and the SR. The NDVI showed poor sensitivity to the changes in LAI. The performance of RSR, however, showed to be weaker at plots around which LAI were relatively constant but the reflectances homogeneous due to a non-vegetation component (e.g. logging roads, rocks, large ditches). In the LAI deviation maps it was observed that the "errors" in LAI_{RSR} (i.e. large deviations from LAI_{mean}) occurred at plots where cutting waste had been left or where there was topographical variation (e.g. a hill). Therefore it is advantageous to use small pixel size. The derived LAI-RSR regression is sensor specific and sensor dependent in two ways: they depend on solar angle and bandwidth. RSR was calculated from the ETM data using the

wavelengths from band 3, 4 and 5 (Sternberg *et al.*, 2004).

Thenkabail *et al.* (2004b) researched the best hyperspectral wavebands for the study of vegetation and agricultural crops over the spectral range of 400 – 2500nm and assessed their classification accuracies through various combinations of narrowbands. The optimal hyperspectral wavebands to study vegetation and agricultural crops were determined through rigorous data mining techniques consisting of principal component analysis, lambda R² models, stepwise discriminant analysis and the derivative vegetation indices (Thenkabail *et al.*, 2004b).

Gong *et al.* (1992) explored the relationship between the original CASI data and the LAI, where the first and second derivatives were correlated with LAI. A piece-wise multiple regression analysis procedure was carried out to produce goodness-of-fit values and standard errors of LAI estimations. Spectral derivative technique was found to considerably increase LAI estimation accuracy. The accuracy increase is attributed to the capability of the derivative technique to reduce the effect caused by the soil background. The first derivative performed slightly better than the second derivative and it was concluded that one type of soil background is advantageous in estimation of LAI using hyperspectral remote sensing (Gong *et al.*, 1992).

Gong *et al.* (2003) tested 12 VI that are originally constructed as simple functions of R and NIR. Some researchers have used bands within the SWIR region (1.0 – 2.5 μ m), especially the ratio of middle infrared (MIR) (1.55- 1.75 μ m) with NIR as a new vegetation index. Leaf reflectances of the SWIR region are dominated by liquid water absorption, therefore to obtain a total canopy equivalent water thickness it was hypothesized that the index is correlated to the LAI through the summation of the individual leaf equivalent of water thickness for each layer. Removal of bands with strong water absorption (1346 – 1447 and 1800 – 1961 nm) and weak and noisy signal bands (wavelengths shorter than 437nm and longer than 2405nm) will leave 168 bands to work with. For each VI a correlation matrix was constructed for a pair of spectral bands. The 12 correlation matrices that were constructed showed that some bands have high potential in LAI estimation. Summarized in APPENDIX 3 are potential bands that were used by Gong *et al.* (2003) and these bands are to be used in this study to select the most suitable bands for each of the nine vegetation indices.

The R^2 column in the table lists two R^2 values, the highest R^2 value for the actual use of NIR and R bands and an optimal R^2 derived from VIs constructed from the SWIR and NIR regions (Gong *et al.*, 2003).

2.9 SUMMARY

2.9.1 Quantification of Lignin

In summary, the chapter has presented a detailed description of the lignin molecule and has also explained its importance in the forest industry. Methods of isolation and quantification have been researched and the benefits of the hyperspectral remote sensing that evolved from the laboratory spectroscopy were briefly discussed. The most recent techniques found in literature utilize the development of lignin indices using bands that correspond to lignin. It was concluded that there are two reference bands for lignin and they are situated at 1680nm and 2100nm. There are other researched bands that correspond to the chemical configuration of the lignin molecule. Construction of lignin indices utilizes one selected lignin band and the reference band closest to the chosen lignin band. Index images that result are related to the laboratory-measured concentrations using statistical analysis (Serrano *et al.*, 2002). Wood chemical analysis has been done in forestry and in the paper industry. Wet chemistry is used concurrently with near infrared spectrophotometers to determine and quantify wood constituents. Laboratory spectrophotometers are calibrated using wet chemistry data and to predict wood chemistry of a large number of samples. The NIR technology has proved to be time and cost effective and has showed more reliable repeatability in prediction results. There is not much accessible literature on meaningful relationships that have been developed between foliar chemistry and wood chemistry for the purposes of application in the pulp and paper industry.

Remote sensing techniques provide the ability to observe, analyze and manipulate data for large areas. The forest industry is researching remote sensing techniques that are beneficial to the industry. In forestry, remote sensing is very cost effective on many applications as long as accurate results are achieved but there is no literature that is focused on finding meaningful relationships between wood lignin and foliar lignin concentrations. Based on the literature above, this study will attempt to obtain a relationship between wood lignin and foliar lignin concentrations. Foliar lignin

concentrations will then be related to lignin indices obtained from the Hyperion data.

2.9.2 LAI and Vegetation Indices

Research is ongoing on the advantages of hyperspectral sensors with regards to LAI estimations using narrow band vegetation indices. Lee *et al.* (2004) found that models with selected AVIRIS channels performed better in LAI predictions than models derived from ETM+ and MODIS. The best models from AVIRIS had up to 23 AVIRIS channels. When Pu *et al.* (2005) compared estimations of forest crown closure and leaf area index from Hyperion, ALI and ETM+; it was found that Hyperion outperformed the LAI and ETM+ sensors. It was concluded that Hyperion's high spectral resolution records subtle spectral information and that the SWIR region is lightly affected by the atmosphere compared to the SWIR region of ALI and ETM+. Therefore, the best spectral region for Hyperion is SWIR and for ALI and ETM+ it is the visible region. Hyperion is demonstrating a high potential for forest management applications (Pu *et al.*, 2005).

It has been discussed by a number of researchers that certain vegetation indices are specific to types of vegetation cover. Muira *et al.* (2006) investigated different sensors for NDVI estimations and it was suggested that distinct algorithms need to be developed for every sensor and that land cover dependency need to be explicitly accounted for to reduce biasness when computing vegetation indices (Muira *et al.* 2006). This study selected vegetation indices that could be applied to *Eucalyptus* plantation.

Fuentes *et al.* (2006) showed that hyperspectral data is effective in measuring net CO₂ and water flux modeled from narrow bands indices. Some vegetation indices, like the NDVI are used for detect nitrogen stress in certain ecosystems and Zhao *et al.* (2005) concluded that hyperspectral remote sensing produces more robust estimation results. There are numerous growth models that require NDVI, many other vegetation indices and LAI as inputs. Hyperspectral narrow bands have proved to be necessary for cost and time effective accurate estimates (Filippi and Jensen, 2006). According to literature provided in this chapter, narrow band vegetation indices are well researched in forestry and they are forming an important part in the formulation of estimation models.

CHAPTER 3: Study Area

3.1 INTRODUCTION

This chapter consists of information on the study area. The study area is described according to its location and composition that explain why it was selected. The study area is also described using topology, geology and soils, climate, and hydrology. The same study area was used for the research on wood and foliar lignin concentrations and research on LAI estimations.

3.2 STUDY AREA

The study area is located in the northern coastal area of Zululand in South Africa. The study area consists of vast plantations of *Eucalyptus* species and *Eucalyptus* clones as well as pine plantations. The study was conducted in twelve *Eucalyptus* commercial forestry plantations. The ages of the compartments ranged between six and nine years, which is the approximate harvesting age. The compartments were selected to permit a comparative analysis of ecosystem biogeochemistry that will hypothetically provide a gradient in relation to foliar lignin and wood lignin concentrations. The selected compartments had light understorey vegetation consisting mainly of broad-leafed vegetation

Every effort was taken to avoid trees that were diseased or trees that showed signs of infestation. Random selection of the trees was also based on the representative varying sizes of the trees in the compartment. Table 3.1 has information on the sites that were chosen for the research on wood and foliar lignin concentrations. Due to time constraints, only seven compartments were chosen from the twelve compartments for LAI measurements (Table 3.1). Other compartmental information can be viewed in APPENDIX 4. Only compartment 11 was thinned and pruned. The rest of the compartments were only fertilized a year after planting.

Table 3.1: Information on the selected compartments for the lignin concentrations and LAI study

Compartment	<i>Eucalyptus</i> Clone	Age at sampling (years)	Spacing (meters)	SI	Plot Radius (m)	Field Measured SI
1	<i>E. urophylla</i>	7.25	3.0 x 3.0	27.50	15	21.29
2	GU-1	7.25	3.0 x 3.0	23.80	15	22.41
3*	GU-2	6.92	3.0 x 2.7	26.50	15	25.90
4	GC-1	7.42	2.7 x 2.4	20.50	15	23.81
5*	<i>E. urophylla</i>	7.25	2.7 x 2.7	27.10	15	24.13
6*	GU-1	8.33	3.0 x 2.0	23.80	15	23.07
7	GU-1	6.33	2.7 x 2.2	20.10	15	22.89
8*	GU-3	6.33	2.7 x 2.2	21.40	15	23.80
9*	GC-2	8.08	3.0 x 2.0	20.60	15	21.96
10*	GU-4	8.00	3.0 x 2.0	20.70	15	17.61
11*	GT	8.75	3.0 x 2.5	20.60	15	27.34
12	<i>E.gra</i>	8.00	2.7 x 2.4	21.90	15	18.05

* Compartments used in the LAI estimation study

3.3 STUDY AREA LOCATION AND DESCRIPTION

3.3.1 Location

The Zululand coastal plain is situated on the eastern seaboard of the KwaZulu Natal Province of South Africa. The study area lies between latitudes 28.29°S and 28.77°S and longitudes 31.92°E and 32.27°E (Figure 3.1).

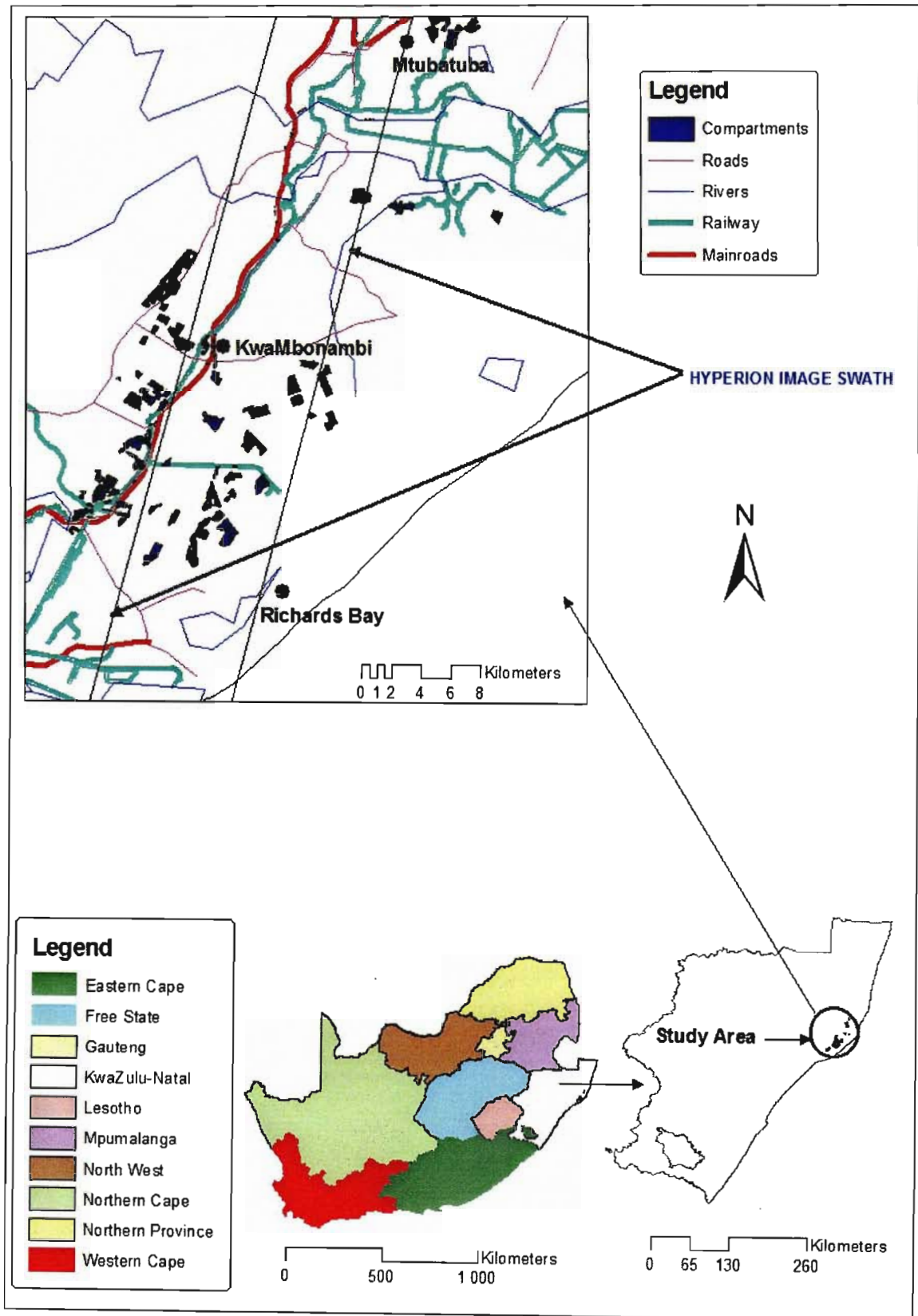


Figure 3.1 Study area, the location of the compartments and the Hyperion swath

3.3.2 Topography

It is well known that topography introduces variations in the radiance detected by the remote sensing sensor and this effect has been researched in many studies (Ekstrand, 1996). The researchers have attempted to model and reduce the influence of local terrain slope and aspect to improve land features identification (Shepherd and Dymond, 2003). Few studies have focused on the effect of topography on hyperspectral data sets, particularly in terms of its influence on the signature of spectral end members. The ability of hyperspectral sensors to detect and identify sub-pixel materials is of great importance to many applications (Feng *et al.*, 2003). Due to the complexities of hyperspectral data the study area was chosen carefully to minimize spectral interference as much as possible. The topography of the study area is flat to gently undulating, with frequent small to medium drainage lines and open water pans (Wolmarans and Du Preez, 1986). The topographic features of Zululand are multi-faceted. The flat coastal region comprises the Natal Coastal Belt and Zululand Coastal Plain with altitudes ranging between sea level to 120m metres (Feleke, 2003).

3.3.3 Climatic Factors

A number of factors influence temperature within forests. Temperature decreases with both latitude and altitude. Proximity to the coast has a moderating influence on temperature and tends to reduce the range in temperature extremes. Climate is an important factor for site quality or classification of sites in forestry. The variation in climate is measured regionally using mean annual precipitation (MAP) and mean annual temperature (MAT) (Schulze, 1997).

MAP is used to characterize the long-term water supply into the region and also defines the potential of a growing area, while taking into consideration other factors such as nutrients, available light and suitable substrate. MAT is an indication of the amount of heat units available that indicate the length of the growing season, the potential of the evapo-transpiration to take place and the rate of assimilation. The main atmospheric conditions that determine growth on regional and local scales are light associated with day length, temperature regimes and available moisture. Maximum temperature is most extreme on the KwaZulu-Natal north coast where mean maximums for the hottest month are in the region of 30°C and mean annual

temperature is 22°C. Due to diverse topography, mean annual rainfall decreases from an average 1200 - 1400mm along the coastal region to an average of 650mm inland. Similarly mean annual temperatures decrease from 22°C along the coast to 16°C 20km inland (Schulze, 1997).

3.3.4 Geology and Soils

The geological material occurring on or near the surface is important in forestry. Some soils are derived from Aeolian deposits, such as those of the coastal dune of Zululand. Others are derived from material deposited by running water (alluvial deposits along riverbanks) and ocean and lake sediments; e.g. some parts along St Lucia (Figure 3.3). South African forest soils often have their origin in more than one parent material, e.g. the topsoil may be from colluvial drift and the subsoil from granitic weathered bedrock. The coastal belt areas include sand stone, shales and mudstones, whose soils have a high agricultural potential. Low potential soils occur along the portions of the Mhlatuze River (Figure 3.2). The St Lucia formation comprises richly fossiliferous glauconitic, olive grey silts and fine sands with large calcareous concretions of marine sediments at various levels. Glauconite, also known as "green sands", is hydrated aluminosilicate of iron and potassium, usually enriched in calcium. This formation is the most important for forestry in this sub-region. It yields poorly drained soils with a clay-loam texture (Ellis, 2000).

The KwaMbonambi (Figure 3.3) area consists of mottled, brown, clayey sand related to vlei or swamp sedimentary environment. This substrate usually forms hydromorphic soils. The Uloa formation occurs closer to Richards Bay (Figure 3.2). It consists of a thin limestone, which is richly fossiliferous (Jacobs *et al.*, 1989).

3.3.5 Hydrology

The hydrological processes of this area which influence the water quality behaviors of the catchments are responsive to a large range of climatic conditions. In the past decades this area has experienced severe storms which have consequently led to sufficient storm events which were linked to trends in water quality and hydrological water paths. The degradation of water resources of Zululand in the past has caused detrimental sediment deposition. Sediment is the most obvious pollutant in the rivers of Zululand, while commercial agriculture is also adding to pollutants through

fertilizers, insecticides and herbicides (Kelbe and Germishuyse, 1999).

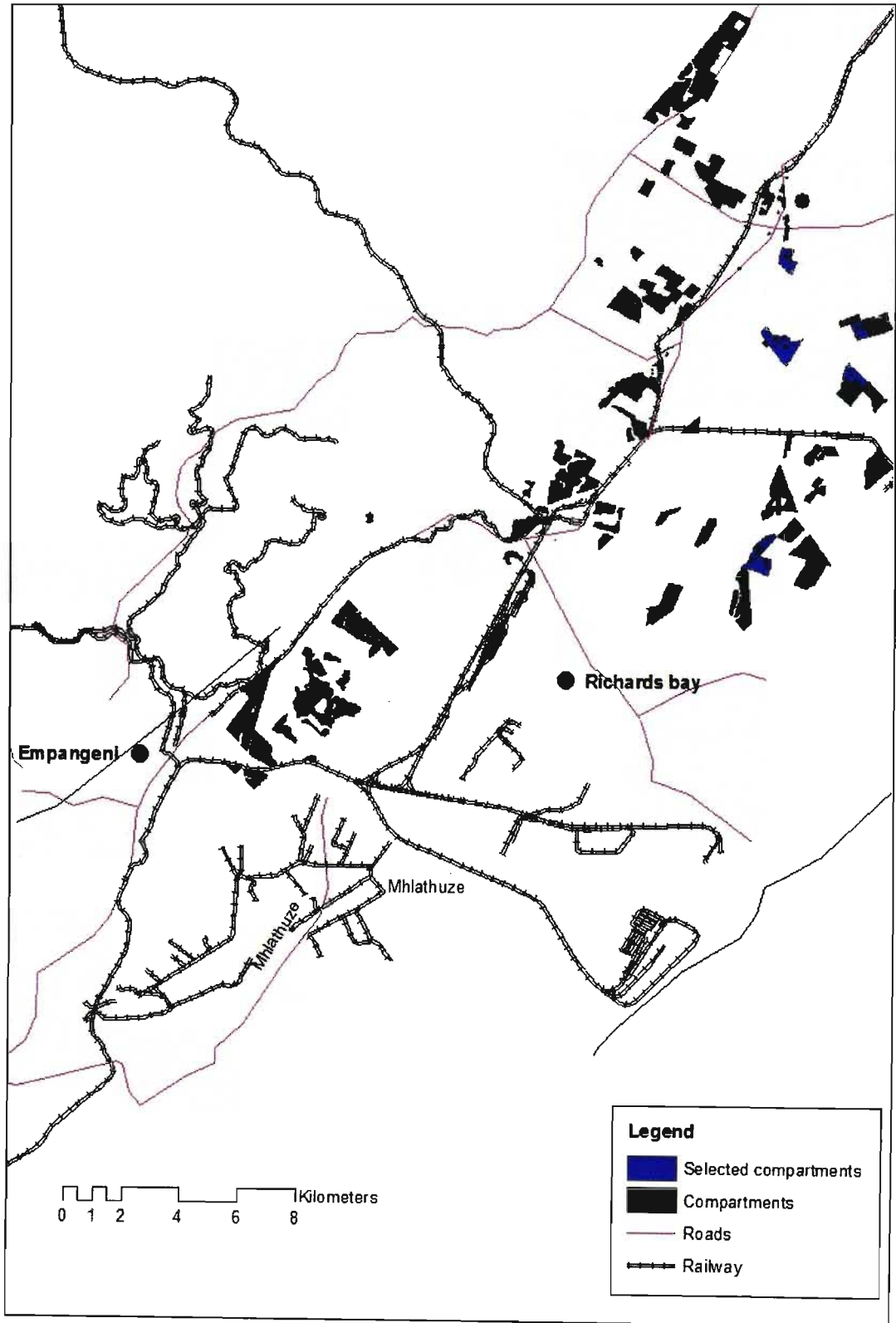


Figure 3.2 Map of Southern part of the study area showing the selected compartments, main towns and catchments

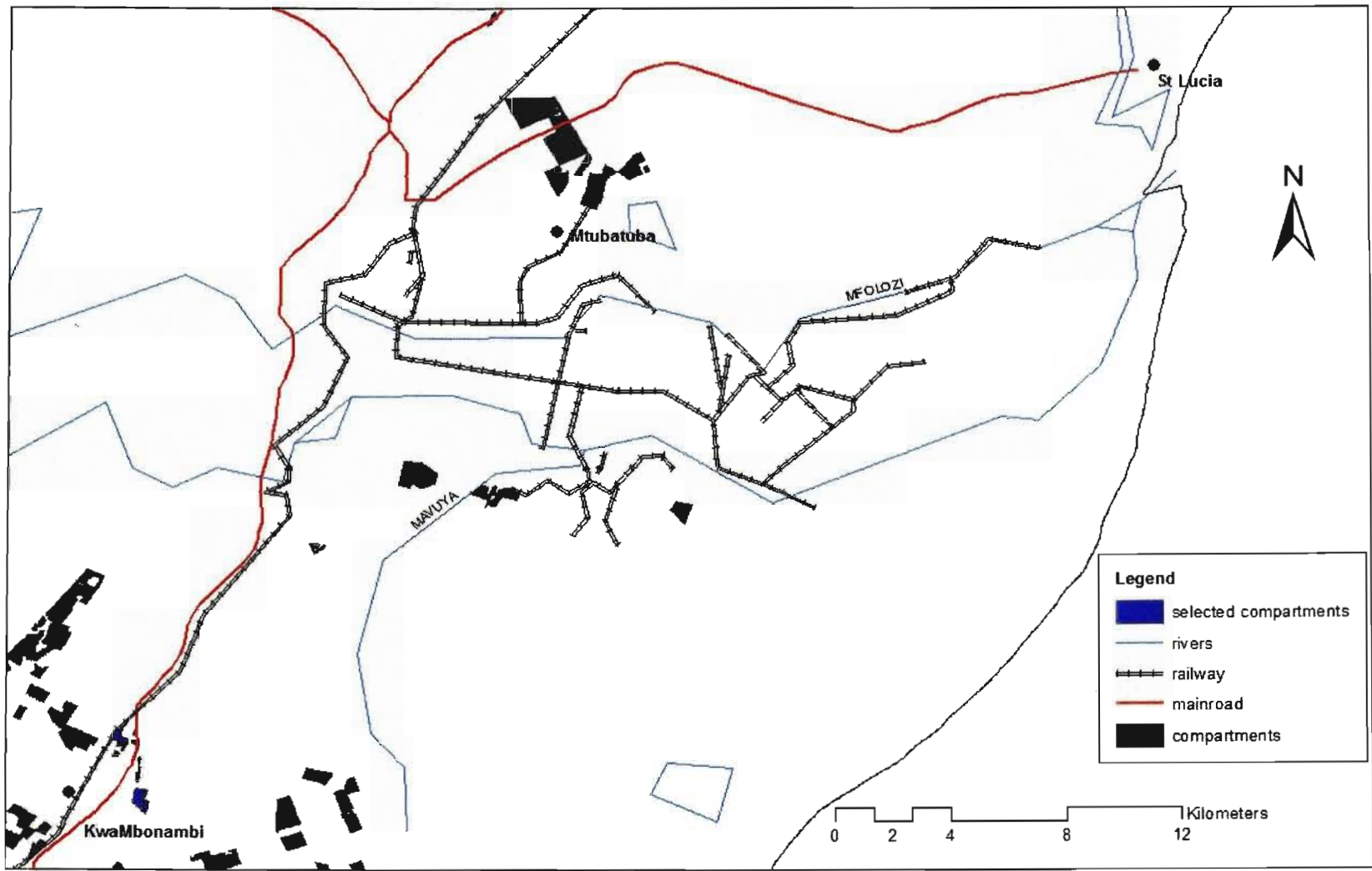


Figure 3.3 Map of Northern Zululand showing the selected compartments, main towns and catchments

CHAPTER 4: Materials and Methods

4.1 INTRODUCTION

The aim of this project is to develop an acceptable framework for estimating lignin concentrations in wood and leaf area index of Eucalyptus species and clones using hyperspectral imagery. As it has been explained in chapter one, work on correlations between wood lignin and foliar lignin in the eucalypts was not available. The use of remotely sensed data to estimate forest attributes, biochemistry or biophysical factors demands calibration of the sensors for the specific study to confirm and assess the accuracy of the obtained data. This means that destructive sampling and direct field-based measurements were carried out in this study. This chapter begins by describing the procedure that was followed when quantifying lignin concentrations. Secondly it describes the procedure followed in satellite image processing, data extraction and statistical analysis to estimate foliar lignin concentrations from hyperspectral imagery. Thirdly, it describes direct and indirect field-based methods of estimating LAI and calculation of vegetation indices from the narrow bands. Lastly, this chapter explains the statistical analyses performed between LAI measurements and vegetation indices.

4.2 ESTIMATION OF WOOD AND FOLIAR LIGNIN CONCENTRATIONS IN THE LABORATORY

4.2.1 Field Sampling

Compartments were selected to permit for a comparative analysis of ecosystem biogeochemistry as well as to provide gradients in foliar lignin; therefore different site qualities were sampled. Twelve compartments that consisted of clones were selected (Table 3.1). All selected compartments were between the ages of six and nine years to obtain estimates of the lignin concentrations in compartments that are at harvesting age. It was assumed that the ages between 6 years and 9 years could be sampled as one age group. Age was thus assumed to be a constant variable. Random sampling was used to select trees within a plot*. The areas where sampling took place overlapped with plots for stand enumeration and LAI measurements. The

* Trees were numbered and a draw was conducted in each plot.

centers of these areas were marked using a GPS (Global Positioning Systems) outside a compartment and distance measuring tapes inside compartment to enable locating these areas on the Hyperion image. Because only clonal material was used, biological variation was anticipated to be minimal; therefore, five trees were sampled per stand. For wood lignin analysis, discs were taken at breast height, 35% and 65% of the height of the tree (Figure 4.1). Leaves were sampled diagonally from the north upper canopy to the south lower canopy for foliar lignin analysis. The leaves were stored in large airtight plastic bags to be stored in the refrigerator for later preparation and use (Wessman, 1987). The weight of the leaves sampled from each tree ranged between 400 and 600 grams.

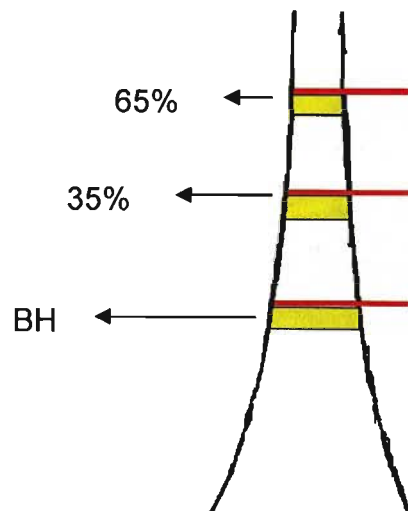


Figure 4.1 Markings on the felled tree and the diagrammatic locations of sampled discs

4.2.2 Sample Preparation

Wood samples were debarked while the leaves were stored in the refrigerator in re-sealable and airtight plastic bags.

4.2.2.1 Preparation of leaves

When sampling, leaf stalks break at different points and some are completely broken off. To reduce erroneous results in quantifying lignin concentration in leaves, leaf stalks in all leaves that were going to be chemically processed were cut off to homogenize the samples. The leaves were then oven-dried at 105 °C overnight to

remove moisture. After grinding the leaves, all the ground foliar particles that passed through a 40-mesh screen were bottled and stored for chemical analysis.

4.2.2.2 Preparation of wood strips

Discs from the DBH, 35% and 65% were cut into wedges using a band saw. One wedge from each disc was used to prepare wood strips using a circular saw and the total number of wood strips was 180. The wood strips were air dried before they were scanned into the NIRS instrument. The typical NIRS spectra can be viewed in APPENDIX 5.



Figure 4.2 The NIRS by FOSS used to scan prepared wood strips

4.2.3 Biochemical analysis

To obtain representative results for lignin concentrations from the foliar sawdust, water soluble and solvent extractives were removed from the leaves. The cold-water procedure removes a part of extraneous components such as inorganic compounds, tannins, gums, sugars and colouring matter. The hot water procedure removes starches in addition to compounds mentioned above (Figure 4.3). The solvent extraction method is for determining the amount of solvent-soluble, non-volatile substances. These substances should be removed before any quantitative chemical

analysis is performed on the sample. The hot water and solvent extractions were carried out as per the Tappi methods (1998). The Klason method, as per Tappi Methods (1998) was then performed on the extracted material. The Klason method separates lignin from sugars (Figure 4.5). The wood strips were scanned into the NIRS instrument for lignin concentration determination (Figure 4.2).

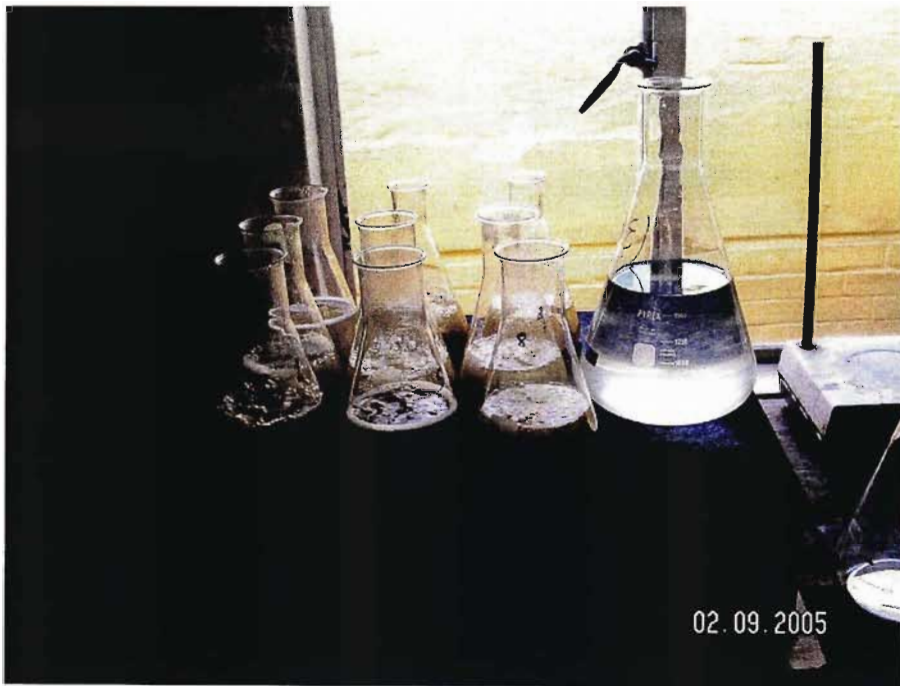


Figure 4.3 Hot water extraction procedure to remove inorganic compounds and starch

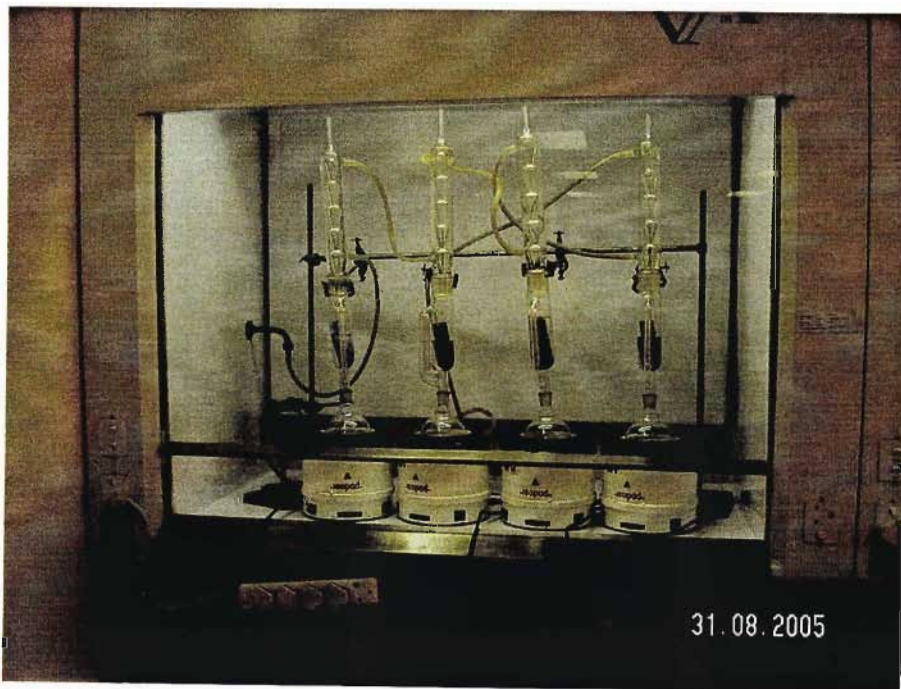


Figure 4.4 Solvent extraction procedure to remove non-volatile chemical substances



Figure 4.5 Products of Klason method; lignin and sugars

4.2.4 Stand enumeration for site index (SI) calculations

Circular plots with a 15m radius were marked using a GPS outside a compartment and distance measuring tapes within a compartment. A calibrated vertex was used to measure heights of the trees and a DBH (diameter at breast height) tape measure was used to measure the diameter of each tree at breast height. Height was only measured for 25% of the trees in a single plot. There is a logarithmic relationship between DBH and height of a tree (Schumacher and Hall, 1933); therefore, the remaining 75% of the tree heights were extrapolated from the regression analysis between the measured DBH and the measured heights. Site indices were derived by calculating the mean height of 20% of the tallest trees in each stand using a base age of five years. Site index was calculated using the Modified Schumacher-difference formulae with coefficients assigned to *Eucalyptus grandis* (Coetzee, 1994). Information used in these equations is presented in APPENDIX 6.

4.3 IMAGE PRE-PROCESSEING, ANALYSIS AND DATA EXTRACTION

4.3.1 Image Data

The image used in this study was acquired by the Hyperion satellite from the Earth Observation (EO-1) platform. The selected scene which covered the study area was of the path 168 and row 80. The image was obtained on July 24, 2004; which was

within 10 days of field sampling. This scene was selected because it covered all the compartments required for this study. The image was not cloud free but it was already radiometrically corrected (Level 1R) by the USGS (United States Geological Survey). The scene dimensions were 42km X 7.5km. This image has a spatial resolution of 30m and a spectral resolution of 10nm. All image processing was done using ENVI 4.2 (RSI-ENVI, 2004). This consisted of ortho-rectification, registration of the bands and sub-setting the image using area of interest. The Red Green and Blue color composite of the image is presented in Figure 4.6. The scene properties can be viewed in APPENDIX 7.

4.3.2 Extracting Reflectance data from Hyperion Imagery

To study surface properties using imaging spectrometer data, the atmospheric absorption and scattering effects should be removed. Several atmospheric correction algorithms for deriving information from the hyperspectral data have been developed in the past decade. Changes in spectral resolution and shifts in channel centre wavelengths may occur when an instrument is airborne or spaceborne due to changes in instrument's temperature and pressure. Therefore, accurate radiometric and spectral calibration of the data must be achieved in order to derive improved surface reflectances. Following calibration, atmospheric correction algorithms are applied to hyperspectral data and to remove the Rayleigh and aerosol scattering (Gao *et al.*, 2004).

The major atmospheric absorption bands present in the spectrum are water vapor bands centered at approximately 940, 1140, 1380 and 1880nm, the oxygen A-band at 760nm and the carbon dioxide bands near 2010 and 2060nm. Additionally a Fraunhofer feature (a set of spectral lines observed as dark features in the optical spectrum of the sun) near 430nm, which is principally associated with the H γ (Hydrogen-gamma) transition, is strong enough to be observed in this region of the spectrum (Lillesand and Kiefer, 2000).

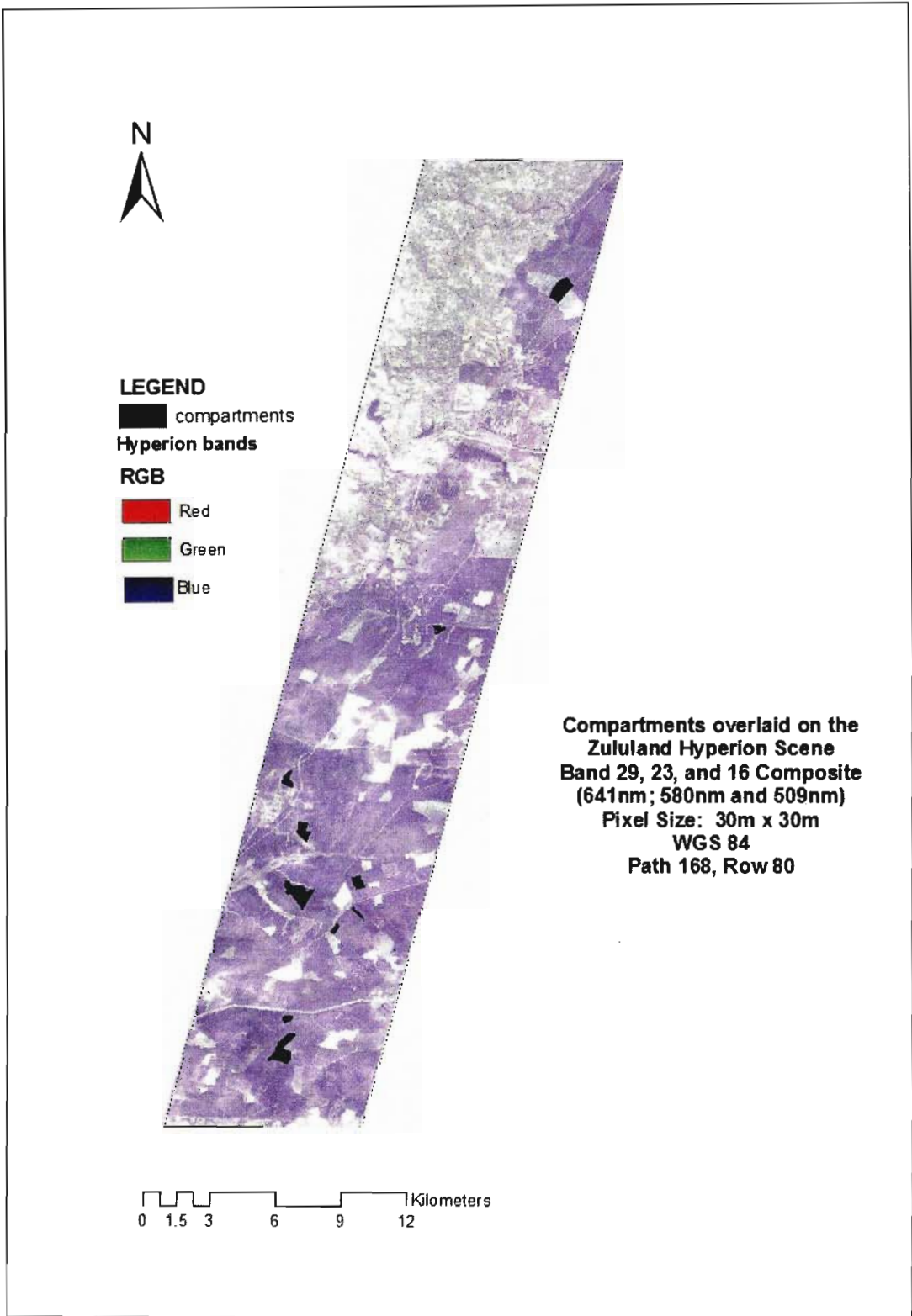


Figure 4.6 Hyperion image for Zululand, 24 July 2004

Hyperion Level 1R data were provided as calibrated radiance ($\text{Wm}^{-2}\text{sr}^{-1}$). ENVI software supports image-to-map registration through Ground Control Points (GCPs), where an image is referenced to geographic coordinates from a vector overlay. GCPs were interactively defined and validated using the error terms displayed for specific warping algorithms. The three different methods supported by ENVI are Rotation/Scaling/Translation (RST), Polynomial, and Delaunay Triangulation, and they correspond to the three re-sampling methods supported by ENVI: nearest neighbor, bilinear interpolation, and cubic convolution respectively. An RST warp, using nearest neighbor, was performed because it produces the least amount of pixel to pixel averaging and yielded the best match to the actual vector data when compared to the other warping and re-sampling methods (Hellman and Ramsey, 2003). The Hyperion image was geo-referenced using ground truthed compartment maps and ortho-photos using Rotation, Scaling and Translation (1st degree RST) warping.

The radiance data were first corrected for variation in balance among vertical columns in the along-track direction of the image data, a product of the sensor's pushbroom design that is most evident in the SWIR channels (1000-2400nm). The correction was based on the use of scaling factors of 40 for the VNIR and 80 for the SWIR (Beck, 2003). Radiance data were then transformed to surface reflectance using the ENVI 4.2 FLAASH that calculates the effect of atmospheric gases as well as molecular and aerosol scattering and removes these effects pixel-by-pixel from the image (RSI-ENVI, 2004). The FLAASH module incorporates the MODTRAN radiation transfer code. The Level 1 Radiometric (L1R) product has a total of 242 bands but there are only 198 bands that are calibrated. The reason for not calibrating all the 242 bands is mainly due to the detector's low responsivity in these channels. The bands that are not calibrated are set to zero in those channels. There is an overlap between the VNIR and SWIR focal planes; therefore, there are 196 unique bands (Beck, 2003). The bands were spectrally subsetted such that bands 8 to 57 from the VNIR and bands 77 to 224 from the SWIR were used and the bands that are not calibrated were deleted.

4.3.3 Computation of the lignin indices

Serrano *et al.* (2002) summarized lignin bands and lignin reference bands based on previous information researched by Curran (1989). There are a number of bands that correspond to lignin but some bands also respond to water absorption as shown in Table 4.1. The bands that unequivocally correspond to lignin were selected and the corresponding reference band closest to the lignin bands was used. The band at 1940nm coincides with water absorption and bands at 2262 and 2380nm had low signal to noise ratio. The selected lignin band was at wavelength 1750nm with a reference band at 1680nm. The indices were computed using ENVI 4.2. Reflectance

based indices were calculated using:
$$LI_R = \frac{\lambda_{1750} + \lambda_{1680}}{(\lambda_{1750} + \lambda_{1680})^2}$$

Bulk lignin is the total lignin concentration sensed from the surface of interest, i.e. the total lignin concentrations sensed from the canopy cover of the *Eucalyptus* plantation excluding the understorey. The bulk lignin concentrations calculations using Leaf Area Index (LAI) or Normalised Difference Vegetation Indices (NDVI) were not necessary since there was no significant variation in understorey among compartments. The understorey was therefore treated as a constant. Index images, with a range of index values per compartment, resulted. The regions of interest (ROI) were developed, using ENVI 4.2, such that they overlap with the area where field sampling took place within a compartment to eliminate error in correlations. The indices to be correlated to foliar lignin concentrations were sampled where the ROIs were developed and these indices were averaged.

Table 4.1: Absorption wavelengths for water and lignin as reported by Serrano *et al.*, 2002

Absorbing biochemical	Wavelength (nm)
Water	970, 1200, 1400, 1450, 1940
Lignin	1120, 1200, 1420, 1450, 1690, 1754, 1940, 2262, 2380

4.3.4 Statistical analysis for the estimation of lignin concentrations

Each point on the regression analysis represents a tree's average lignin concentration when regressing foliar against wood lignin concentrations that were measured in the laboratory. Each point is a mean value of two duplicates per tree. Foliar lignin concentrations were then averaged per compartment and then laboratory measured lignin concentrations were regressed against all the lignin bands individually. Linear

regression was performed on the twelve averages of the computed spectral lignin indices and the compartments averages of foliar lignin concentrations measured in the laboratory. The resulting equations were then used to convert the computed lignin indices to create images of predicted or derived foliar lignin concentrations. The foliar lignin concentrations derived from the lignin indices were then converted to wood lignin concentrations using the site-specific wood-foliar lignin regression equations that were developed using the laboratory determined wood and foliar lignin concentrations. The averages of the predicted wood lignin concentrations were calculated for each compartment, and they were compared to the laboratory-measured wood lignin concentrations using linear regression.

4.4 ESTIMATION OF LEAF AREA INDEX FROM HYPERION DATA

4.4.1 Measuring LAI in the field using A Li-Cor LAI 2000 canopy analyser

Only seven compartments were measured for LAI because of time constraints. These are compartments 3, 5, 6, 8, 9, 10 and 11 (Table 3.1). The central areas where the LAI readings were taken were marked using a differential GPS (Global Positioning Systems) and a compass outside a compartment, and distance within a compartment. A Licor instrument was used and the values measured were within 10% of the mean values with a 0.95 confidence level (LI-COR, 1990). The remote mode method was used because of the substantial height of the trees. Three sets of readings were taken for five points under the canopy in each plot. These points were chosen randomly. The multiple readings below the canopy and the fish-eye field of view ensure that LAI calculations are based on a large sample of foliage canopy. All readings were taken with the instrument pointing away from the sun. A separate synchronized instrument was located in the centre of a clearing of at least 40m in diameter, the minimum area necessary at these sites to ensure an uninterrupted view of open sky conditions. The sensor was taking readings every 15 seconds representing the above-canopy readings. During the data processing stage, below-canopy readings were compared with the above-canopy readings closest in time and averaged.

4.4.2 Correlation analysis of vegetation indices extracted from Hyperion data with field LAI measurements

While the NIR is influenced by canopy structure, the SWIR region is mainly influenced by water content (Huber *et al.*, 2005). Research conducted has shown that there is a strong correlation between water content of leaves and SWIR reflectance. SWIR region is associated with water absorption such that its reflectance alone can be utilized to estimate moisture content at landscape level (Toomey and Vierling, 2005). It has also been shown that large variations in results derived from the SWIR region are attributed to the differences in moisture content between the data collection and satellite data collection period. Broader bands are highly affected by the water content whereas narrow bands show specificity to the bands affected by water and moisture content. In MODIS data, channel 6 (1628-1652 nm) mainly corresponds to the moisture and water content (Fensholt *et al.*, 2004). In hyperspectral data, it was found that the water channels are at 970, 1200, 1400, 1450 and 1940nm. This renders most bands usable in the SWIR region when using hyperspectral data, as long as they do not coincide with the water narrowbands.

Gong *et al.* (2003) and Pu *et al.* (2005) established that combinations of bands in the NIR and SWIR regions of Hyperion produce better correlations with measured LAI compared to the combinations of bands from red and NIR regions. Therefore in the context of LAI calculations, bands from the NIR and SWIR regions were termed optimal bands. Only the optimal bands were explored in this study and therefore all the vegetation indices are modified, e.g. Normalized Difference Vegetation Index (NDVI) in this study is Modified Normalized Difference Vegetation Index (MNDVI). According to Gong *et al.* (2003), there are several bands in the NIR and SWIR regions that can be used to calculate vegetation indices. Using the table (APPENDIX 8) of possible bands that can be used to calculate vegetation indices, compiled by Gong *et al.* (2003), linear regression was performed between all the possible bands and the LAI values that were averaged per compartment. Vegetation indices were then constructed using the selected bands from the NIR and SWIR. Each vegetation index was constructed using all the possible combinations of selected bands from the NIR and the SWIR regions. Indices constructed were simple ratio (SR); modified normalized difference vegetation index (MNDVI); re-normalized difference vegetation index (RDVI); non-linear vegetation index (NLI); modified non-linear vegetation index

(MNLi); soil adjusted vegetation index (SAVI), SAVI*SR; NDVI*SR and modified simple ratio (MSR) (the descriptions and equations of the vegetation indices are in APPENDIX 3a). The soil line slope, soil line intercept and the soil minimizing adjustment factor were not calculated or measured in the field therefore, TSAVI, PVI and WdVI were not calculated. $L = 0.5$ was used in this study because it is applicable to a wide range of LAI values.

Figure 4.7 summarizes the analysis procedures that were followed from field sampling to the establishment of the lignin and LAI models. Other bands for VI calculations can be viewed in APPENDIX 9.

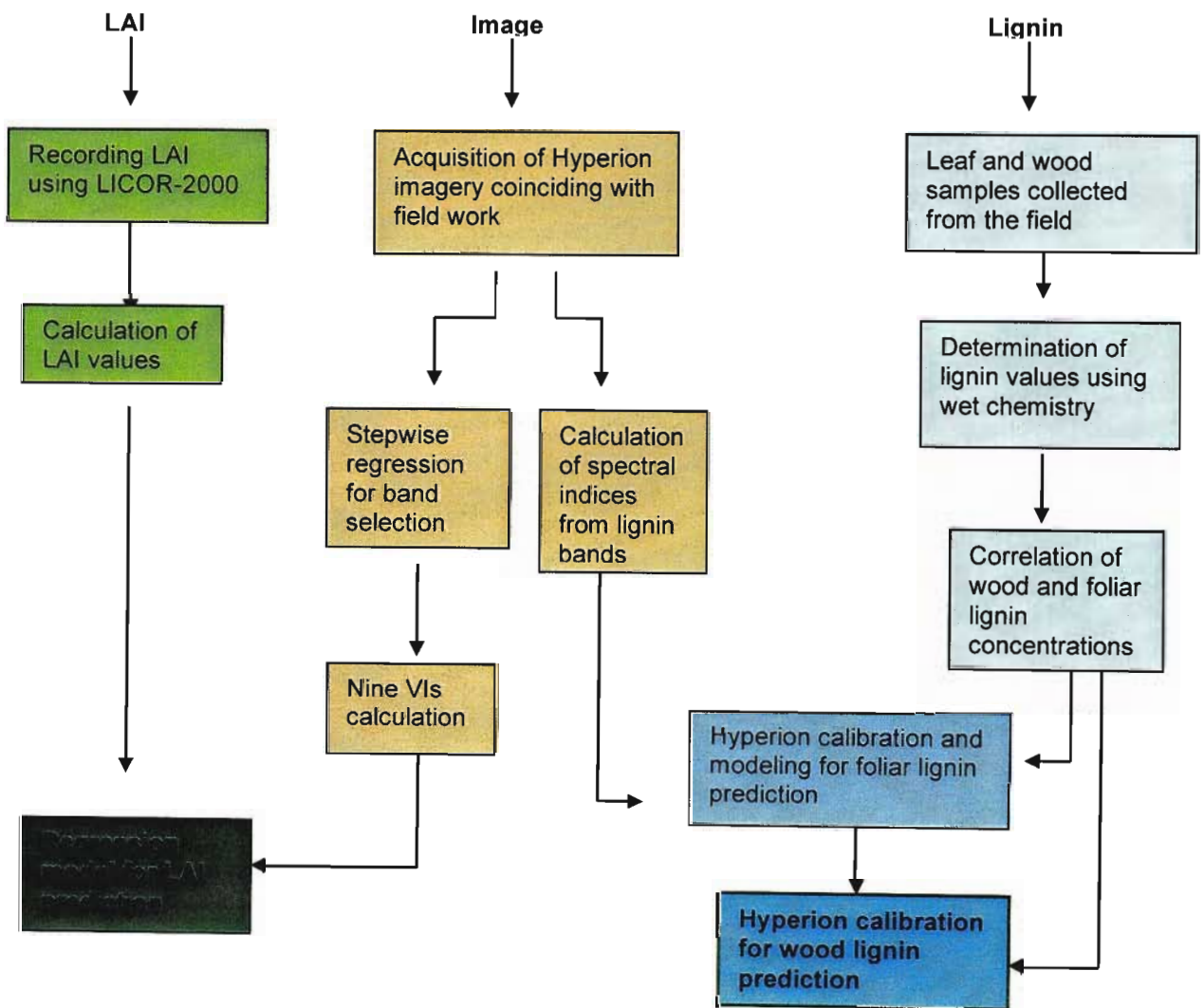


Figure 4.7 Summary of the analysis procedures and outcomes of the study

CHAPTER 5: Results and Discussion

5.1 INTRODUCTION

This chapter presents results of the work that was carried out to quantify concentrations of wood and foliar lignin in each tree, wood and foliar lignin relationships results and image analysis for the lignin indices. The chapter includes the statistical analysis results for the establishment of the lignin estimation model using regression analysis. Field measured LAI results are presented as well as the vegetation indices values calculated from the narrow bands. Results on regression analysis between the calculated vegetation indices and field measured LAI are also presented. Discussions are also included in this chapter.

5.2 WOOD LIGNIN ESTIMATION USING HYPERION DATA

5.2.1 Wood and foliar lignin concentrations determination in the laboratory

Wood and foliar lignin were analyzed for each sampled tree in a compartment. The resulting values of wood lignin concentrations were regressed against the resulting values of foliar lignin concentrations to obtain a general model for wood lignin prediction from foliar lignin concentrations as shown in Figure 5.1. Linear regression analysis indicated that there is no general relationship between foliar and wood lignin concentrations for *Eucalyptus* clones in the age group between six and nine years, although the relationship is significant with a p value of 0.044 .

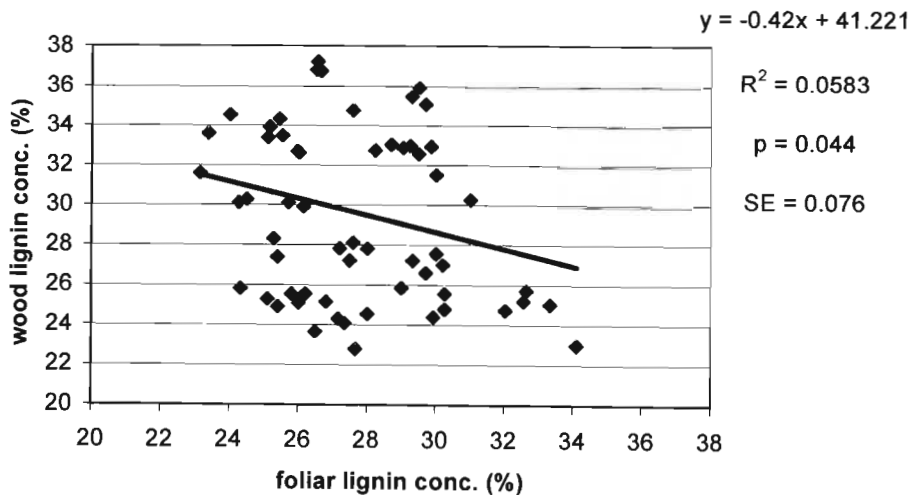


Figure 5.1 Relationship between foliar and wood lignin in all trees

The R^2 is very low at 0.068 and it was concluded that there is a meaningful trend but not useful for the purpose of the study. It was suspected that the wood-foliar lignin relationship could be site specific or compartment-specific; therefore, wood and foliar lignin concentrations were first regressed for individual compartments. The results of the regression analysis for each compartment are presented in Table 5.1. Average laboratory-measured values of wood and foliar lignin concentrations for each compartment are presented in APPENDIX 10.

Table 5.1: A summary of regression analysis between wood lignin concentrations and foliar lignin concentration per compartment

Compartment	R^2	p-value	Standard Error (SE)
1	0.861	0.023	0.104
2	0.834	0.030	0.844
3	0.799	0.041	0.612
4	0.696	0.079	0.134
5	0.824	0.033	0.956
6	0.787	0.045	0.188
7	0.790	0.044	0.134
8	0.777	0.048	0.240
9	0.803	0.040	0.203
10	0.853	0.025	0.130
11	0.871	0.020	0.422
12	0.519	0.170	0.308

The regression analysis for each compartment produced results that indicated that wood and foliar lignin relationship could be compartment-specific. The results showed significant relationships between wood lignin and foliar lignin concentrations in ten compartments. Compartment 4 and 12 did not show significant relationships between wood and foliar lignin concentrations. The R^2 for each of the ten compartments was very high and ranged between 0.777 and 0.871. The compartment-specific relationships led an investigation into a correlation matrix between wood lignin concentrations, foliar lignin concentrations, age and SI. The results of the correlation matrix are presented in Table 5.2.

Table 5.2: A summary of the correlation matrix for foliar, wood lignin, site index and Age (Size = 60)

	Foliar lignin	Wood lignin	Age	Site index
Wood lignin	-0.260*			
Age	-0.287*	0.519**		
SI	-0.282*	-0.089	-0.111	
Clone type	0.424*	0.194	0.491*	-0.529*

* Relationship is significant at the 0.05 level (2-tailed).

** Relationship is significant at the 0.01 level (2-tailed).

The results presented in Table 5.2 showed that age has a significant influence on wood and foliar lignin concentrations. Site index also significantly influences wood lignin concentrations. These findings led to attempts to find more meaningful relationships between wood and foliar lignin, therefore, compartments were grouped according to age and site index.

A. Grouping according to similar age

Grouping of compartments of same or similar ages was also explored, such as compartments 1, 2, 3 and 4; compartments 7 and 8; and compartments 6, 9, 10 and 12 (Table 5.3). The results of groupings, according to age, that showed significant relationships are presented in Figure 5.2 (A-F).

Table 5.3: the compartments grouped according to similar ages

Compartment	<i>Eucalyptus</i> Clone	Age at sampling	Spacing	Plot Radius (m)	Field Measured SI
1	<i>E. Urophylla</i>	7.25	3.0 x 3.0	15	21.29
2	GU-1	7.25	3.0 x 3.0	15	22.41
3*	GU-2	6.92	3.0 x 2.7	15	25.90
4	GC-1	7.42	2.7 x 2.4	15	23.81
5*	<i>E. Urophylla</i>	7.25	2.7 x 2.7	15	24.13
6*	GU-1	8.33	3.0 x 2.0	15	23.07
7	GU-1	6.33	2.7 x 2.2	15	22.89
8*	GU-3	6.33	2.7 x 2.2	15	23.80
9*	GC-2	8.08	3.0 x 2.0	15	21.96
10*	GU-4	8.00	3.0 x 2.0	15	17.61
11*	GT	8.75	3.0 x 2.5	15	27.34
12	<i>E.gra</i>	8.00	2.7 x 2.4	15	18.05

Similar age and similar clone (rows 1-5)

Same age and similar clone (rows 7-8)

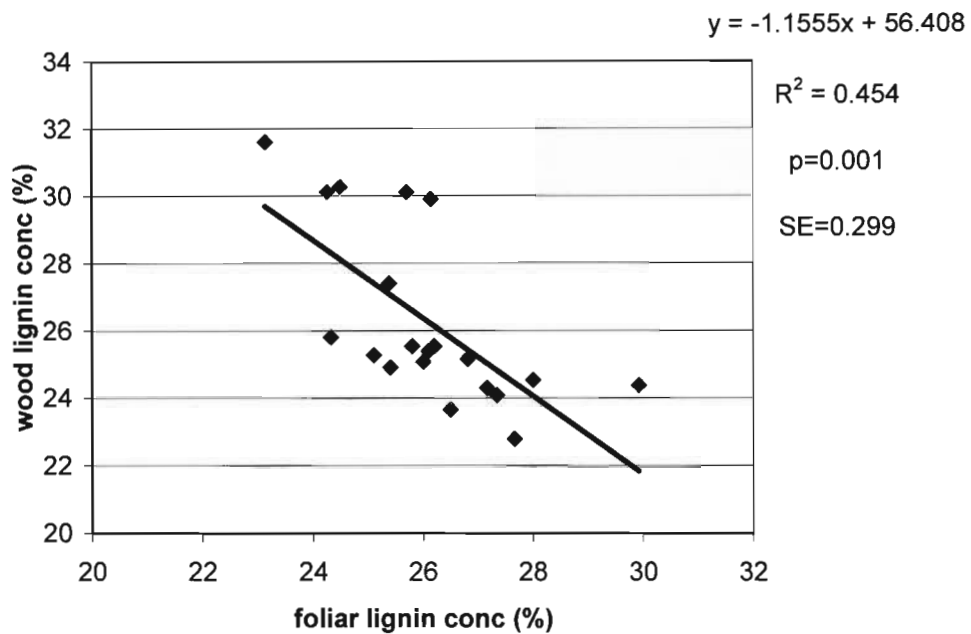
Very similar age (rows 9-12)

More similar age; close to 8 years (rows 6, 9-12)

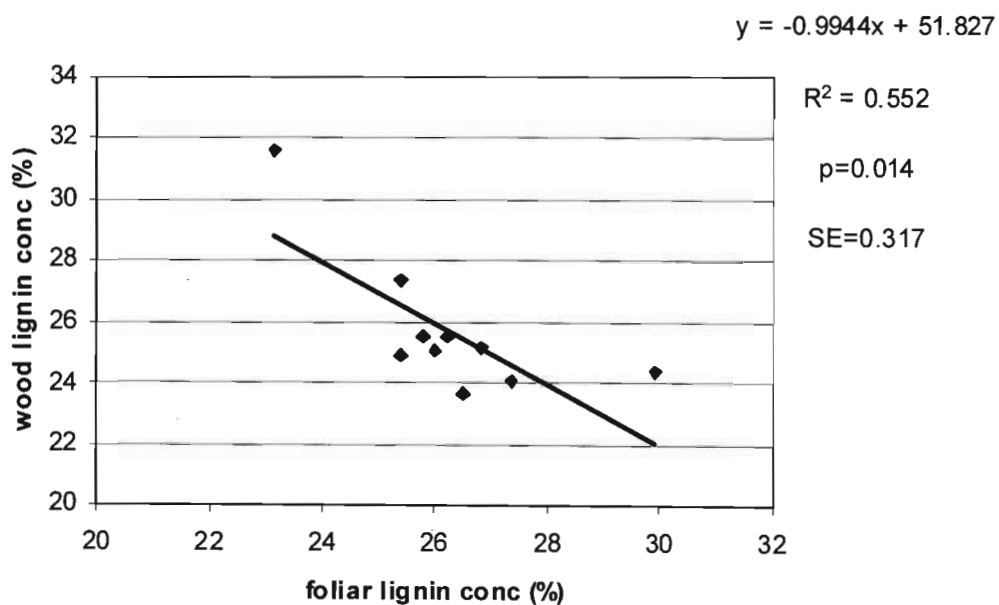
Legend (Main Group coding)

- Heading row
- Compartment 1, 2, 3, 4 and 5
- Omitted compartment from a group
- Compartment 6, 9, 10, 11 and 12
- Compartment 7 and 8

Table 5.3 shows compartments that were grouped according to similar ages. Three main groups resulted from the 12 compartments when they were grouped according to similar age. Within each group there were more suitable sub-groups that showed more significant results with respect to the relationship between wood and foliar lignin concentrations. These sub-groups were more suitable because the compartments that fell within these sub-groups were either of similar clones or of more similar or same age.

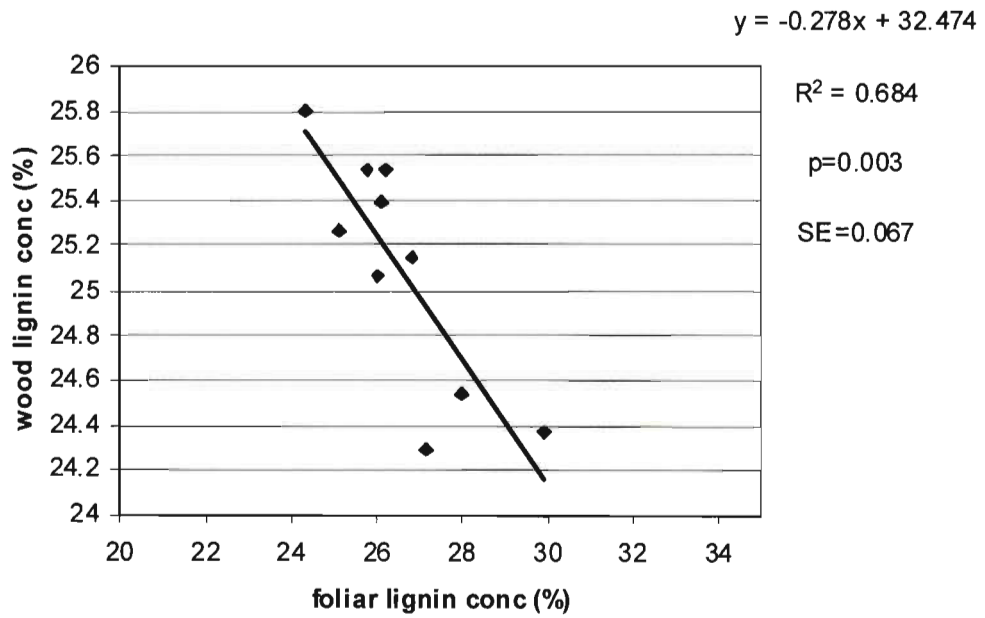


A: Compartments 1, 2, 3 and 4 (main group)

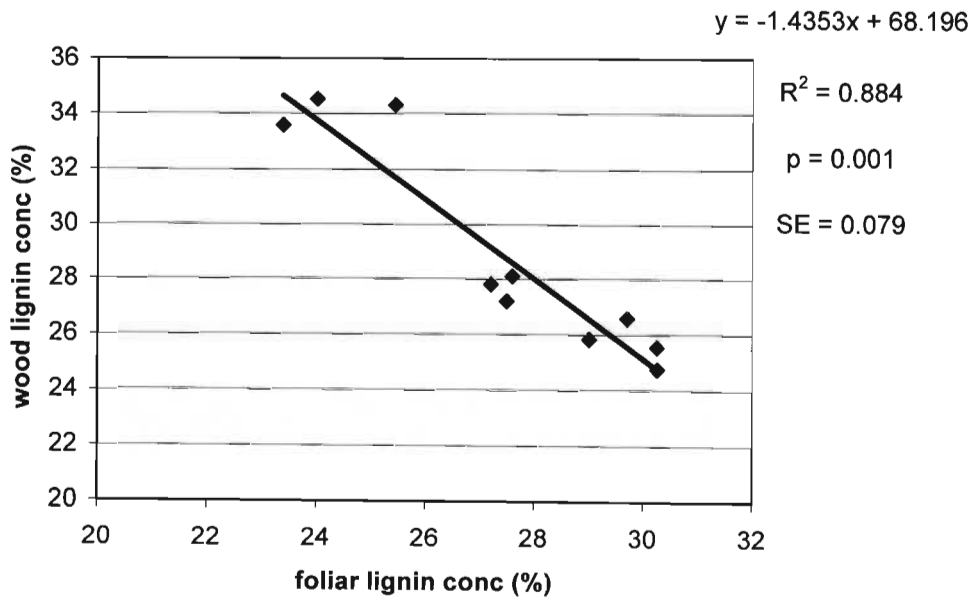


B: Compartments 1 and 2 (sub-group)

Figure 5.2 Graphs (A-B) demonstrating the resulting age groupings that showed significant relationships between wood and foliar lignin concentrations

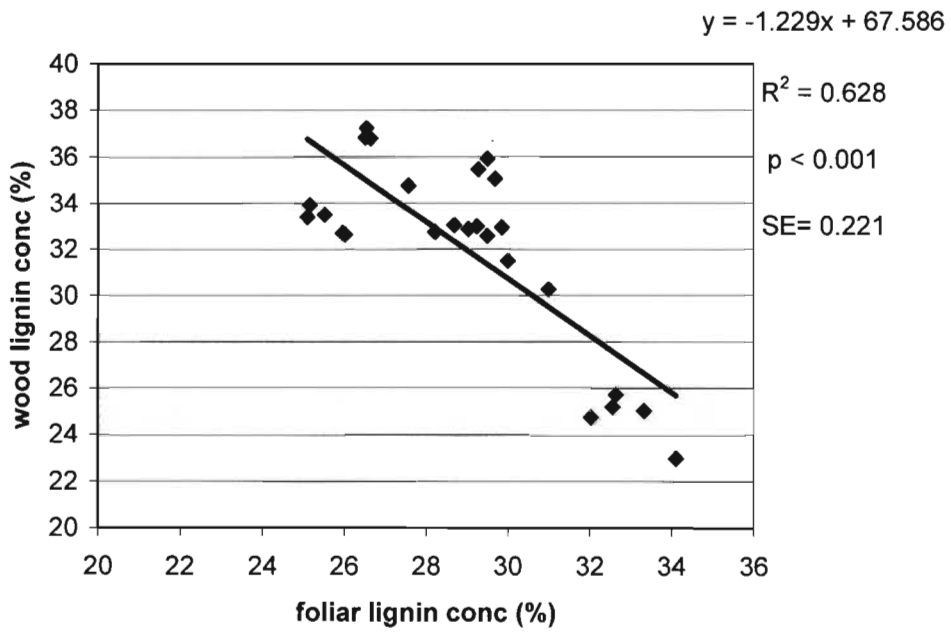


C: Compartments 2 and 3 (sub-group)

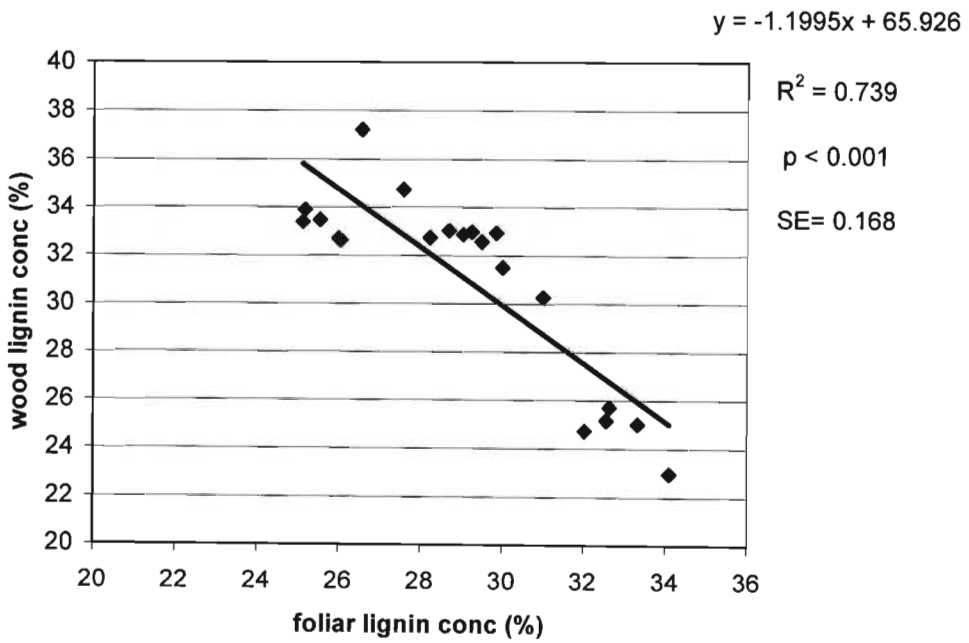


D: Compartments 7 and 8 (main group)

Figure 5.2 Graphs (C-D) demonstrating the resulting age groupings that showed significant relationships between wood and foliar lignin concentrations

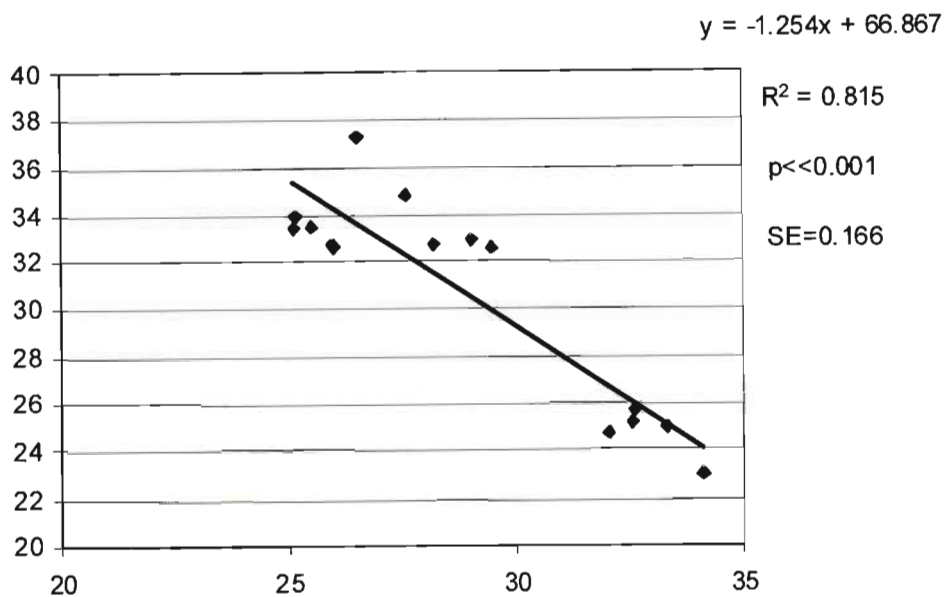


E: Compartments 6, 9, 10, 11 and 12



F: Compartments 6, 9, 10 and 12

Figure 5.2 Graphs (E-F) demonstrating the resulting age groupings that showed significant relationships between wood and foliar lignin concentrations



G: Compartments 9, 10 and 12

Figure 5.2 Graphs (G) demonstrating the resulting age groupings that showed significant relationships between wood and foliar lignin concentrations

Compartment 1, 2, 3, 4 and 5 were grouped together, however when compartment 5 was included there was no significant relationship between wood and foliar lignin. Even though compartment 5 had the same age as compartment 1 and 2, the site index was slightly higher than the SI of compartment 1, 2, and 4; it was lower than SI of compartment 3. Compartment 1 and 5 are of the same *Eucalyptus* species, but there was no significant relationship between wood and foliar lignin when these two compartments were grouped together. When an *E. Urophylla* and a GU of the same age were grouped together the R^2 was 0.552 and the relationship between wood and foliar lignin was significant (Figure 5.2B). When two GU compartments (compartments 2 and 3) of similar ages (7.25 and 6.92 years respectively) were grouped, R^2 was high at 0.684, and the p-value was low, indicating a significant relationship (Figure 5.2C). Compartment 7 and 8 are of exact age and the relationship between wood and foliar lignin when these compartments were grouped and the R^2 was high at 0.884 (Figure 5.2D). The p-value was also low indicating a significant relationship. This significant relationship with a high R^2 can be attributed to the fact that compartments 7 and 8 are of a similar clone as well as exact age. Compartment 6, 9, 10, 11 and 12 were grouped together because they were of similar ages at 8.33, 8.08, 8.00, 8.75 and 8.00 respectively (Figure 5.2 E). The

relationship between wood and foliar lignin concentration when these five compartments were grouped was significant with a p-value lower than 0.001 and an R^2 of 0.628. When compartment 11 was omitted because it was closer to 9 years of age when the other four compartments were closer to 8 years of age, the relationship between wood and foliar lignin improved and the R^2 was 0.739 (Figure 5.2 F). It must be noted that this group consisted of very different clones; two GU, one GC, one GT and one *E. grandis*. The high R^2 and low p-value indicate that age in this case is a major influence of the relationship between wood and foliar lignin and not necessarily the clone type. When compartment 9, 10 and 12 were grouped together because their age group is very similar, the R^2 improved at 0.815 with a p value of 4.03^{-06} (figure 5.2 G)

B. Compartments grouped according to similar SI

Compartments with similar site indices were grouped together to investigate significant relationships between wood and foliar lignin concentrations (Table 5.4). The results of the grouping according to site index that showed significant relationships are presented below in Figure 5.3 (A-D).

When grouping the compartments according to similar site indices, only one sub-group resulted. Compartment 4 and 8 had more similar site indices and they formed a sub-group.

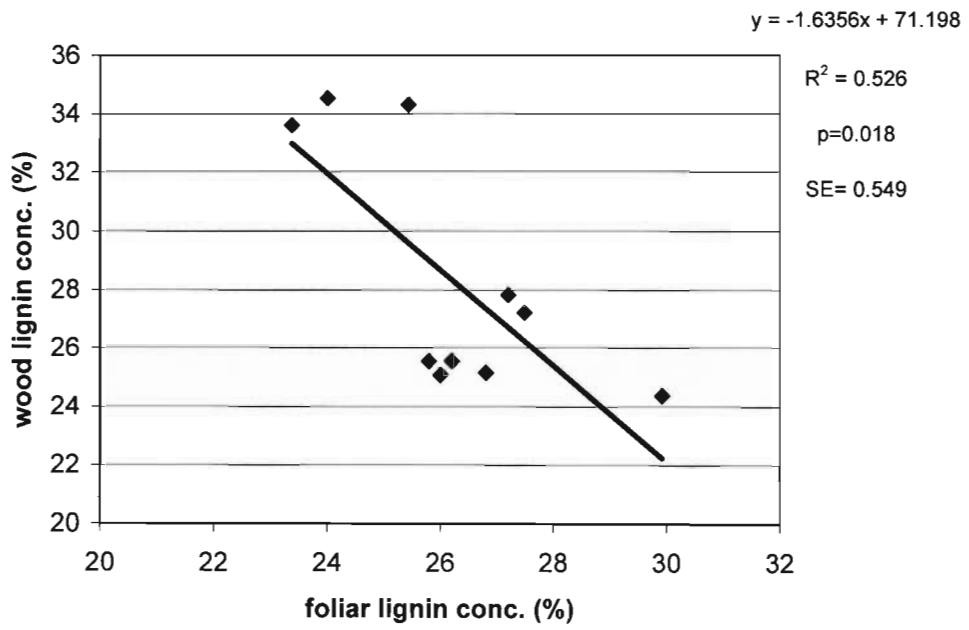
Table 5.4: compartments grouped according to similar site indices

Compartment	<i>Eucalyptus</i> Clone	Age at sampling	Spacing	Plot Radius (m)	Field Measured SI
1	<i>E. Urophylla</i>	7.25	3.0 x 3.0	15	21.29
2	GU-1	7.25	3.0 x 3.0	15	22.41
3*	GU-2	6.92	3.0 x 2.7	15	25.90
4	GC-1	7.42	2.7 x 2.4	15	23.81
5*	<i>E. Urophylla</i>	7.25	2.7 x 2.7	15	24.13
6*	GU-1	8.33	3.0 x 2.0	15	23.07
7	GU-1	6.33	2.7 x 2.2	15	22.89
8*	GU-3	6.33	2.7 x 2.2	15	23.80
9*	GC-2	8.08	3.0 x 2.0	15	21.96
10*	GU-4	8.00	3.0 x 2.0	15	17.61
11*	GT	8.75	3.0 x 2.5	15	27.34
12	<i>E.gra</i>	8.00	2.7 x 2.4	15	18.05

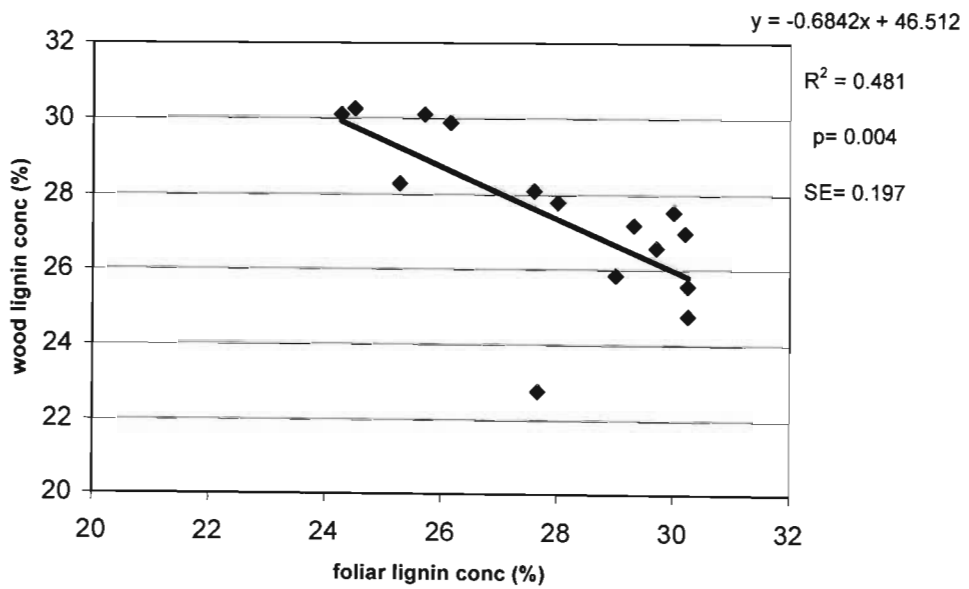
More similar SI

Legend (Main group coding)

- Heading row and compartments that could not be grouped with other compartments
- Compartments 2 and 7
- Compartments 4, 5 and 8
- Compartments 10 and 12
- Compartment 1 and 9

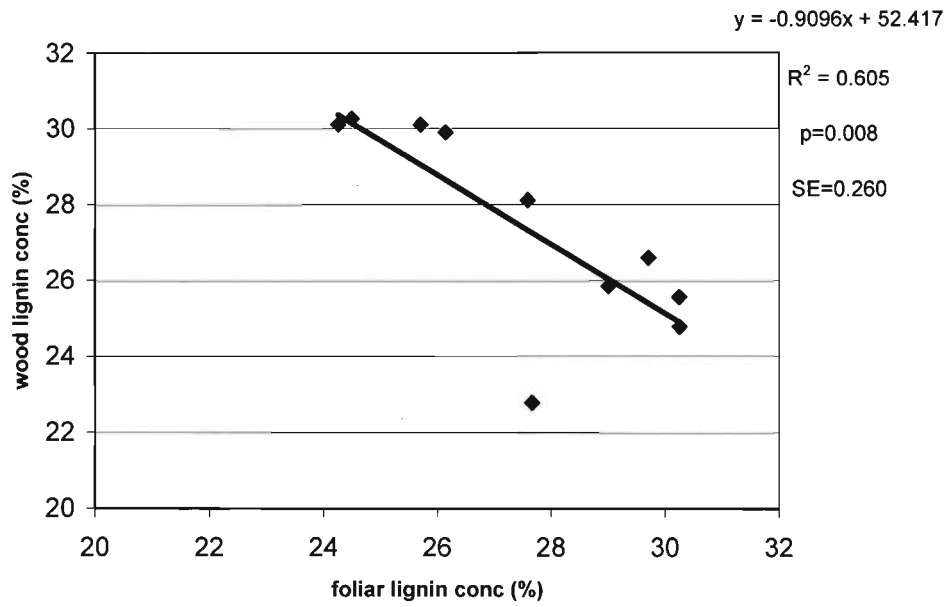


A: Compartments 2 and 7 (main group)

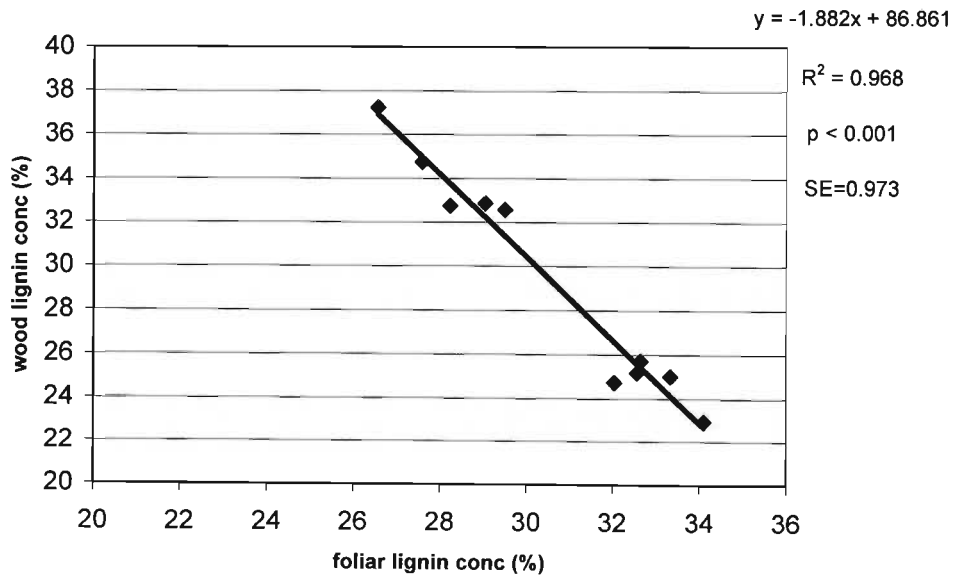


B: Compartments 4, 5 and 8 (main group)

Figure 5.3 Graphs (A-B) demonstrating the resulting SI groupings that showed significant relationships between wood and foliar lignin concentrations



C: Compartments 4 and 8 (sub-group)



D: Compartments 10 and 12 (main group)

Figure 5.3 Graphs (C-D) demonstrating the resulting SI groupings that showed significant relationships between wood and foliar lignin concentrations

Compartment 1 and 9 had similar SI at 21.29 and 21.96 respectively, but compartment 1 was closer to 7 years of age at 7.25 years and compartment nine was closer to 8 years of age at 8.08 years. This grouping did not produce a significant relationship between wood and foliar lignin concentrations. Compartments 2, 6 and 7 were grouped and there was no significant relationship between wood and foliar lignin that resulted. However, when compartment 6 was omitted in this group because this compartment was over 8 years old and the site index was slightly higher than the other two compartments, there was a significant relationship between wood and foliar lignin concentrations (Figure 5.3 A). The R^2 was just above 0.5. Compartments 4, 5 and 8 were grouped together; there was a significant relationship between wood and foliar lignin concentrations with an R^2 of 0.48. However, compartments 4 and 8 had the exact SI, and when the two compartments were grouped, the relationship between wood and foliar lignin concentrations improved to an R^2 of 0.61 (Figure 5.3 C). Compartments 10 and 12 were grouped and the relationship between wood and foliar lignin was significant with an R^2 of 0.97 (Figure 5.3D). The high R^2 can be attributed to the fact that these two compartments have exactly the same age (8.0 years). Compartments 10 and 12 are a GU and *E. grandis* respectively. Both the age and SI groupings proved that age and SI influence the relationship between wood and foliar lignin concentrations.

This project aims at predicting wood lignin using canopy spectral reflectance. To achieve this aim, wood and foliar lignin concentrations had to be determined since the satellite sensor can only sense information at the canopy level.

5.2.2. Relationship between foliar lignin concentrations from the laboratory and lignin indices

After the atmospheric correction, spectral bands are supposed to be clear of any atmospheric influence; however, that is not usually easily achievable. Some researchers use atmospheric correction together with ground spectroradiometer measurements to modify and produce improved reflectance images (Pu *et al.*, 2005).

Most lignin bands were either affected by the water absorption or the spectral noise in the region of longer wavelengths (Lillesand and Kiefer, 2000). Each band was regressed against the averages of lignin indices extracted from the ROIs.

Reflectances from each lignin band were regressed against the laboratory-measured lignin concentrations (Table 5.5.)

Table 5.5: A summary of linear regression analysis between all possible bands for the calculation of spectral lignin indices and laboratory measured foliar lignin concentrations

Spectral region	Band λ (nm)	R ²	p-value	Standard error (SE)
NIR	1120	0.059	0.4454	386.469
	1200	0.073	0.3964	365.952
Ref. band	1680	0.761	0.0002	91.462
SWIR	1690	0.771	0.0002	88.359
	1750	0.719	0.0005	102.800
	2100	0.518	0.0083	156.782
	2262	0.515	0.0086	127.126

The reflectance values from the band situated at 1690nm have the highest correlation with the foliar lignin concentrations; however, this band is also situated close to the reference band situated at 1680nm (Table 5.5). This means that the data from the reference band and data from the band at 1690nm are highly correlated. Therefore the band at 1750nm was selected over the band at 1690nm. The bands that were used to construct the lignin indices were, thus, bands at 1750nm and the reference band at 1680nm. The equation was used to construct the lignin index image using the two selected bands. The mean values of the indices were extracted from the ROIs within each compartment. These mean values were regressed against the laboratory-measured foliar lignin concentrations for each compartment (figure 5.4)

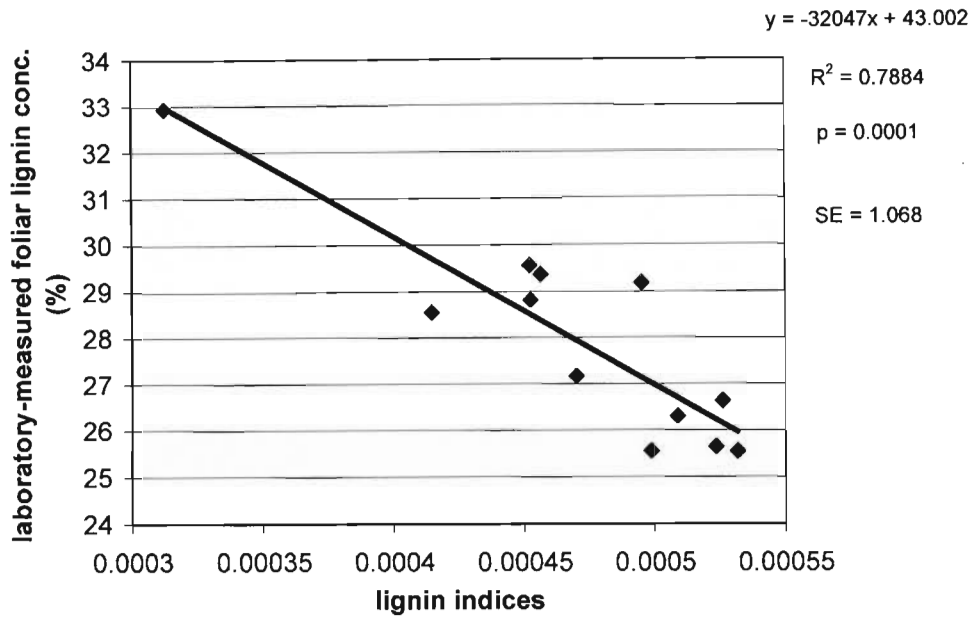


Figure 5.4 Relationship between laboratory-measured foliar lignin concentrations and the reflectance-based non-linear lignin indices (1690nm and 1680nm_{ref})

Figure 5.4 shows a significant relationship between lignin indices and laboratory-measured foliar lignin concentrations. The equation was used to convert the lignin index image to the foliar lignin concentration image. Figure 5.5 demonstrates foliar lignin concentrations across the whole image and Figure 5.6 demonstrate the distribution of foliar lignin and wood lignin concentrations across each compartment. The distribution of foliar lignin concentration varies within each compartment. The advantage of remote sensing is that variation across a compartment can be mapped. In this study the laboratory measured averages of a compartment correspond to ROI averages and therefore the distribution of foliar lignin wood lignin concentrations in the images below is extrapolated across the rest of the compartment and image.

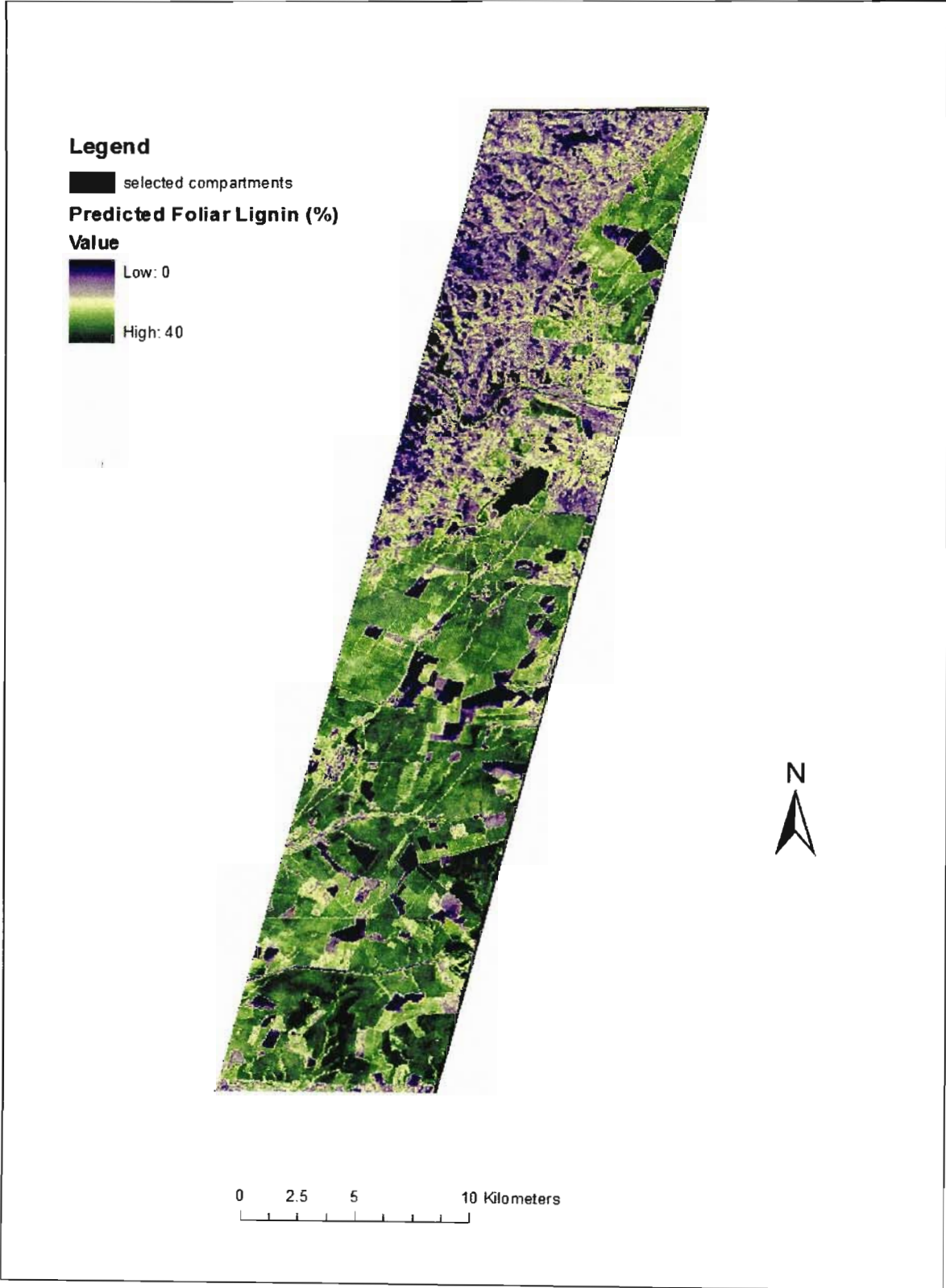


Figure 5.5 An illustration of foliar lignin concentrations calculated from the lignin indices across the image

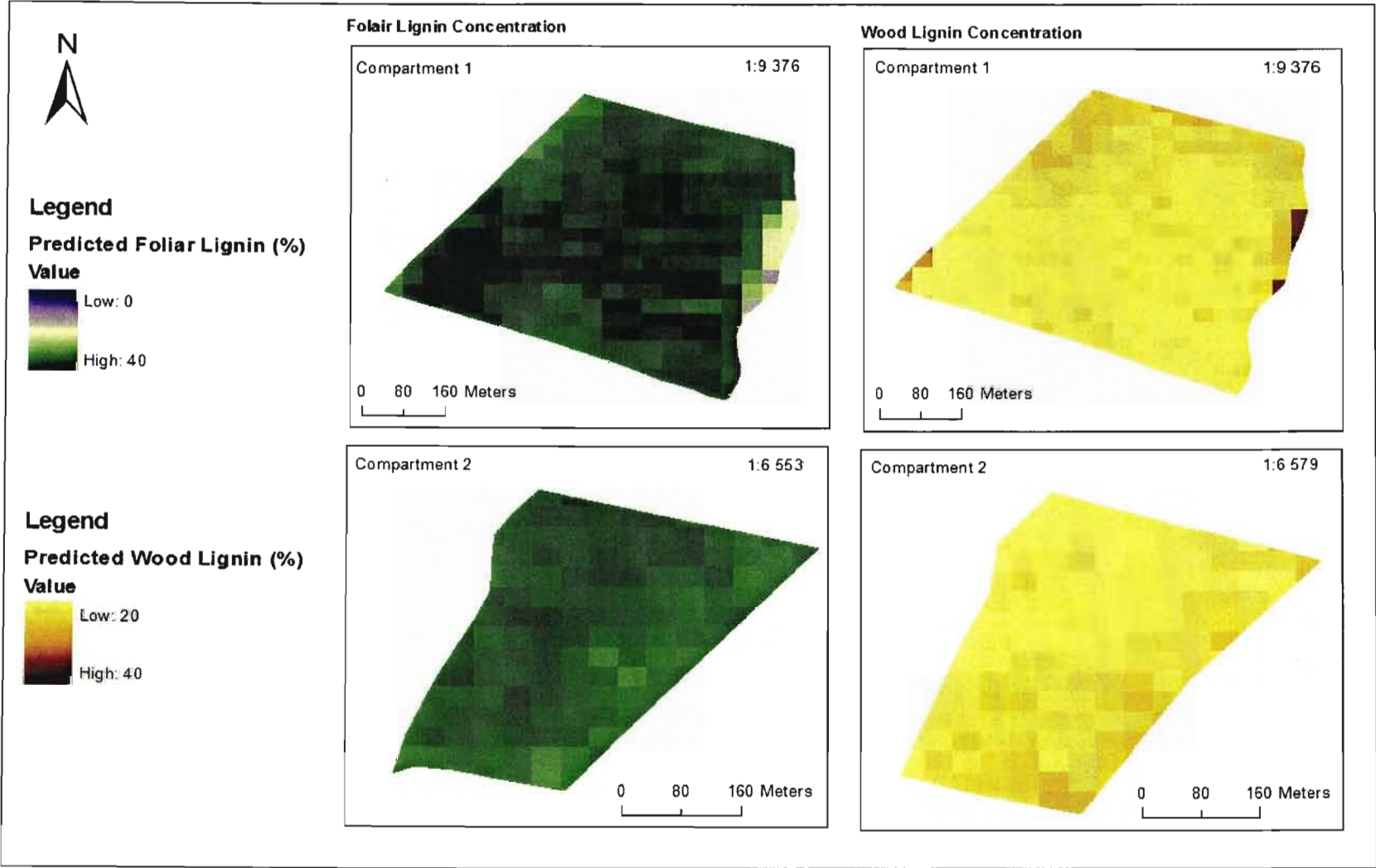


Figure 5.6 An illustration of foliar lignin and wood lignin concentrations calculated from the lignin indices across each compartment (1 and 2)

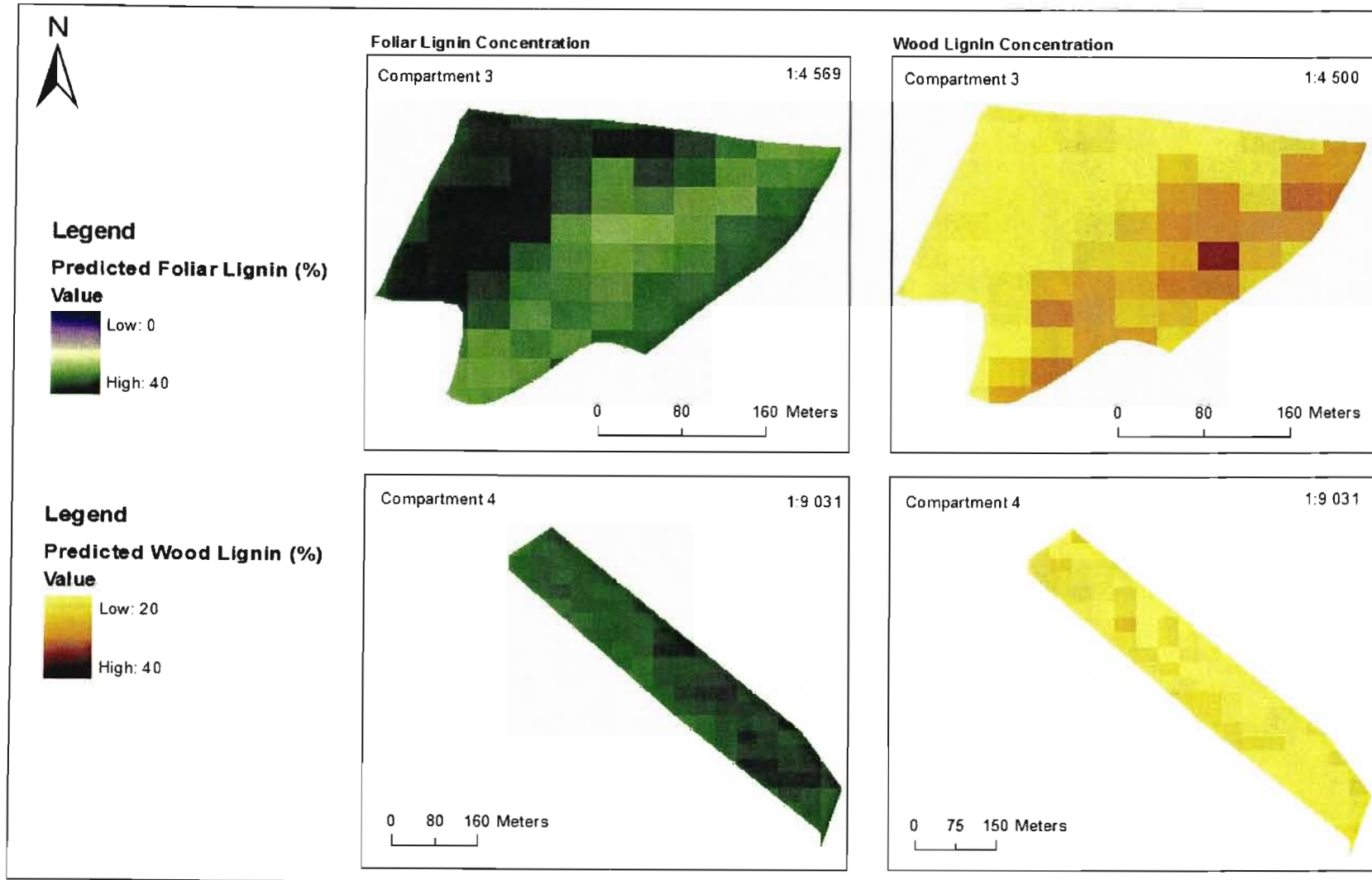


Figure 5.6 An illustration of foliar lignin and wood lignin concentrations calculated from the lignin indices across each compartment (3 and 4)

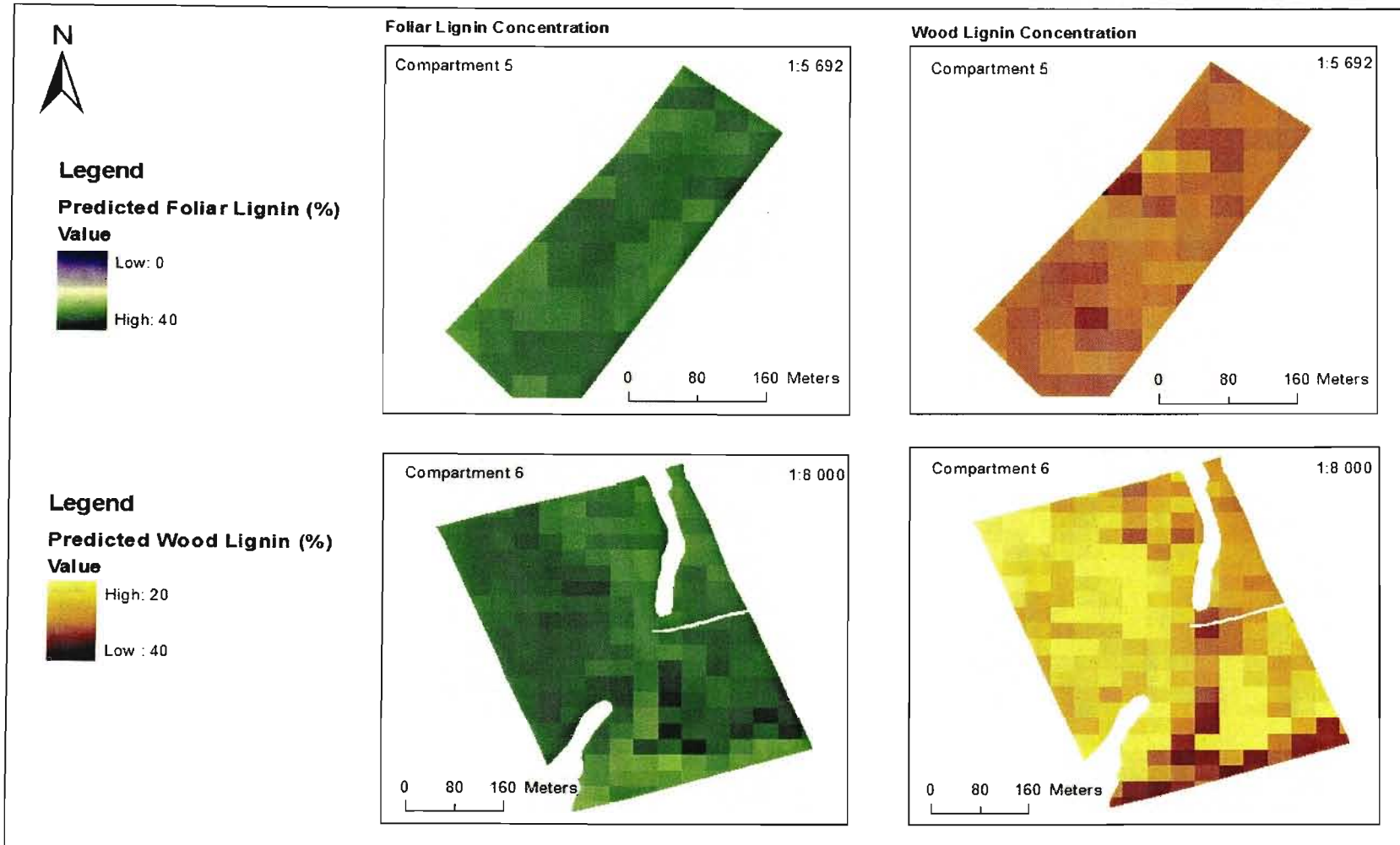


Figure 5.6 An illustration of foliar lignin and wood lignin concentrations calculated from the lignin indices across each compartment (5 and 6)

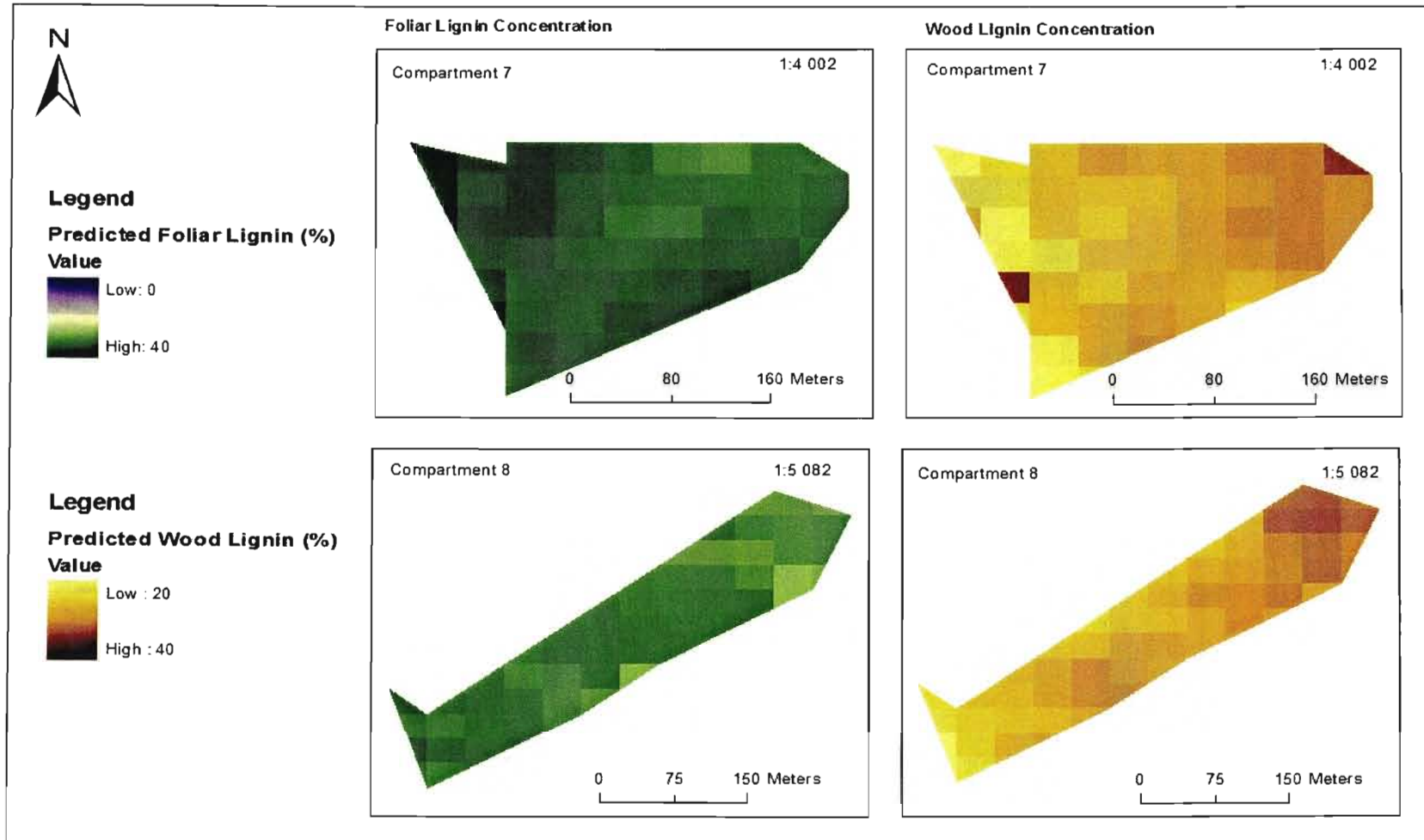


Figure 5.6 An illustration of foliar lignin and wood lignin concentrations calculated from the lignin indices across each compartment (7 and 8)

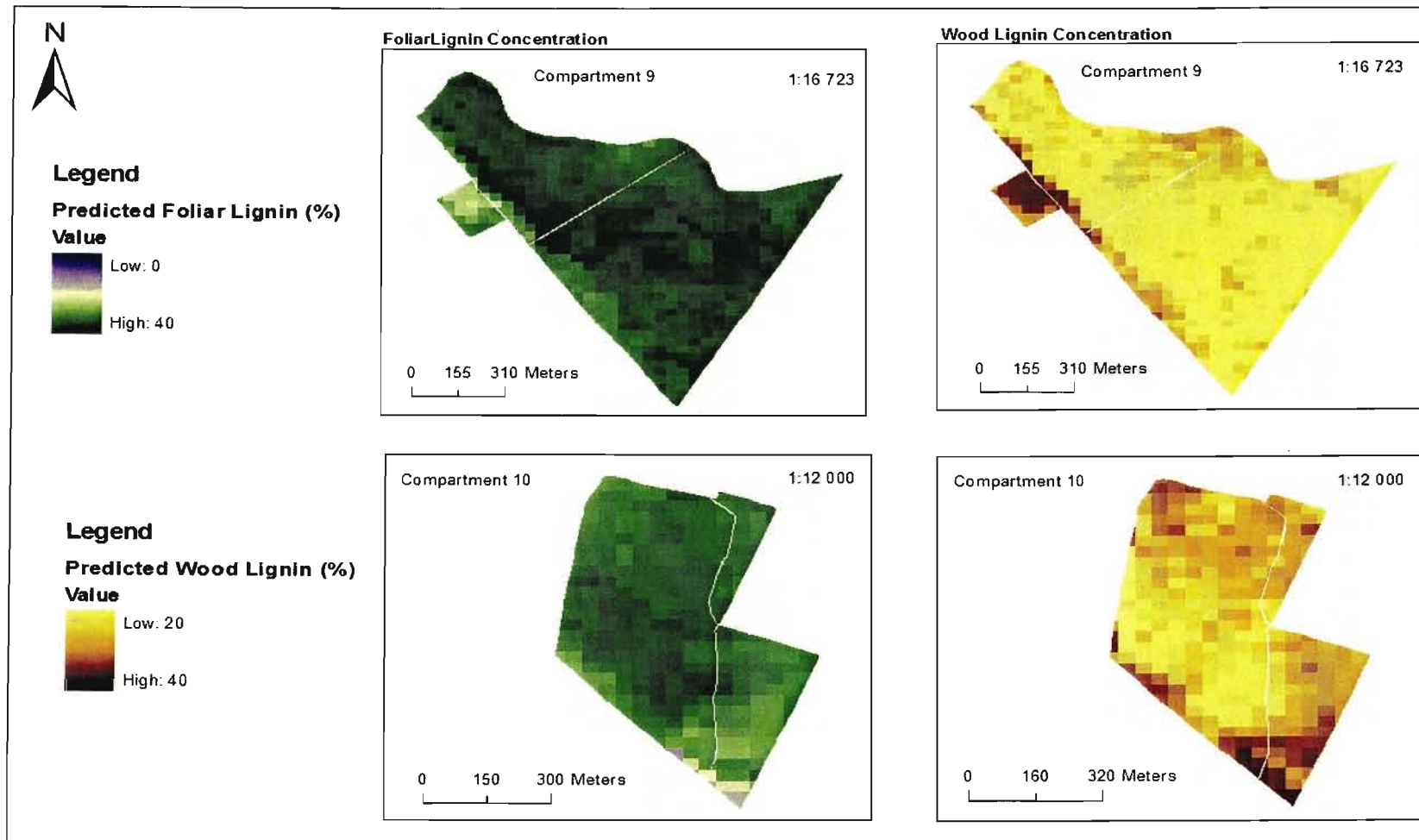


Figure 5.6 An illustration of foliar lignin and wood lignin concentrations calculated from the lignin indices across each compartment (9 and 10)

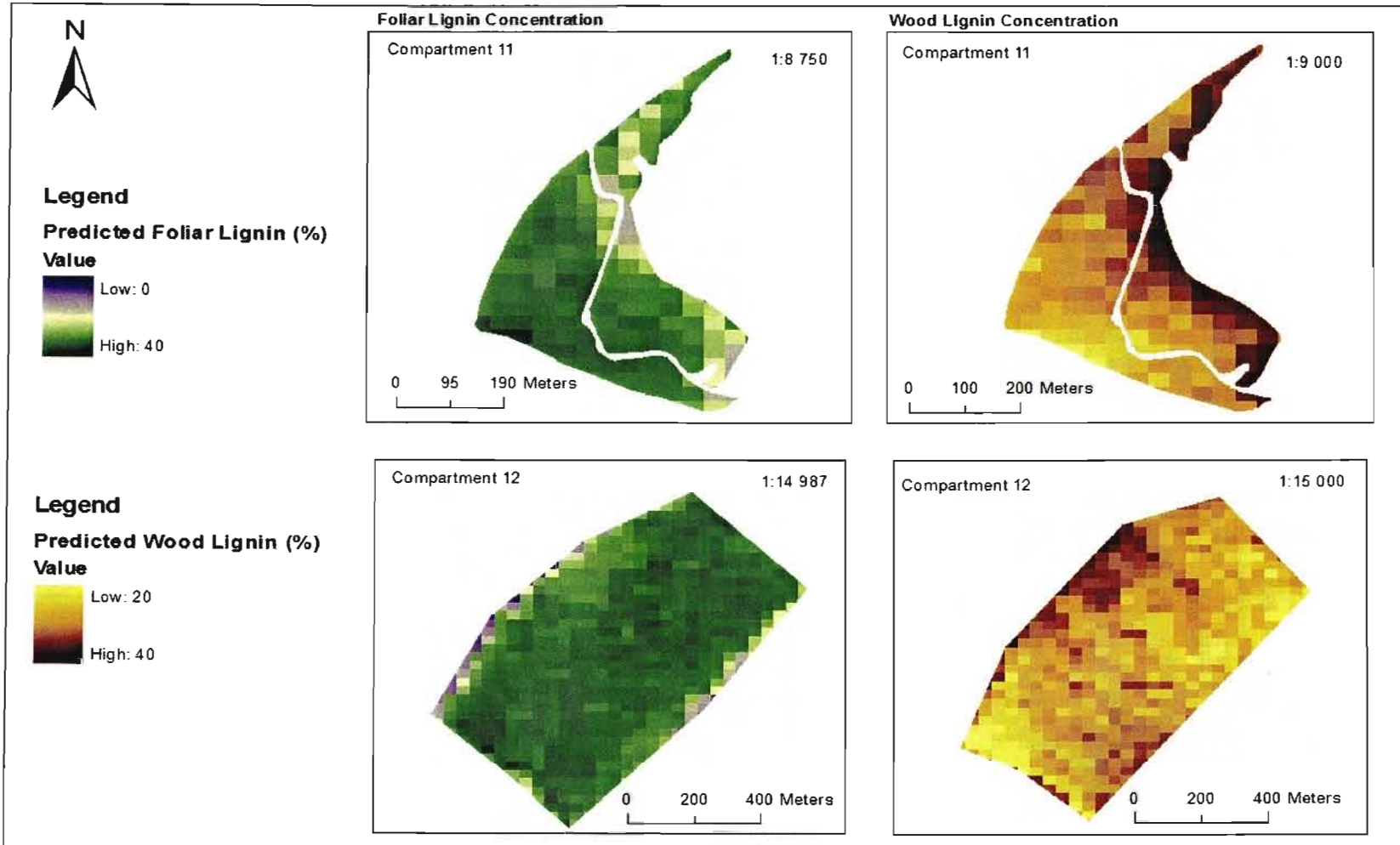


Figure 5.6 An illustration of foliar lignin and wood lignin concentrations calculated from the lignin indices across each compartment (11 and 12)

5.2.3 Prediction of Wood Lignin Concentrations

The resulting derived foliar lignin concentrations from the image were firstly converted to wood lignin concentrations using compartment specific equations which were established using the laboratory data (refer to Table 5.1). Compartment 4 and 12 did not have significant relationships individually but when they were grouped with other compartments of similar age and SI the relationships between wood and foliar lignin concentration were significant. The equation in figure 5.3 C was used to convert foliar lignin concentration of compartments 4 and 8 to wood lignin concentrations. The equation in Figure 5.2 F was used to calculate the predicted wood lignin from the predicted foliar lignin concentrations of compartment 12. The predicted wood lignin concentrations were averaged per ROI of each compartment and then regressed against the averages of the laboratory-measured wood lignin concentrations. Figure 5.7 shows a positive relationship between laboratory-measured and predicted wood lignin concentrations with an R^2 of 0.91 and a very low p-value.

Secondly, foliar lignin concentrations from the image were converted to wood lignin concentrations using the age and site index dependant equations. Equations from Figure 5.2 B, C, D, E and Figure 5.3 B were used to convert foliar lignin concentrations to wood lignin concentrations. Figure 5.8 shows the positive relationship between laboratory-measured and predicted wood lignin concentrations. This relationship implies that wood lignin concentrations can be predicted using hyperspectral lignin bands and meaningful relationships between wood and foliar lignin concentrations.

From this study a multiple regression model was attempted to obtain an indication of the variables that contribute largely to the variations in wood lignin concentrations. The multiple-regression analysis was performed to assess if the wood lignin concentration prediction model could be significant with the inclusion of the SI and age and clone type. The results of the multiple-regression are presented in Table 5.6.

Table 5.6 Summary of results of the multiple-regression analysis

Dependent	wood lignin concentrations
Input independent variables	age, SI and foliar lignin concentrations, clone type
Variables that significantly explain the variation in wood lignin concentrations	age and foliar lignin concentrations
Multiple R	0.683
R²	0.466
No. of cases	60
Standard error	3.187
p	<0.0001
Resulting model	wood lignin concentrations = 3.71A – 0.74F + 21.90, where A = age and F = foliar lignin concentrations

Table 5.6 summarizes that foliar lignin concentrations and age have a combined significant influence on the variations of wood lignin concentrations. The R² improved from 0.06 (Figure 5.1) to 0.47 when age was included in the wood lignin concentration prediction model for all trees in one regression analysis. The p value shows that the relationship is adequately significant to conclude that clone type, SI and age could further be modeled using a wide range of ages and site qualities. This model is subject to inherent errors due to the sample size. This study has formed a basis to model specific variables for the prediction of wood lignin concentrations using hyperspectral lignin indices.

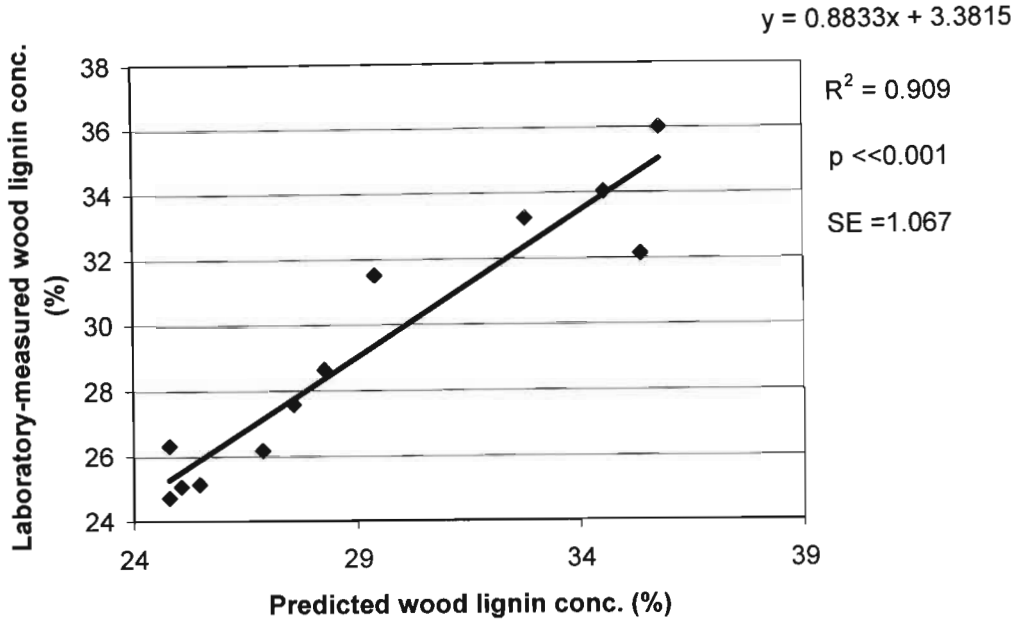


Figure 5.7 A comparison between laboratory-measured wood lignin concentrations and wood lignin concentrations derived from the hyperspectral image using mostly compartment specific equations

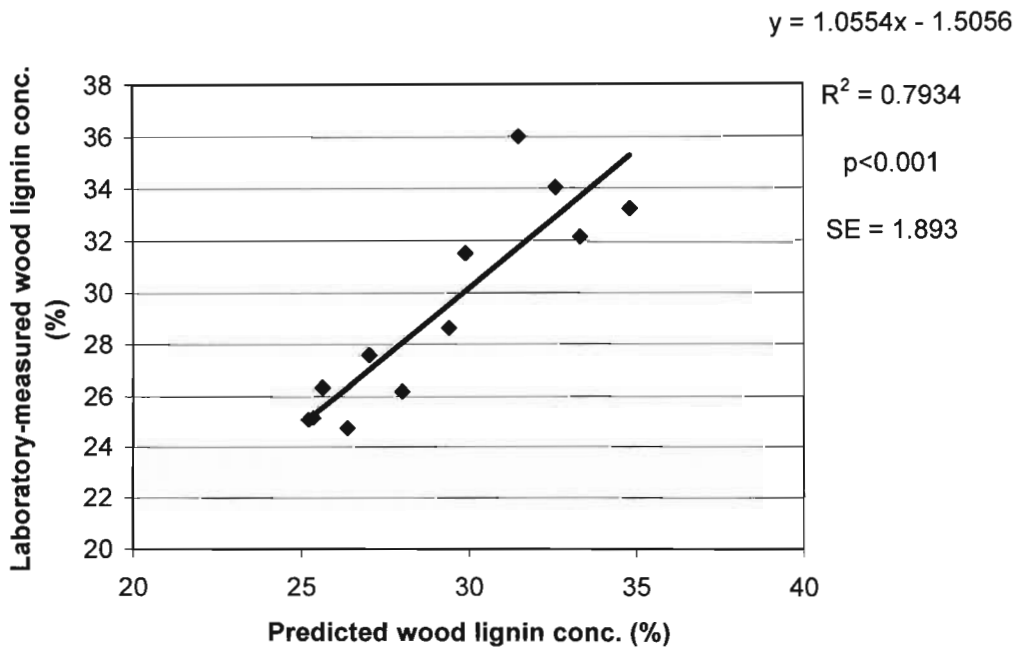


Figure 5.8 A comparison between laboratory-measured wood lignin concentrations and wood lignin concentrations derived from the hyperspectral image using age and site specific equations

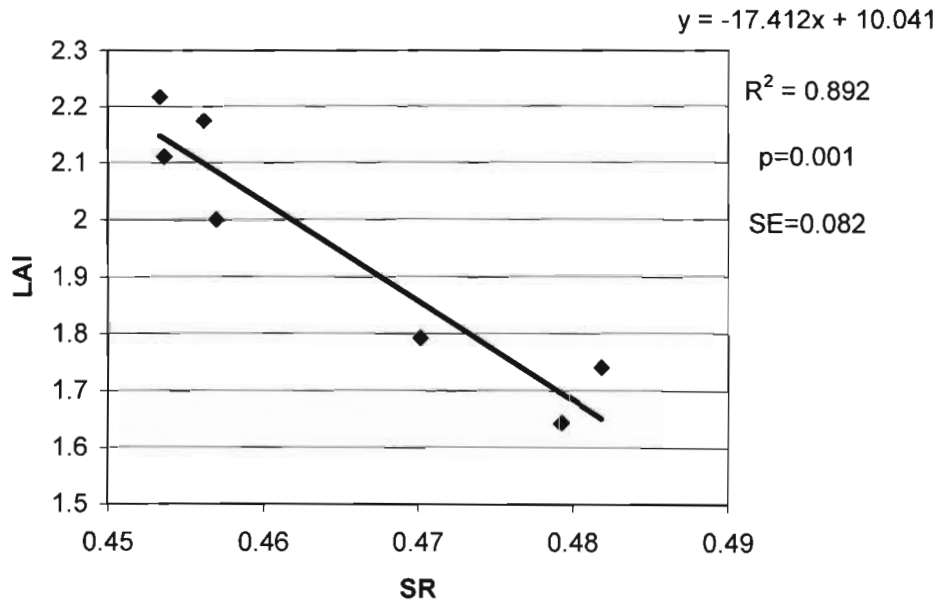
5.3 LEAF AREA INDEX DETERMINATION USING HYPERION DATA

The regression analysis between all the possible bands for calculating vegetation indices and the field measured LAI resulted in certain specific bands showing significant relationships with the LAI measurements. The bands that showed significant relationship are situated at 814 and 824nm in the NIR region and at 1250, 1630, 1640, 1650, 1660 and 1670nm in the SWIR region. In total, eight bands were selected. The results of regression analysis for the eight selected bands are presented in Table 5.7.

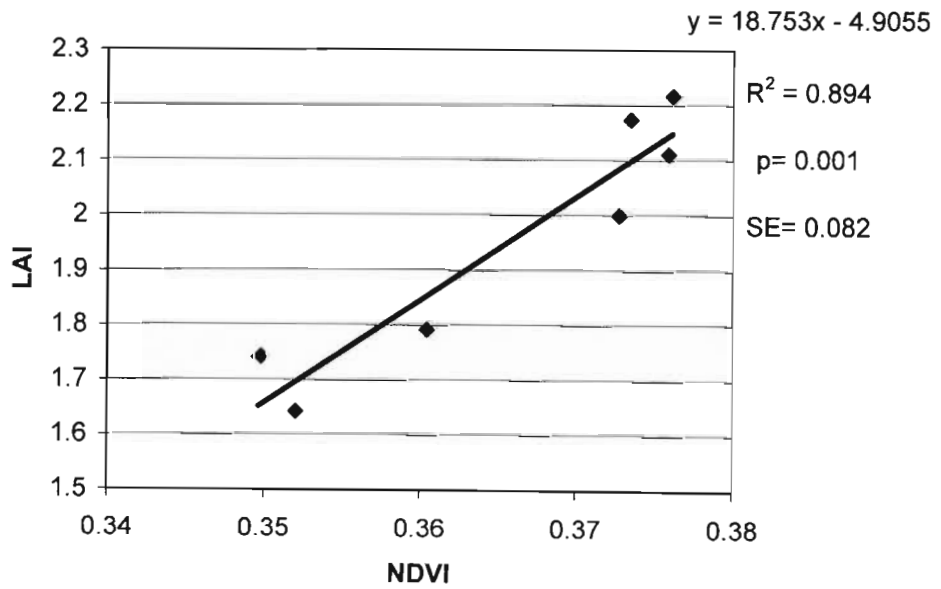
Table 5.7: A summary of the linear regression analysis between the selected possible bands and the field measured LAI

Spectral region	Band λ (nm)	R ²	p-value	Standard error (SE)
NIR	814	0.819	0.013	1082.025
	824	0.926	0.002	653.280
SWIR	1250	0.853	0.009	582.889
	1630	0.704	0.037	340.831
	1640	0.873	0.006	267.151
	1650	0.876	0.006	265.040
	1660	0.656	0.051	404.441
	1670	0.590	0.074	398.575

Plant cell walls scatter NIR energy, leading to generally high reflectance values in the NIR region than in SWIR region in the spectrum of a plant canopy (Lillesand and Kiefer, 2000). Therefore, when calculating the indices R was substituted with SWIR. Nine vegetation indices: SR; MNDVI; RDVI; NLI; MNLI; SAVI*SR; MNDVI*SR; SAVI and MSR were computed using average spectral reflectance values of two bands in each compartment using all the eight selected bands for possible combinations. The two bands that produced vegetation indices that correlated best with the field measured LAI were situated at 824nm in the NIR region and at 1650nm in the SWIR region. Linear regression coefficients were calculated between the VIs and measured LAI for each of the seven compartments (refer to Table 3.1). The results of the regression analysis for the LAI values of all the seven compartments against SR, NDVI, RDVI, MNDVI*SR, SAVI*SR, MNLI SAVI and MSR are in Figure 5.8.

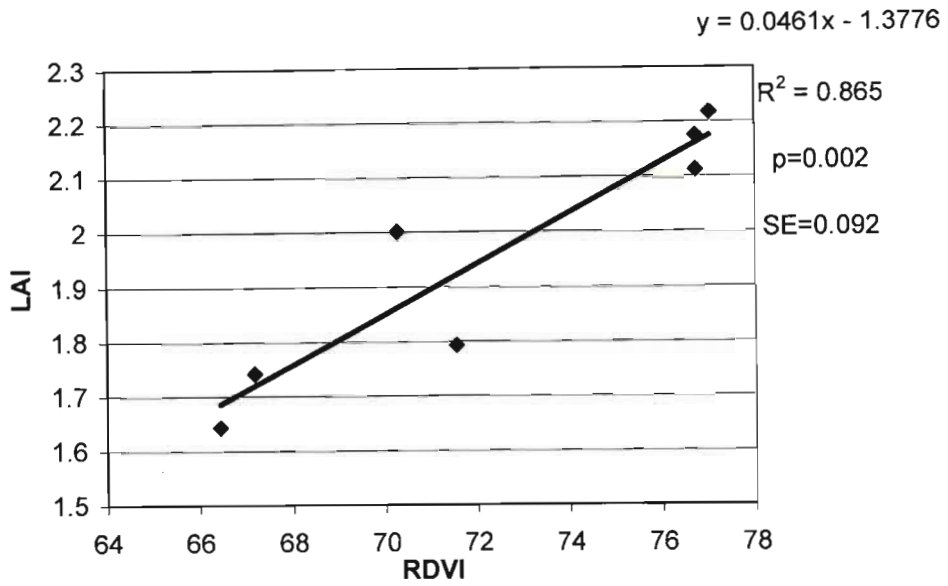


A: SR vs. LAI

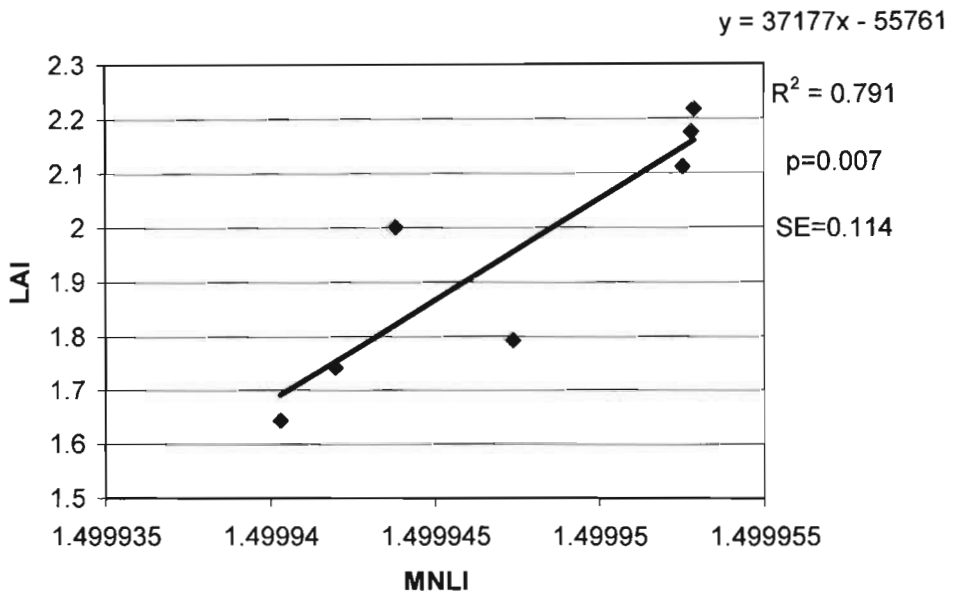


B: NDVI vs. LAI

Figure 5.9 (A-B) Graphs summarizing the regression analysis for all the calculated Vegetation Indices and field-measured LAI

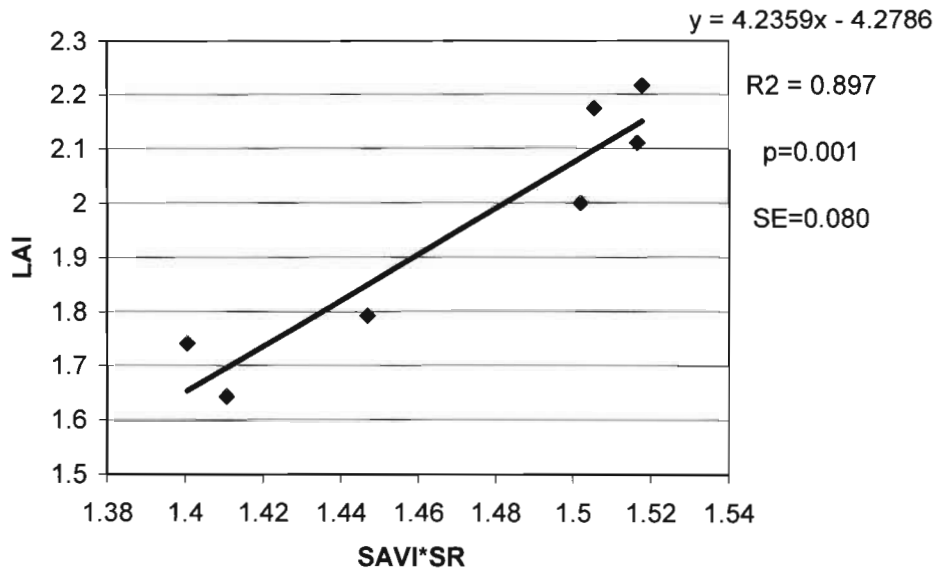


C: RDVI vs. LAI

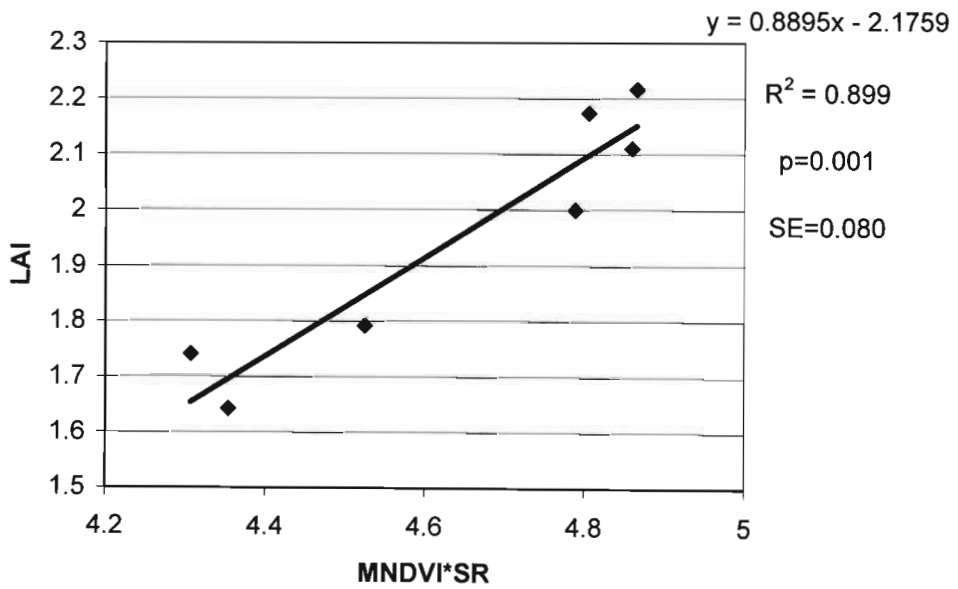


D: MNLI vs. LAI

Figure 5.9 (C-D) Graphs summarizing the regression analysis for all the calculated Vegetation Indices and field-measured LAI

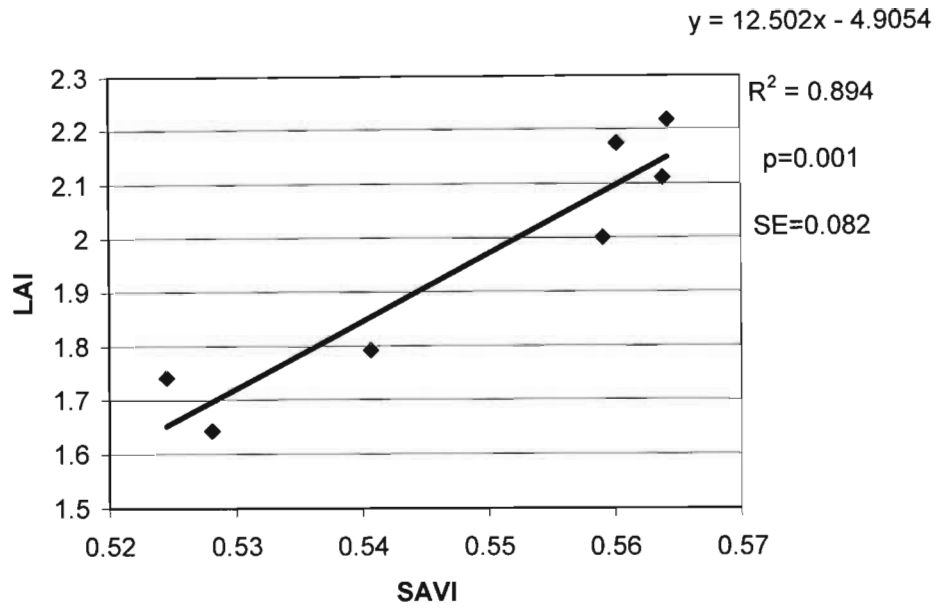


E: SAVI*SR vs. LAI

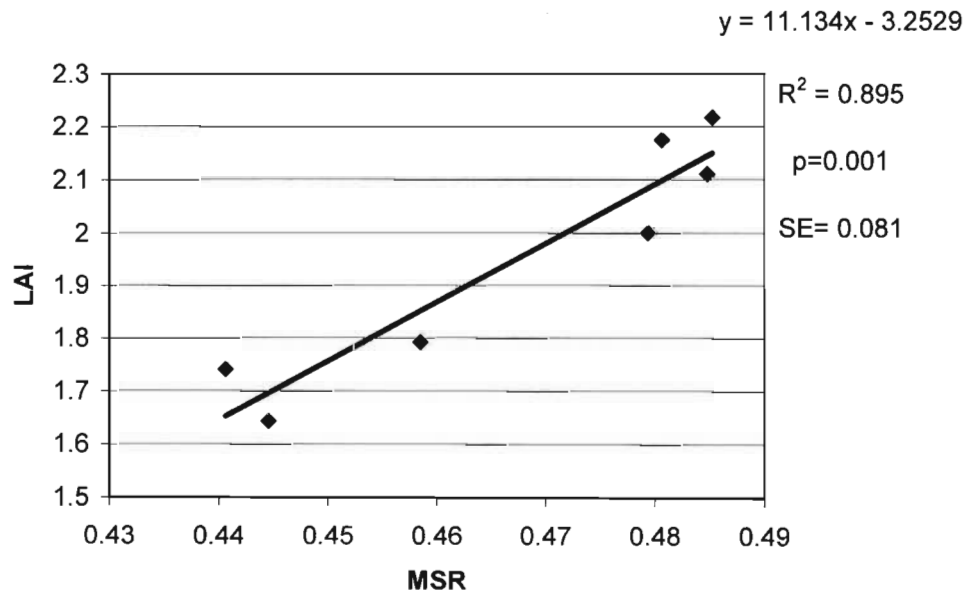


F: NDVI*SR vs. LAI

Figure 5.9 (E-F) Graphs summarizing the regression analysis for all the calculated Vegetation Indices and field-measured LAI



G: SAVI vs. LAI



H: MSR vs. LAI

Figure 5.9 (G-H) Graphs summarizing the regression analysis for all the calculated Vegetation Indices and field-measured LAI

NLI results for all the LAI values were 0.999. For this reason this graph was not presented, and therefore only eight graphs were presented in Figure 5.8. Gong *et al.* (2003) stated that NLI and MNLI are indices that can linearize relationships with surface parameters that tend to be non-linear and are therefore more suitable for semiarid environments. The study area in this project, Zululand, is a land used for commercial plantations and therefore cannot be categorised as a semi-arid land. This could be the reason the NLI produced values of 0.999 and the MNLI produced values between 1.499935 and 1.499955. These values are close together and might saturate with higher or wider range of LAI values. The MNLI and NLI are, therefore, not recommended for use in the commercial forestry land. The MNLI correlation to LAI also had a lower R^2 of 0.791 compared to all the other seven index-correlations. The relationship between LAI and the MNLI also had the highest p-value (0.007) and standard error (SE) of 1.114 (Figure 5.8 D). The seven other vegetation indices had significant relationships with the field measured LAI.

The results of the eight vegetation indices and LAI regression analysis are summarised in Table 5.8. In six cases (SR vs. LAI; MNDVI vs. LAI; SAVI*SR vs. LAI; MNDVI*SR vs. LAI, SAVI vs. LAI and MSR vs. LAI) had a p-value of 0.001 when RDVI vs. LAI produced a p-value of 0.002 and MNLI vs. LAI gave a p-value of 0.007. RDVI is nonetheless recommended for LAI predictions because the relationship between LAI values and RDVI is significant. The standard error (SE) was relatively low for all the correlations; the lowest SE was 0.080 and the highest was 0.092. SAVI*SR and MNDVI*SR correlations had the lowest SE of 0.080, followed by MSR with SE of 0.081. SR, NDVI and SAVI had the SE of 0.082. RDVI had the highest SE of 0.092. SAVI*SR and MNDVI*SR had the highest R^2 of 0.897 and 0.899 respectively, followed by the MSR with the R^2 of 0.895. SAVI and MNDVI produced very similar statistics for their correlations, with the R^2 of 0.894. The SR also has almost similar results with the SAVI and MNDVI except for the R^2 values. The SR produced an R^2 of 0.892, which is slightly lower. The RDVI had the second lowest R^2 of 0.865 out of the eight correlations. All the investigated indices produced very significant results when regressed against LAI. SAVI*SR and MNDVI*SR produced the best results when regressed with the field-measured LAI. Eight of the nine vegetation indices that were regressed against the field-measure LAI are suitable for estimating and predicting ground LAI, however MNLI is not recommended for a

forest plantation because the LAI values corresponded to a very narrow range of MNLi in this study.

Table 5.8 A summary of the results of the regression analysis between the eight VI and LAI

Regression analysis	R ²	p-value	Standard error (SE)
SR vs. LAI	0.892	0.001	0.082
NDVI vs. LAI	0.894	0.001	0.082
RDVI vs. LAI	0.865	0.002	0.092
MNLi vs. LAI	0.791	0.007	0.144
SAVI*SR vs. LAI	0.897	0.001	0.08
NDVI*SR vs. LAI	0.899	0.001	0.08
SAVI vs. LAI	0.894	0.001	0.082
MSR vs. LAI	0.895	0.001	0.081

The SAVI*SR index combines the SAVI merits of adjusting variations induced by the soil brightness and the SR merits where there are changes in the amount of green biomass, pigment content and leaf water stress. Generally with higher LAI, where the reflectance is higher in NIR region and lower in the R or SWIR regions, a change in the NIR region will induce a larger change in the SR than in the MNDVI. The MNDVI*SR is therefore expected to balance the phenomenon to increase correlation accuracies for a wider range of LAI values (Pu *et al.*, 2005). MSR, RDVI and NLI linearize the non-linear relationships between the VIs and any biophysical parameter such as LAI (Goel and Qin, 1994).

SAVI was derived from the NDVI but the soil/ background adjustment factor was introduced to produce vegetation isolines that are more independent of the background. SAVI with L=0 is equivalent to NDVI. In this study a factor of 0.5 was used because this factor can reduce the soil noise problems for a wide range of LAI values. However, taking into consideration that in the forest plantations there is hardly any evidence of exposed soil within the compartments, it can be concluded that the 0.5 only uniformly affected the reflectance of all the compartments. The illustrations of the widely used vegetation index: the MNDVI; and the two indices that had the best relationship with the field-measured LAI in this study: the MNDVI*SR and the SAVI*SR are shown in Figure 5.9. Only two compartments are shown for

each index. Different vegetation indices represent vegetation cover differently as shown in Figure 5.9, based on the different calculations using the two narrow bands. LAI is therefore calculated from the regression models in Figure 5.8. Figure 5.10 presents a map of LAI across the image that resulted from the MNDVI*SR vs. LAI model in Figure 5.8 F. It is possible to map LAI across each compartment using remote sensing as demonstrated in Figure 5.11. These LAI maps were developed from the MNDVI*SR index because it produced the best correlation results with the field measured LAI.

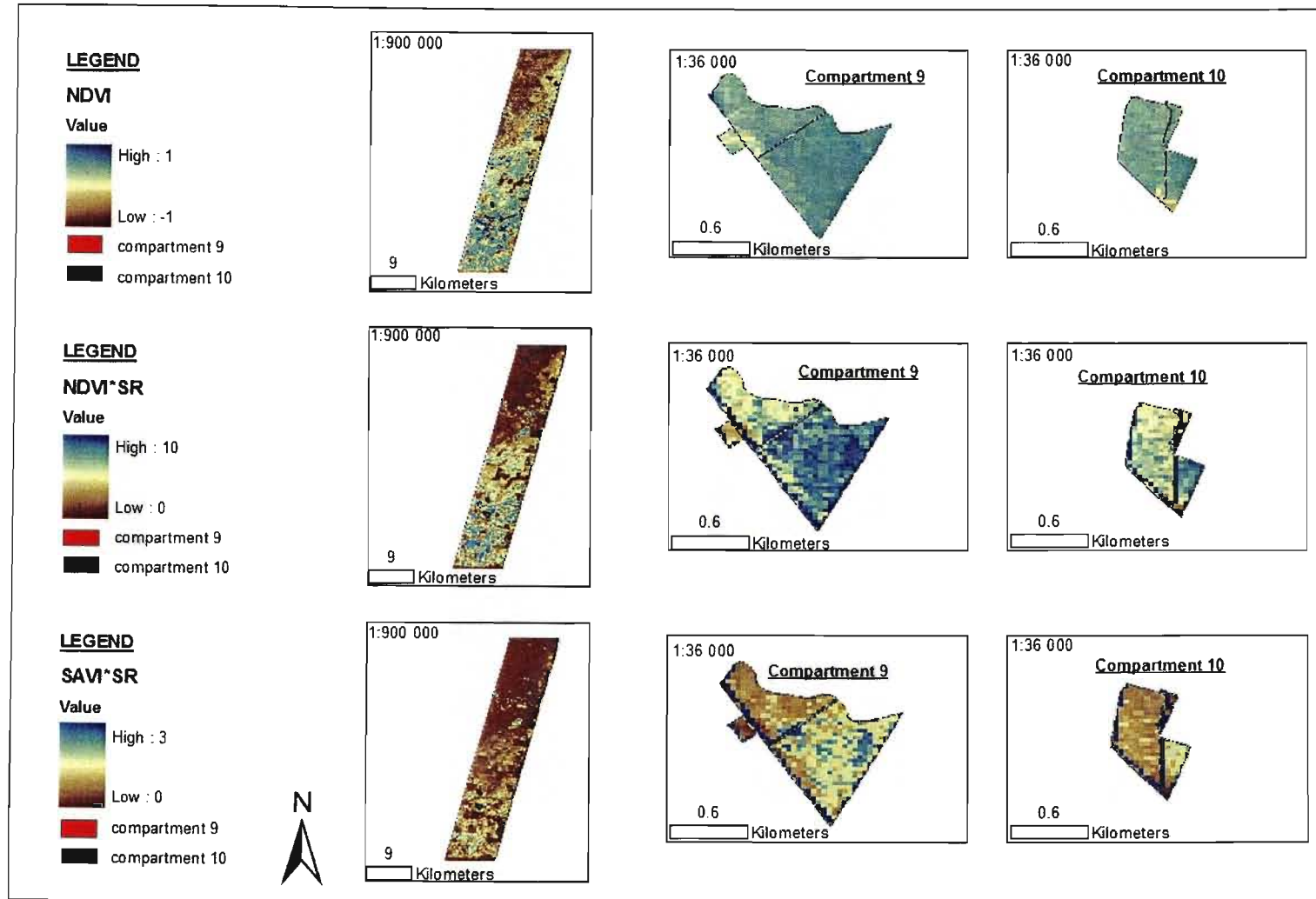


Figure 5.10 illustrations across a compartment of NDVI, of NDVI*SR and SAVI*SR calculated from two Hyperion bands in compartment 9 and 10

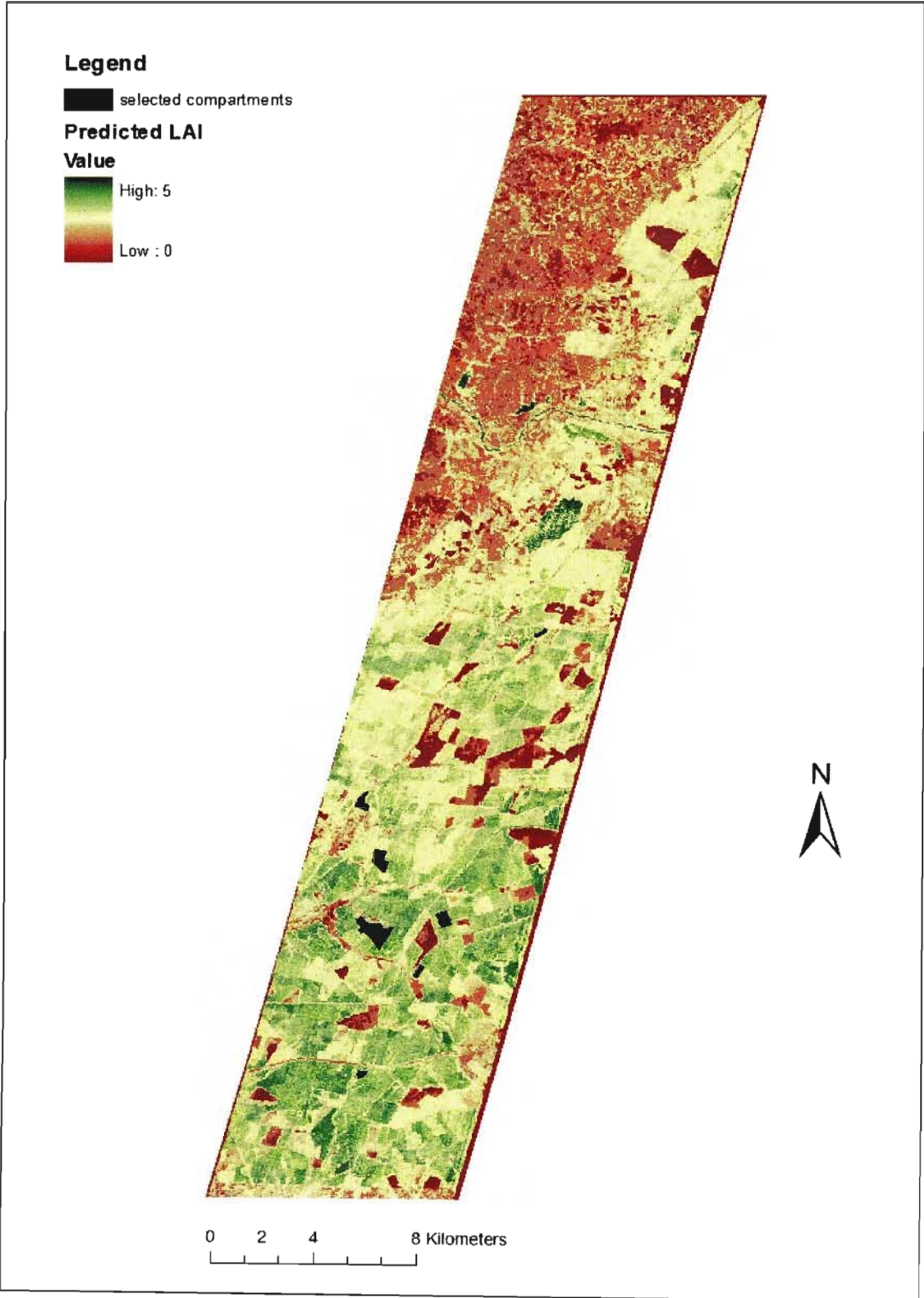


Figure 5.11 The LAI map for the Hyperion image

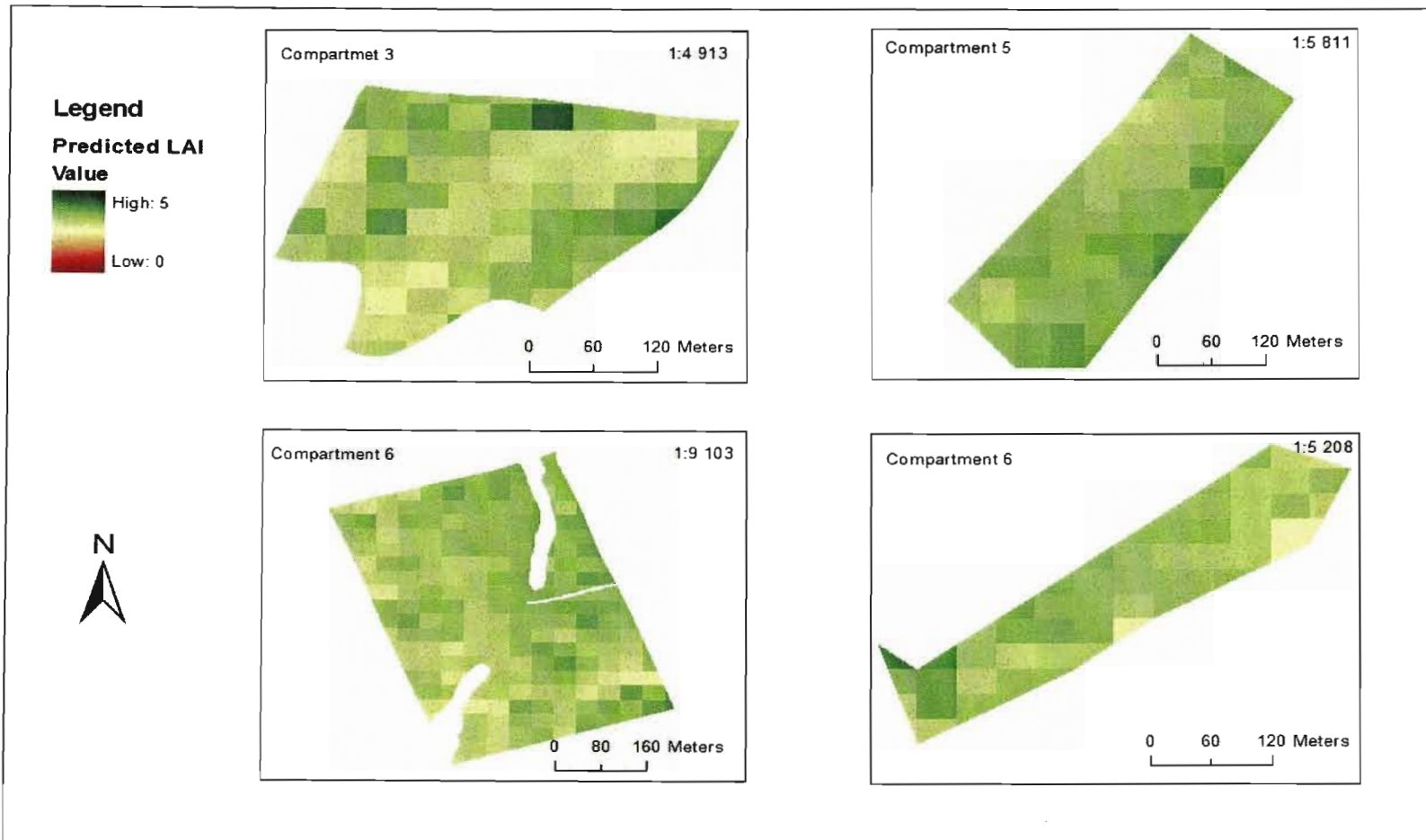


Figure 5.12 Illustrations of LAI variation across each compartment (3, 5, 6 and 8)

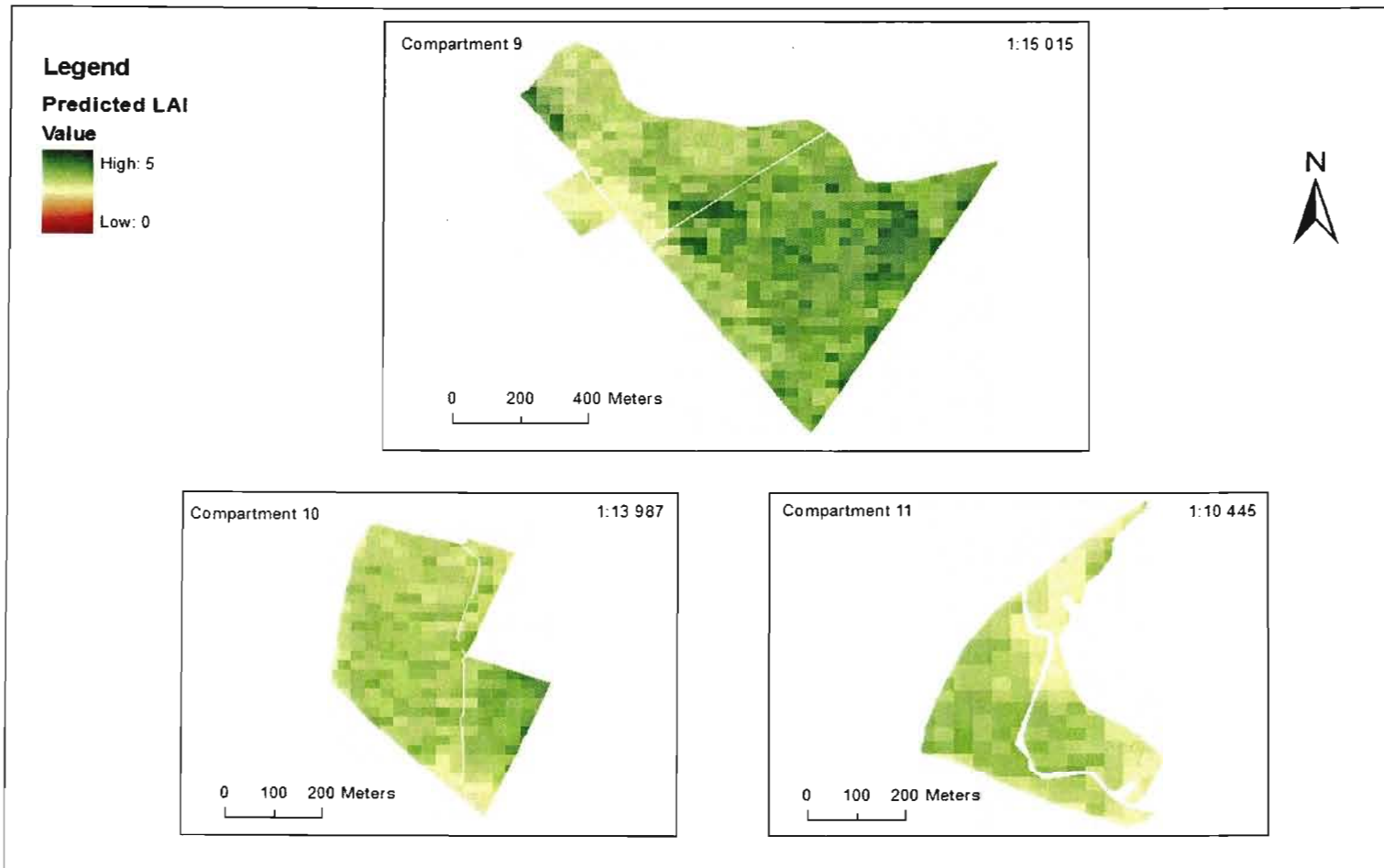


Figure 5.12 Illustrations of LAI variation across each compartment (9, 10 and 11)

CHAPTER 6: Conclusions and Recommendations

6.1 Conclusions

The aim of this project was to investigate if satellite-borne hyperspectral data can be used to estimate wood lignin concentrations using calculated lignin indices, and also to investigate the robustness of the narrowband vegetation indices for estimating LAI. For the estimation of wood lignin concentrations, selected compartments were between the ages of six and nine years to obtain estimates of the lignin concentrations in compartments that are at harvesting age. The age between 6 and 9 years is the approximate age of pulpwood harvesting. It was assumed that the ages between 6 years and 9 years could be grouped as one age group. Age was thus assumed to be a constant variable. Large variation among the *Eucalyptus* clones was not anticipated since clones and not *Eucalyptus* species were used. Biological variation was also, assumed to be a constant. Site indices were, however, not kept constant to allow for a comparative study. The results showed that there is no general model to predict wood lignin concentrations from foliar lignin concentrations. The relationships between wood and foliar lignin concentrations could be compartment-specific but to generalise the model, a correlation matrix revealed that these relationships are influenced by site index (SI) and age. This implies that for a model to be successful to implement, age and SI have to be taken into consideration. There was no evidence of correlation between wood and foliar lignin concentration when the two *E. urophylla* compartments of the same age were grouped together

The two bands at 1680nm and 1750nm were selected because they were not correlated and they produced indices that correlated best to the laboratory measured foliar lignin. The results show that there is potential to predict foliar lignin concentrations from lignin indices in *Eucalyptus* clones plantation forests. These indices correlated to the laboratory measured foliar lignin concentrations. When the predicted wood lignin concentrations were regressed against the laboratory measured wood lignin concentrations, the relationship was very significant with an R^2 of 0.91. It is therefore concluded that it is possible to predict wood lignin concentrations if the

wood and foliar lignin concentration model is pre-determined and accurately modelled.

Atmospheric correction of Hyperion produced an image with bands that were explored for the construction of vegetation indices. Eight bands (two in NIR and six in SWIR) that correlated to field measured LAI were used to construct nine vegetation indices using all possible combination of any two bands (one band from NIR and the other from SWIR). The resulting vegetation indices were regressed against the average field measured LAI of seven compartments. The regression analysis showed that vegetation indices that best correlate to field-measured LAI are situated at 824nm and 1650nm; therefore these two bands were selected to construct the nine vegetation indices.

The results of the NLI (non-linear vegetation index) calculation using the reflectances from the selected bands showed saturation since all the LAI values corresponded to the NLI value of 0.999 and there was no correlation. This index is mainly used in the semi-arid regions and it is therefore not suitable for LAI predictions in areas like Zululand which is populated with forest plantations. The index also showed possible signs of saturation because the index values that showed correlation with the LAI values corresponded to a range between 1.499935 and 1.499955. This vegetation index is therefore not recommended for LAI predictions because it also had the lowest R^2 , highest SE and p-value, compared to the other vegetation indices, when regressed against LAI values. SAVI*SR and NDVI*SR proved to have the best results when regressed against the measured LAI. NDVI*SR had a higher R^2 . Any of the vegetation indices can be used to predict LAI depending on the soil brightness in the image or the extent of bare soil present within the compartments, except for the NLI. MNLI could be used with caution because it might easily saturate at extreme values. With regards to this study area, soil is not of concern since there is very little or no bare soil present within the compartments. This might be the reason the NDVI*SR is the best for this study area. Judging by the results obtained in this study, it can be postulated that hyperspectral-based indices pose many opportunities for formulation of more accurate models to predict biophysical parameters.

6.2 RECOMMENDATIONS

The study showed that it is possible to predict wood and foliar lignin using hyperspectral remote sensing. The results also show that site index and age have an influence on the wood and foliar lignin model. It will therefore be beneficial to explore the possibilities of age and site quality models within an individual clone. Sampling within a compartment should be extensive such that a substantial number of trees are sampled for statistically viable conclusions about the wood and foliar lignin concentration relationship and to understand the compartmental relationship between wood and foliar lignin concentrations. From the results of this study, it is recommended that models that were developed to predict wood lignin from foliar lignin concentrations and hyperspectral indices be used for other similar compartments for pulp and paper processing purposes.

When sampling or acquiring measurements within a compartment, a more specific ground plot location could be used. This plot can then be marked using distance such that it can be identified on the image. This will enable a more accurate calibration model for foliar lignin concentration and LAI predictions if the laboratory-measured foliar lignin concentrations and field measured LAI are regressed against means of image data from areas that overlap with the ground plots. The actual foliar lignin concentrations or LAI can then be extrapolated to the rest of the image. More accurate estimations of foliar lignin concentrations and NDVI values will be developed and consequently more accurate wood lignin concentrations and LAI estimations will result.

It is imperative to use an appropriate atmospheric correction model for the atmospheric correction of Hyperion data. Leaf area index is one of the frequently measured biophysical parameters, therefore to confidently conclude that hyperspectral is more accurate for LAI estimation; a larger number of compartments should be sampled. This study was conducted on a flat terrain; therefore studies conducted on more rough terrain should incorporate an accurate digital elevation model (DEM) for the calculation of correct vegetation indices. Hyperspectral data hold great potential in providing relatively more accurate LAI estimation, however, more work needs to be done to arrive at conclusive evidence. The use of Hyperion data for

predicting LAI values and subsequently use these estimations in physiological and ecological models is recommended.

REFERENCES

- Alves, A.; Schwanninger, M.; Pereira, H. and Rodrigues, J. 2006. Analytical pyrolysis as a direct method to determine the lignin content in wood. Part 1: Comparison of pyrolysis lignin with Klason lignin. *Journal of Analytical and Applied Pyrolysis* 76, pp 209 – 213
- Anderson, L. O.; Shimabukuro, Y. E. and Arai, E. 2005. Multitemporal fraction images derived from Terra MODIS data for analysing land cover change over the Amazon region. *International Journal of Remote Sensing* 26 (11), pp 2251 – 2257
- Arsenault, E. and Bonn, F. 2005. Evaluation of soil erosion protective cover by crop residues using vegetation indices and spectral mixture analysis of multispectral and hyperspectral data. *Catena* 62, 157 – 172
- Asner, G. P.; C. A. Wessman, and C. A. Bateson. 1998. Sources of variability in plant canopy hyperspectral reflectance data in a savanna ecosystem. *Proceedings of the 7th Annual Airborne Earth Science Workshop* 1, pp 23 – 32
- Asner, G. P. Carlso, K. M. and Martin, R. M. 2005. Substrate age and precipitation effects on Hawaiian forest canopies from spaceborne imaging spectroscopy. *Remote Sensing of Environment* 98, pp 457 – 467
- Bailleres, H.; Davrieux, F. and Ham-Pichavant, F. 2002. Near infrared analysis as a tool for rapid screening of some major wood characteristics in a eucalyptus breeding program. *Annals for Science* 59, pp 479 – 490
- Bajcsy, P. and Groves, p. 2004. Methodology for hyperspectral band selection. *Photogrammetric Engineering and Remote Sensing Journal* 70 (7), pp 793 – 802.
- Baptista, C.; Robert, D. and Duarte, A. P. 2006. Effect of pulping conditions on lignin structure from maritime pine kraft pulps. *Chemical Engineering Journal* 121, pp 153 – 158

Beck, R. 2003. EO-1 User Guide version 2.3. USGS Earth Resources Observation Systems Data Center. Sioux Falls, USA. Pp 22 – 32

Benz, U. C.; Hoffman, P.; Willhauck, G.; Lingenfelder, I. and Heynen, M. 2004. Multi-resolution, object-oriented fuzzy analysis of remote sensing data for GIS-ready information. *ISPRS Journal of Photogrammetry and Remote Sensing* 58, pp 239 – 258

Benhardt-Reversat, F. and Schwartz, D. 1997. Change in lignin content during litter decomposition in tropical forest soils (Congo): comparison of exotic plantations and native stands. *Earth and Planetary Sciences* 325, pp 427 – 432.

Bharati, M. H.; McGregor, J. F. and Champagne, M. 2004. Using near-infrared multivariate image regression to predict pulp properties. *Tappi Journal* 3 (5), pp 8 – 14

Boegh, E.; Soegaard, H.; Broge N.; Hasager, C. B.; Jensen, N. O.; Schelde, K. and Thomsen, A. 2002. Airborne multispectral data for quantifying leaf area index, nitrogen concentration, and photosynthetic efficiency in agriculture. *Remote Sensing of Environment* 81 (2), pp. 179-193

Brauns. F. E. 1952. The chemistry of lignin. Academic Press Inc, New York. Pp 120 – 160

Brundle, C. R. 1974. The application of electron spectroscopy to surface studies. *Journal of Vacuum Science and Technology* 11 (1), pp 212 – 224

Campbell, P. K. E.; Rock, B. N.; Martin, M. E.; Neefus, C. D.; Irons, J. R.; Middleton, E. M. and Albrechtova, J. 2004. Detection of initial damage in Norway spruce canopies using hyperspectral airborne data. *International Journal of Remote Sensing* 20, pp 5557 – 5583

Casa, R. and Jones, H. G. 2005. LAI retrieval from multiangular image classification and inversion of a ray tracing model. *Remote Sensing of Environment* 98, pp 414 – 428

Casey, J. P. 1952. Pulp and Paper: Chemistry and chemical technology. Interscience Publishers Ltd. London. Pp 5 – 40

Cho*, M. A. and Skidmore, A. K. 2006. A new technique for extracting the red edge position from hyperspectral data: the linear extrapolation method. *Remote Sensing of Environment* 101, 181 – 193

Chen, C. -M.; Hepner, G. F. and Forster, R. R. 2003. Fusion of hyperspectral and radar data using the HIS transformation to enhance urban surface features. *Photogrammetry and Remote Sensing* 58, pp 19 – 30

Chen, S. and Yip, S. 1974. *Spectroscopy in Biology and Chemistry*. Academic Press Inc. London. Pp 20 – 45

Cheng, Y.; Gamon, J. A.; Fuentes, D. A.; Mao, Z.; Sims, D. A.; Qiu, H.; Claudio, H.; Clark, M. L.; Roberts, D. A. and Clark, D. B. 2005. Hyperspectral discrimination of tropical rain forest tree species at leaf to crown scales. *Remote Sensing of Environment* 96, pp 375 – 398

Christiernin, M.; Ohlsson, A. B.; Berglund, T. and Henriksson, G. 2005. Lignin isolated from primary walls of hybrid aspen cell cultures indicates significant differences in lignin structure between primary and secondary cell wall. *Plant Physiology and Biochemistry*, 43 (8) 777 - 785

Cocks, T. Jenssen, R.; Stewart, A.; Wilson, I. and Shields, T. 1998. The HyMapTM airborne hyperspectral sensor: the system, calibration and performance. *1st Earsel Workshop on Imaging Spectroscopy*, pp 1 – 7

Coetzee, J., 1994, The development of top height with age for application to short rotation and thinning crops: *E. grandis*. ICFR Bulletin Series 9/94. Pietermaritzburg

Cohen, W. B.; Maersperger, T. K.; Yang, Z.; Gower, S. T., Turner, D. P.; Ritts, W. D.; Berterretche, M. and Running, S. W. 2003. Comparisons of land cover and LAI estimates derived from ETM+ and MODIS for four sites in North America: a quality assessment of 2000/2001 provisional MODIS products. *Remote Sensing of Environment* 88, pp 233 – 255

Colombo, R.; Bellingeri, D., Fasolini, D. and Marino, C. M. 2003. Retrieval of leaf area index in different vegetation types using high-resolution satellite data. *Remote Sensing of the Environment* 86, pp 120 – 131

Combe, J.; Launeau, P. Carrere, V.; Despan, D.; Meleder, V.; Barille, L. and Sotin, C. 2005. Mapping microphytobenthos biomass by non-linear inversion of visible infrared hyperspectral images. *Remote Sensing of Environment* 98, pp 371 – 378

Coops, N.; Austin, M. and Ryan, P. 1997. Temporal response in the spectral response of *Eucalyptus*. MDP forest productivity. *CSIRO Forestry and Forest Products, Wildlife and Ecology, and Land and Water*, pp 1 – 3

Coops, N.; Bi, H.; Barnett, P.; and Ryan, P. 1999 Estimating mean and current annual increments of stand volume in regrowth *Eucalypt* forest using historical Landsat MSS imagery. *Journal of Sustainable Forestry* 9 (3/4), pp 149 – 167

Coops, N. 1999. Improvement in predicting stand growth of *pinus radiata* across landscapes using NOAA AVHRR and Landsat MSS imagery combined with a Forest Growth Process Model. *Photogrammetric Engineering of Remote Sensing* 65 (10), pp 1149 – 1156

Coops, N. C.; Waring R. H.; Brown S. R. and Running S. W. 2001. Comparisons of predictions of net primary production and seasonal patterns in water use derived with two forest growth models in Southwestern Oregon. *Ecological Modelling* 142, pp 61–81

Coops, N.; Smith, M.; Martin, M. E. and Ollinger, S. V. 2003 Prediction of eucalypt foliage nitrogen content from satellite-derived hyperspectral data. *IEEE Transactions on Geoscience and Remote Sensing* 41(6), pp 1338 – 1346

Coops, N. C.; Smith, M.; Martin, M. E.; Ollinger, S. V.; Held, A. and Dury, S. J. undated. Assessing the performance of Hyperion in relation to eucalypt biochemistry: preliminary project design and specifications. *CSIRO Forestry and Forest Products*, Australia

Curran, P. J. 1989. Remote Sensing of foliar chemistry. *Remote Sensing of Environment* 30, pp 271 – 278

Curran, P. J.; Dungan, J. L. and Peterson, D. L. 2001. Estimating foliar biochemical concentration of leaves with reflectance spectrometry: testing the Kokaly and Clarke methodologies. *Remote Sensing of Environment* 76, pp 349 – 359

[CITATION] In: **Dale JE, Milthorpe FL** eds. The growth and functioning of leaves
EWK BARLOW - Gambridge, London: Gambridge University Press, **1983**

del Rio, J. C.; Gutierrez, A.; Rodriguez, I. M.; Romero, J.; Martinez, M. J. and Martinez, A. T. 2001. Identification of residual lignin markers in eucalypt kraft pulps by Py-GC/MS. *Journal of Analytical and Applied Pyrolysis* 58-59, pp 425 – 439

del Rio, J. C.; Gutierrez, A.; Hernando, M.; Landin, P.; Romero, J. and Martinez, A. T. 2005. Determining the influence of eucalypt lignin composition in paper pulp yield using Py-GC/MS. *Journal of Analytical and Applied Pyrolysis* 74, pp 110 – 115

Donaldson, L. A. 2001. Lignification and lignin topochemistry- an ultrastructural view. *Phytochemistry* 57, pp 859 – 873

Eduardo, L.; Aragao, L. E. O. C.; Shimabukuro, Y. E.; Santo, F. D. B. E. and Williams, M. 2005. Landscape pattern and spatial variability of leaf area index in Eastern Amazonia. *Forest Ecology and Management* 211, pp 240 – 256

Eklundh, L.; Harrie, L. and Kuusk, A. 2001. Investigating relationships between Landsat ETM+ sensor data and leaf area index in a boreal conifer forest. *Remote Sensing of Environment* 78, pp 239 – 251

Ekstrand, S. 1996. Landsat TM-based forest damage assessment – correction for topographic effects. *Photogrammetric Engineering and Remote Sensing* 62(2), pp 151 – 161

El-Araby, E. El-Ghazawi, T.; Le Moigne, J. and Gaj, K. undated. Wavelet spectral dimension reduction of hyperspectral imagery on a reconfigurable computer. NASA/Goddard Space Flight Center, George Mason University, USA

Ellis, F. 2000. Timber Plantation Silviculture: Geology. In: D. L. Owen (Ed.) *South African Forestry Handbook*, Vol 1. The Southern African Institute of Forestry, Pretoria

Ellis, R. J. and Scott, P. W. 2004. Evaluation of hyperspectral remote sensing as a means of environmental monitoring in the St. Austell China clay (kaolin) region, Cornwall, UK. *Remote Sensing of Environment* 93, pp 118 – 130

Endo, T.; Okuda, T.; Tamura, M. and Yasouka, Y. undated. Estimation of net photosynthetic rate based in in-situ hyperspectral data. National Institute for Environmental Studies, University of Tokyo. Japan

Erdas Imagine .1999. *Tour guide*. Erdas Inc. USA. Pp 200 – 250

Feleke, A.K., 2003, Land use and land cover in Relation to *Chromolaena odorata* distribution; mapping and change detection in St. Lucia wetland area, South Africa. Masters thesis, International Institute for Geo-information Science and Earth Observation, Enschede, The Netherlands

Fensholt, R.; Pederson, M. W. and Sandholt, I. 2004. Evaluation of a shortwave infrared water stress index (SIWSI) from MODIS near and shortwave infrared data. *Geophysical Research Abstracts* 6, pp 06783

Feng, J. Rivard, B. and Sanchez-Azofeifa, A. 2003. The topographic normalization of hyperspectral data: implications for the selection of spectral end members and lithologic mapping. *Remote Sensing of Environment* 85, pp 221 – 231

Filippi, A. M. and Jensen, J. R. 2006. Fuzzy learning vector quantization for hyperspectral coastal vegetation classification. *Remote Sensing of Environment* 100, pp 512 – 530

Foley, W. J.; McIwee, A.; Lawler, I., Aragonés, L.; Woolnough, A. P. and Berding, N. 1998. Ecological applications of near infrared reflectance spectroscopy - a tool for rapid, cost-effective prediction of the composition of plant and animal tissues and aspects of animal performance. *Oecologia* 116 (3), pp 293 – 305

Foody, G. M. 2003. Geographical weighting as a further refinement to regression modelling: an example focused on the NDVI-rainfall relationship. *Remote Sensing of Environment* 88, pp 283 – 293

Fourty, T.; Baret, F.; Jacquemoud, S.; Schmuck, G. and Verdebout, J. 1996. Leaf optical properties with explicit description of its biochemical composition: direct and inverse problems. *Remote Sensing of Environment* 56, pp 104 – 117

Frank, M. and Menz, G. 2003. Detecting seasonal changes in semi-arid environment using hyperspectral vegetation indices. *3rd EARSel Workshop on Imaging spectrometer*, pp 504 – 512

Freudenberg, K. 1964. *The formation of lignin in the tissue and in vitro: The formation of wood in forest trees*. Springer-Verlag, New York. Pp 150 – 170

Fuentes, D. A.; Gamon, J. A.; Cheng, Y.; Claudio, H. C.; Qiu, H.; Mao, Z.; Sims, D. A.; Rahman, A. F.; Oechel, W. and Lou, H. 2006. Mapping carbon and water vapour fluxes in a chaparral ecosystem using vegetation indices derived from AVIRIS. *Remote Sensing of Environment* 103, pp 312 – 323

Galvao, L. S.; Formaggio, A. R. and Tisot, D. A. 2005. Discrimination of sugar cane varieties in south eastern Brazil with EO-1 Hyperion data. *Remote Sensing of Environment* 94, pp 523 – 534

Gao, B.; Montes, M. J. and Davis, C. O. 2004. Refinement of wavelength calibrations of hyperspectral imaging data using a spectrum-matching technique. *Remote Sensing of Environment* 90, pp 424 – 433

Gastellu-Etchegorry, J. P.; Zagolski, F.; Mougín, E.; Marty, G.; and Giordano, G. 1995. An Assessment of canopy chemistry with AVIRIS- a case study in the Landes Forest, South-West France. *International Journal of Remote Sensing* 16(3), pp 487 – 501

Gausman, H. W. 1985. *Plant leaf optical properties*. Texas Tech Press. Texas. Pp 35 – 45

Gibson, P. J. 2000. *Introducing remote sensing principles and concepts*. Routledge, New York. Pp 2 – 35

Gindaba, J.; Rozanov, A. and Negash, L. 2005. Photosynthetic gas exchange, growth and biomass allocation of two *Eucalyptus* and three indigenous tree species of Ethiopia under moisture deficit. *Forest Ecology and Management* 205, pp 127 – 138

Glasser, W. G. and Sarkanen, S. 1989. *Lignin: properties and materials*. American Chemical Society, Washington DC. Pp 67 – 83

Gong, P.; Pu, R.; Miller, J. R. 1992. Correlating leaf area index of ponderosa pine with hyperspectral CASI data. *Canadian Journal of Remote Sensing* 18(4), pp 275 – 281

Gong, P.; Pu, R.; Biging, G.S. and Larrieu, M. R. 2003. Estimation of forest leaf area index using vegetation indices derived from Hyperion hyperspectral data: *IEEE Transactions on GeoScience and Remote Sensing* 41(6), pp 1355 – 1362

Guo, Z. L.; Zheng, J. P.; Ma, Y. D.; Li, Q. K.; Yu, G. R.; Han, S. J.; Fan, C. N.; Liu, W. D. 2006. Researches on litter fall decomposition rates and model simulating of main species in various forest vegetations of Changbai Mountains, China. *Acta Ecologica Sinica* 26 (14), pp 1037 –1046

Guo, B., Gunn, S. R., Damper, R. I. and Nelson, J. 2005. Adaptive band selection for hyperspectral image fusion using mutual information (Speech). In *Proceedings of 8th International Conference on Information Fusion* 1, pp. 630 – 637, Philadelphia, PA.

Haboudane, D.; Miller, J. R.; Pattey, E.; Zarco-Tejada, P. J. and Strachan, I. B. 2004. Hyperspectral vegetation indices and novel algorithms for predicting green LAI of crop canopies: Modeling and validation in the context of precision agriculture. *Remote Sensing of Environment* 90, pp 337 – 352

Hall, S. A.; Burke, I. C.; Box, D. O.; Kaufman, M. R. and Stoker, J. M. 2005. Estimating stand structure using discrete-lidar: an example from low density, fire prone ponderosa pine forests. *Forest Ecology and Management* 208, pp 189 – 209

Hall, R. J.; Davidson, D. P. and Peddle, D. R. 2003. Ground and remote estimation of leaf area index in Rocky Mountain forest stands, Kanaaskis, Alberta. *Canadian Journal of Remote Sensing* 29(3), pp 411 – 427

Hansen, P. M. and Schjoerring, J. K. 2003. Reflectance measurement of canopy biomass and nitrogen status in wheat crops using normalized difference vegetation indices and partial least squares regression. *Remote Sensing of Environment* 86, pp 542 – 553

Hess, D. (1975) *Plant Physiology*. Springer Verlag. New York, US. Pp 65 – 84

Hellman, M. J. and Ramsey, M. S. 2004. Analysis of hot springs and associated deposits in Yellowstone National Park using ASTER and AVIRIS remote sensing. *Journal of Volcanology and Geothermal Research* 135, pp 95 – 219

Holden, H. and leDrew, E. 2002. Measuring and modeling water column effects on hyperspectral reflectance in a coral reef environment. *Remote Sensing of Environment* 81, pp 300 – 308

Holmgren, J.; Nilsson, M. and Olsson, H. 2003. Estimation of tree height and stem volume on plots using airborne laser scanning. *Forest Science* 49(3), pp 419 – 428

^aHu, B.; Miller, J. R.; Chen, J. M. and Hollinger, A. 2004. Retrieval of the canopy leaf area index in the BOREAS flux tower sites using linear spectral mixture analysis. *Remote Sensing of Environment* 89, pp 176 – 188

^bHu, B.; Qian, S.; Haboudane, D.; Miller, J. R.; Hollinger, A. B.; Tremblay, N. and Pattey, E. 2004. Retrieval of crop chlorophyll content and leaf area index from decompressed hyperspectral data: the effects of data compression. *Remote Sensing of Environment* 92, pp 139 – 152

Huang, Z.; Turner, B. J.; Dury, S. J.; Wallis, I. R. and Foley, W. 2004. Estimating foliage nitrogen concentration from HyMap data using continuum removal analysis. *Remote Sensing of Environment* 93, pp 18 – 29

Huber, S.; Kneubuhler, M.; Zimmerman, N. E. and Itten, K. 2005. Potential of spectral feature analysis to estimate nitrogen concentration in mixed canopies. 4th workshop on imaging spectroscopy. Warsaw, Switzerland

Huete, A. and Rahman, A. F. 2006. A multi-scale analysis of dynamic optical signals in a Southern California chaparral ecosystem: a comparison of field, AVIRIS and MODIS data. *Remote Sensing of Environment* 103, pp 369 – 378

Humphreys, J. M.; Hemm, M. R. and Chapple, C. 1999. New routes for lignin biosynthesis defined by biochemical characterization of recombinant ferulate 5-hydroxylase, a multifunctional cytochrome P450-dependent monooxygenase. *Proceedings of National Academia Science Biochemistry* 96 (18), pp 10045 – 10050

Hyypa, J.; Hyypa, H.; Inkinen, M.; Engdahl, M.; Linko, S. and Zhu, Y. 2000. Accuracy comparison of various remote sensing data sources in the retrieval of

forest and stand attributes. *Forest Ecology and Management* 128, pp 109 – 120

Ibarra D.; del Rio, J. C.; Gutierrez, A.; Rodriguez, I. M.; Romero, J.; Martinez, M. J. and Martinez, A. T. 2005. Chemical characterization of residual lignins from eucalypt paper pulps. *Journal of Analytical and Applied Pyrolysis* 74, pp 116 – 122

Ibarra D.; del Rio, J. C.; Gutierrez, A.; Rodriguez, I. M.; Romero, J.; Martinez, M. J. and Martinez, A. T. 2004. Isolation of high-purity residual lignins from eucalypt paper pulps by cellulose and proteinase treatments followed by solvent extraction. *Enzyme and Microbial Technology* 35, pp 172 – 181

Jacobs, E. O.; Schafer, G. N. and Robertson, T. A. 1989. The classification of forest sites: Zululand key area. *South African Forestry research Institute*, Report no. S89/3, pp 37

Jia, G. J.; Burke, I. C.; Kaufmann, M. R.; Goetz, A. F. H.; Kindel, B. C. and Pu, Y. 2006. Estimates of forest canopy fuel attributes using hyperspectral data. *Forest Ecology and Management* 229, pp 27 – 38

Kalacska, M.; Sanchez-Azofeifa, A.; Caelli, T; Rivard, B. and Boerlage, B. 2005. Estimating leaf area index from satellite imagery using Bayesian networks. *IEE transactions on Geoscience and Remote Sensing* 43, pp 1867 – 1873

Kangas, A. and Maltamo, M. 2002. Anticipating the variance of predicted stand volume and timber assortments with respect to stand characteristics and field measurements. *Silva Fennica* 36(4), 799 – 811

Kelbe, B. and Germishuys, T. 1999. *A Study of the relationship between hydrological processes and water quality characteristics in the Zululand coastal region*. Water Research Commission, Pretoria, pp1-1 – 3-5

Kirk, T. K.; Higuchi, T. and Chang, H. 1980. Lignin biodegradation: microbiology, chemistry and potential applications. CRC Press Inc, Florida. Pp 57 – 100

Kishino, M.; Tanaka, A. and Ishizaka, J. 2005. Retrieval of chlorophyll a, suspended solids, and colored dissolved organic matter in Tokyo Bay using ASTER data. *Remote Sensing of Environment* 99, pp 66 – 74

Koger, C. H.; Bruce, L. M.; Shaw, D. R. and Reddy, K. N. 2003. Wavelet analysis of hyperspectral reflectance data for detecting pitted morningglory in soybean. *Remote Sensing of the Environment* 86, pp 108 – 119

Kumar, I.; Schmidt, K.; Dury, S. and Skidmore, A. 2001. *Imaging Spectrometry and Vegetation Science*. Kluwer Academic Publishers, Netherlands. Pp 23 – 45

LaCapra, V. C.; Melack, J. M.; Gastil, M. and Valeriano, D. 1996. Remote sensing of foliar chemistry of inundated rice with imaging spectrometry. *Remote Sensing of Environment* 55, pp 50 – 58

Lamar, W. R. and McGraw, J. B. 2005. Evaluating the use of remotely sensed data in matrix population modeling for eastern hemlock (*Tsuga Canadensis* L.). *Forest Ecology and Management* 212, pp 50 – 64

Lee, K.; Cohen, W. B.; Kennedy, R. E.; Maier-Sperger, T. K. and Gower, S. T. 2004. Hyperspectral versus multispectral data for estimating leaf area index in four different biomes. *Remote Sensing of Environment* 91, pp 508 – 520

Lee, Z. and Carder, K. L. 2004. Absorption spectrum of phytoplankton pigments derived from hyperspectral remote sensing reflectance. *Remote Sensing of Environment* 89, pp 361 – 368

le Marie G.; Francois, C. and Dufrene, E. 2004. Towards universal broad leaf chlorophyll indices using PROSPECT simulated database and hyperspectral reflectance measurements. *Remote Sensing of Environment* 89, pp 1 – 28

Li, Z.; Goloub, P.; Devaux, C.; Gu, X. Dueze, J. Qiao, Y. and Zhao, F. 2006. Retrieval of aerosol optical and physical properties from ground-based spectral, multi-angular and polarized sun-photometer measurements. *Remote Sensing of*

Environment 101, pp 519 – 533

LI-COR. 1990. *LAI-2000 Plant Canopy Analyzer Instruction Manual*. LI-COR Lincoln, Nebraska, USA.

Lillesand T. M. and Kiefer, R. W. 1994. *Remote sensing and Image Interpretation*. John Wiley and Sons Inc. New York, USA. Pp 1 – 60

Lillesand T. M. and Kiefer, R. W. 2000. *Remote sensing and Image Interpretation*. John Wiley and Sons Inc. New York, USA. Pp 1 – 150

Lindberg, J. J.; Kuusela, T. A. and Levon, K. 1989. *Specialty Polymers from Lignins*. American Chemical Society. New York, USA. Pp 12 – 56

Louw, J. H. and Scholes, M. C. 2003. Foliar nutrient levels as indicators of site quality for *Pinus patula* in the Mpumalanga escarpment area. *Southern African Forestry Journal* 197, pp 21 – 30

Makela, H. and Pekkarinen, A. 2004. Estimation of forest stand volumes by Landsat TM imagery and stand-level field-inventory data. *Forest Ecology and Management* 196, pp 245 – 255

Malan, F. S. 1993. The wood properties and qualities of three South African-grown Eucalypt hybrids. *South African forestry Journal* 167, pp 35 – 44

Malan, F. S. and Verry, S. D. 1996. Effects of genotype-by-environment interaction on the wood properties and qualities of four-year-old *Eucalyptus grandis* and *E. grandis* hybrids. *South African Forestry Journal* 176, pp 47 – 53

Manninen, T.; Sternberg, P.; Voipio, P. and Smolander, H. 2005. Leaf area index estimation of boreal forest using ENVISAT ASAR. *IEEE Transactions on Geoscience and Remote Sensing* 43(11), pp 2627 – 2635

Martin, M. E. and Aber, J. D. 1997. High Spectral resolution remote sensing of forest canopy lignin, nitrogen and ecosystem process. *Ecological applications* 7(2), pp 431 – 443

Maselli, F. 2004. Monitoring forest conditions in a protected Mediterranean coastal area by the analysis of multiyear NDVI data. *Remote Sensing of Environment* 89, pp 423 – 433

Matson, P.; Johnson, L.; Billow, C.; Miller, J. and Pu, R. 1994. Seasonal patterns and remote spectral estimation of canopy chemistry across the Oregon transect. *Ecological Applications* 4(2), pp 280 – 298

McLellan, T. M.; Aber, J. D. Martin, M. E.; Mellilo, J. M. and Nadelhoffer, K. J. 1991. Determination of nitrogen, lignin and cellulose content of decomposing leaf material by near infrared reflectance spectroscopy. *Canadian Journal of Remote Sensing* 21, pp 1684 – 1688

Meroni, M. Colombo, R. and Panigada, C. 2004. Inversion of a radiative transfer model with hyperspectral observations for LAI mapping in poplar plantations. *Remote Sensing of Environment* 92, pp 195 – 206

Muira, T.; Huete, A. Yoshioka, H. 2006. An empirical investigation of cross-sensor relationships of NDVI and red/ near-infrared reflectance using EO-1 Hyperion data. *Remote Sensing of Environment* 100, pp 223 – 236

Mundt, J. T.; Glenn, N. F.; Weber, K. T.; Prather, T. S.; Lass, L. W. and Pettingill, J. 2005. Discrimination of hoary cress and determination of its detection limits via hyperspectral image processing and accuracy assessment techniques. *Remote Sensing of Environment* 96, pp 509 – 517

Mnyeni, R. B.; Hoffman, S.; Knyazikhin, Y.; Privette, J. L.; Glassy, J., Tian, Y.; Wang, Y.; Song, X.; Zhang, Y.; Smith, G. R.; Lotsch, A.; Friedl, M.; Morisette, J. T.; Votava, P.; Nemani, R. R. and Running, S. W. 2002. Global products of vegetation leaf area and fraction absorbed PAR from year one of MODIS data. *Remote Sensing*

of *Environment* 83, pp 214 – 231

Nada, A. M. A.; El-Sakhawy, M. and Kamel, S. M. 1998. Infrared spectroscopic study of lignins. *Polymer Degradation and Stability* 60, pp 247 – 251

Nada, A. M. A.; Yousef, M. A.; Shaffej, K. A. and Salah, A. M. 1998. Infrared spectroscopy of some treated lignins. *Polymer Degradation and Stability* 62, pp 157 – 163

Nemani, R.; Pierce, L. and Running, S. 1993. Forest ecosystem process at the watershed scale: sensitivity to remotely-sensed leaf area index estimates. *International Journal of Remote Sensing* 14, pp 2519 – 2534

Nogueira, E. M.; Nelson, B. W. and Fearnside, P. M. 2005. Wood density in dense forest in central Amazonia, Brazil. *Forest Ecology and Management*: 208, pp 261 – 286

Neto, C. P.; Evtuguin, D.; Pinto, P.; Silvestre, A. and Freire, C. 2005. Chemistry of plantation eucalypts: Specificities and influence on wood and fibre processing. *Appita* 2005, pp 431 – 438

Neville, R. a., Levesque, J.; Staenz, K.; Nadeau, C.; Hauff, P. and Borstad, G. A. 2003. Spectral unmixing of hyperspectral imagery for mineral exploration: comparison of results from SFSI and AVIRIS. *Canadian Journal of Remote Sensing* 29(1), pp 99 – 110

Pacheco, A. and Bannari, A. 2001. Application of hyperspectral remote sensing for LAI estimation in precision farming. *23rd Canadian Remote Sensing Symposium*, Department of Geography. University of Ottawa, Canada

Pearlman, J. S.; Dyk, A.; Goodenough, D.; Ma, Z.; Crawford, M.; Neuenschwander, A. and Ham, J. undated. Analysis of forest environments – classification as a metric of hyperspectral instrument performance. Department of Computer Science, Center for Space Research University of Texas, Texas, USA

Pekkarinen, A. 2002. Image segment-based spectral features in the estimation of timber volume. *Remote Sensing of Environment* 82, pp 349 – 359

Pepper, J. M. 1959. Chemical aspects of hardwood lignins. *Tappi*: 42(9), pp 793 – 800

Peterson, D. L.; Aber, J. D.; Matson, P. A.; Card, D. H.; Swanberg, N.; Wessman, C.; and Spanner, M. 1988. Remote sensing of forest canopy and leaf biochemical contents. *Remote Sensing of Environment* 24, pp 85 – 108

Phua, M and Saito, H. 2003 Estimating biomass of a mountainous tropical forest using Landsat TM data. *Canadian Journal of Remote Sensing* 29 (4), pp 429 – 440

Pinachas, S. and Laulicht, I. 1971. *Infrared spectra of labelled compounds*. Academic Press. New York. Pp 58 – 130

Plaza, A.; Valencia, D.; Plaza, J. and Martinez, P. 2006. Commodity cluster-based parallel processing of hyperspectral imagery. *Journal of Parallel and Distributed Computing* 66, pp 345 – 358

Poke, F. S.; Wright, J. K. and Raymond, C. A. 2004. Predicting extractives and lignin contents in *Eucalyptus globulus* using near infrared reflectance analysis. *Journal of wood chemistry and technology* 24 (1), pp 55 – 67

Privette, J. L.; Mnyeni, R. B.; Knyazikhin, Y.; Mukelabai, M.; Roberts, G.; Tian, Y.; Wang, Y.; Leblanc, S. G. 2002. Early spatial and temporal validation of MODISLAI product in the Southern Africa Kalahari. *Remote Sensing of Environment* 83, pp 232 – 243

Pu, P. and Gong, P. 2004. Wavelet transform applied to EO-1 hyperspectral data for forest LAI and crown closure mapping. *Remote Sensing of Environment* 91, pp 212 – 224

Pu, R.; Yu, Q.; Gong, P. and Biging, G. S. 2005. EO-1 Hyperion, ALI and Landsat 7 ETM+ data comparison for estimating forest crown closure and leaf area index. *International Journal of Remote Sensing* 26 (3), pp 457 – 473

Raison, R. J. and Myers, B. J. 1992. The biology of forest growth experiment: linking water and nitrogen availability to the growth of *Pinus radiata*. *Forest Ecology and Management* 52, pp 279 – 308

Ramsey, E. and Nelson, G. 2005. A whole image approach using field measurements for transforming EO-1 Hyperion hyperspectral data into canopy reflectance spectra. *International Journal of Remote Sensing* 26 (8), pp 1589 – 1610

Richardson, A.D. and Reeves, J.B., 2005, Quantitative reflectance spectroscopy as an alternative to traditional wet lab analysis of foliar chemistry: near infrared and mid infrared calibrations compared. *Canadian Journal of Forest Resources* 35, 1122 – 1130.

Roberts, J. L. 1996. *The chemistry of paper*. The Royal Society of Chemistry. Cambridge, UK. Pp 1 – 72

Rosema, A., Verhoef, W., Noorbergen, H., Borgesius, J.J. 1992 A new forest light interaction model in support of forest monitoring, *Remote Sensing of Environment* 42, pp 23 – 41

Rowan, L. C.; Simpson, C. J. and Mars, J. C. 2004. Hyperspectral analysis of the ultramafic complex and adjacent lithologies at Mordor, NT, Australia. *Remote Sensing of Environment* 91, pp 419 – 431

Sandercock, C. F., Sands, R.; Ridoutt, B. G.; Wilson, L. F. and Hudson, I. 1995. Factors determining wood microstructure in eucalypts. *Proceedings of the CRCTHF-IUFRO Conference. Eucalypt Plantations: Improving Fibre Yield and Quality*, CRCTHF-IUFRO (ed), pp 128-135. Hobart, Tasmania: CRCTHF-IUFRO.

Schiefer, S.; Hostert, P. and Damm, A. 2006. Correcting brightness gradients in hyperspectral data from urban areas. *Remote Sensing of Environment* 101, pp 25 – 37

Schimleck, L. R.; Mora, C. and Daniels, R. F. 2003. Estimation of the physical wood properties of green *Pinus taeda* radial samples by near infrared spectroscopy *Canadian Journal for Forest Research* 33(12), pp 2297-2305

Schlerf, M.; Atzberger, C. and Hill, J. 2005. Remote sensing of forest biophysical variables using HyMap imaging spectrometer data. *Remote Sensing of Environment* 95, 177 – 194

Schlerf, M. and Atzberger, C. 2006. Inversion of a forest reflectance model to estimate structural canopy variables from hyperspectral remote sensing data. *Remote Sensing of Environment* 100, pp 281 – 294

Schmidtlein, S. and Sassin, J. 2004. Mapping of continuous floristic gradients in grasslands using hyperspectral imagery. *Remote Sensing of Environment* 92, pp 126 – 138

Schonau, A. P. G. and Herbert, M. A. 1982. Relationship between growth rate and foliar concentration of Nitrogen, Phosphorus and Potassium for *Eucalyptus grandis*. *South African Forestry Journal* 120, pp 19 – 23

Schuerger, A. C.; Capelle, G. A.; Benedetto, J. A. D.; Mao, C.; Thai, C. N.; Evans, M. D.; Richards, J. T.; Blank, T. A. and Stryjewski, E. C. 2003. Comparison of two hyperspectral imaging and laser-induced fluorescence instruments for the detection of zinc stress and chlorophyll concentration in bahia grass (*Paspalum notatum* Flugge). *Remote Sensing of Environment* 84, pp 572 – 588

Schultze, R. E. 1997. *South African atlas of agrohydrology and climatology*. Department of Agriculture Engineering, *Water Research Commission*. Report TT86/96, pp 276

Schumacher, F. X. and Hall, F. D. S. 1933. Logarithmic expression of timber-tree volume. *Journal of Agricultural Research* 47, pp 719 – 734

Segl, K.; Roessner, S.; Heiden, U. and Kaufmann, H. 2003. Fusion of spectral and shape features for identification of urban surface cover types using reflective and thermal hyperspectral data. *Photogrammetry and Remote Sensing* 58, pp 99 – 112

Senay, G. B. and Elliott, R. L. 2000. Combining AVHRR – NDVI and land-use data to describe temporal and spatial dynamics of vegetation. *Forest Ecology and Management* 128, pp 83 – 91

Serrano, L.; Penuelas, J. and Ustin, S. L. 2002. Remote sensing of nitrogen and lignin in Mediterranean vegetation from AVIRIS data: Decomposing biochemical from structural signals. *Remote Sensing of Environment* 81, pp 355 – 364

Schenk, J. S.; Landa, I. Hoover, M. R. and Westerhaus, M. O. 1981. Description and evaluation of near infrared reflectance spectro-computer for forage and grain analysis. *Crop Science*. 21, pp 355 – 358

Shettigara, V. K.; O'mara, D.; Bubner, T. and Kempinger, S. G. 2000. Hyperspectral and band selection using entropy and target to clutter ratio measures. *10th Australian Remote Sensing and Photogrammetry Conference*, pp 1008 – 1018

Shepherd, J. D. and Dymond, J. R. 2003. Correcting satellite imagery for the variance of reflectance and illumination with topography. *International of Remote Sensing* 24 (17), pp 3503 – 3514

Silverstein, R. M.; Bassler, G. C. and Morrill, T. C. 1974. Spectrometric Identification of organic compound. John and Wiley Inc. New York. Pp 5 – 43

Sims, D. A. and Gamon, J. A. 2002. Relationships between leaf pigment content and spectral reflectance across a wide range of species, leaf structures and development stages. *Remote Sensing of Environment* 81, pp 337 – 354

Sims, D. A.; Luo, H.; Hastings, S., Oechel, W. C.; Rahman, A. F. and Gamon, J. A. 2006. Parallel adjustment in vegetation greenness and ecosystem CO₂ exchange in response to drought in Southern California chaparral ecosystem. *Remote Sensing of Environment* 103, pp 289 – 303

Smith, G. M. and Curran, P. J. 1995. The estimation of foliar biochemical content of a slash pine canopy from AVIRIS imagery. *Canadian Journal of Remote Sensing* 21(3), pp 234 – 242

Smith, K. L.; Steven, M. D. and Colls, J. J. 2004. Use of hyperspectral derivative ratios in the red-edge region to identify plant stress responses to gas leaks. *Remote sensing of Environment* 92, pp 207 – 217

Smith, M.; Martin, M. E. Plourde, L. and Ollinger, S. V. 2003. Analysis of Hyperspectral Data for Estimation of Temperate Forest Canopy Nitrogen Concentration: Comparison Between an Airborne (AVIRIS) and Spaceborne (Hyperion) Sensor. *IEE transactions on Geoscience and Remote Sensing* 41(6), pp 1332 – 1337

Smook, G. A. 1992 *Handbook for pulp and paper technologists*. Angus and Wilde Publications. Vancouver, USA. Pp 24 – 58

Soukupova, J.; Rock, B. N. and Albrechtova, J. 2002. Spectral characteristics of lignin and soluble phenolics in the near infrared- a comparative study. *International Journal of Remote Sensing* 23(15), pp 3039 – 3055

Sternberg, P.; Rautiainen, T.; Voipio, P. and Smolander, H. 2004. Reduced Simple Ratio better than NDVI for Estimating LAI in Finnish Pine and Spruce Stands. *Silva Fennica* 38(1), pp 3 – 14

Takahashi, T.; Yasouka, Y. and FUJII**, T. 2004. Estimation of and comparison of acid-detergent lignin and acetyl bromide lignin in fallen leaves using near-infrared spectroscopy. *International Journal of Remote Sensing* 25 (24), pp 5585 – 5600

Takahashi, T.; Yasouka, Y. and FUJII**, T. *undated*. Hyperspectral remote sensing of riparian vegetation and leaf chemistry content. Yasouka Lab., Institute of Industrial Science (IIS), the University of Tokyo, Japan

Tappi. 1996 – 1997. Tappi Test Methods. Tappi Press. Atlanta, Georgia, USA. T222 om - 88

^aThenkabail, P. S.; Enclona, E. A. Ashton, M. S. and Van Der Meer, B. 2004. Accuracy assessments of hyperspectral waveband performance for vegetation analysis applications. *Remote Sensing of Environment* 91, pp 354 – 376

^bThenkabail, P. S.; Enclona, E. A.; Ashton, M. S.; Legg, C. and De Dieu, M. J. 2004. Hyperion, IKONOS, ALI, and ETM+ sensors in the study of African Rainforests. *Remote Sensing of Environment* 90, pp 23 – 43

Thiemann, S. and Kaufman, H. 2002. Lake water quality monitoring using hyperspectral airborne data – semiempirical multisensor and multitemporal approach for the Mecklenburg Lake District, Germany. *Remote Sensing of Environment* 81, pp 228 – 237

Thulin, S. M.; Hill, M, J, and Held, A. A. *undated*. Hyperspectral detection of chemical properties within management and fertility treatments on a dairy farmlet experiment in eastern Victoria, Australia. Department of Geospatial Science. RMIT University. Melbourne, Australia

Tian, Y.; Wang, Y.; Zhang, Y.; Knyazikhin, Y.; Bogaert, J. and Myneni, R. B. 2002. Radiative transfer based scaling of LAI retrievals from reflectance data of different resolutions. *Remote Sensing of Environment* 84, pp 143 – 159

Ting, P. I. 1982. Plant Physiology. Addison- Wesley Publishing Company. Massachusetts, USA. Pp 101 – 200

Tokola, T. and Heikkila, J. 1997. Improving satellite image based forest inventory by using a priori site quality information. *Silva Fennica* 31(1), pp 67 – 78

Toomey, M. and Vierling, L. A. 2005. Multispectral remote sensing of landscape level foliar moisture: techniques and applications for forest ecosystem monitoring. *Canadian Journal for Forest Research* 35, 1087 – 1097

Townsend, P. A.; Foster, J. R. and Currie, W. S. 2003. Application of imaging spectroscopy to mapping canopy nitrogen in the forests of the central Appalachian Mountains using Hyperion and AVIRIS. *IEEE Transactions on Geoscience and Remote Sensing* 41 (6), pp1347 – 1354

Treitz, P. M. and Howarth, P. J. 1999. Hyperspectral Remote Sensing for estimation biophysical parameters of forest ecosystems. *Progress in Physical Geography* 23(3), pp 359 – 390

Trishchenko, A. P.; Cihlar, J. and Li, Z. 2002. Effects of spectral response function on surface reflectance and NDVI measured with moderate resolution satellite sensors. *Remote Sensing of Environment* 18, pp 1 – 18

Tuo, H. and Liu, Y. 2005. A new coarse-to-fine rectification algorithm for airborne push-broom hyperspectral images. *Pattern Recognition Letters* 26, pp 1782 – 1791

Underwood, E. Ustin, S. and DiPietri, D. 2003. Mapping nonnative plants using hyperspectral imagery. *Remote Sensing of Environment* 86, pp 150 – 161

Vaiphasa, C. 2006. Consideration of smoothing techniques for hyperspectral remote sensing. *ISPRS Journal of Photogrammetry and Remote Sensing* 60, pp 91 – 99

Van der Meer, F. 2001. *Basic physics of spectroscopy*. Kluwer Academic Publishers, Netherlands. Pp 9 – 34

Van der Meer, F.; De Jong, S. and Bakker, W. *Imaging spectrometry, basic analytical techniques*. Kluwer Academic Publishers, Netherlands. Pp 45 – 67

Varma, V. K.; Ferguson, I. And Wild, I. 2000. Decision support system for the sustainable forest management. *Forest Ecology and Management* 128, pp 49 – 55

Watanabe, Y.; Kojima, Y.; Ona, T.; Asada, T.; Sano, Y.; Fukazwa, K. and Funada, R. 2004. Histochemical study on heterogeneity of lignin in *Eucalyptus* species II. The distribution of lignins and polyphenols in the walls of various cell types. *IAWA Journal* 25(3), pp 283 – 295

Wardrop, A. B. 1981. *Lignification and xylogenesis in xylem cell Development*. Castle House, Tunbridge Wells. Pp 87 – 134

Watson, E. 1992. Mathematical modeling and experimental study of the kinetics of the acid-sulphite pulping of *Eucalyptus* wood. University of Natal, Durban. Pp 56 – 88

Wessman, C.; Aber, J. D.; Peterson, D. L.; and Melillo, J. M. 1987. Foliar analysis using near infrared reflectance spectroscopy. *Canadian Journal of Forest Research* 18, pp 6 – 11

Wettle, M.; Brando, V. E. and Dekker, A. G. 2004. A methodology for retrieval of environmental noise equivalent spectra applied to four Hyperion scenes of the same tropical coral reef. *Remote Sensing of Environment* 93, 188 – 197

White, K. 1998. Remote Sensing. *Progress in Physical Geography* 22, pp 95 – 102

Will, R. E.; Narahari, N. V.; Shiver, B. D. and Teskey, R. O. 2005. Effects of planting density on canopy dynamics and stem growth for intensively managed loblolly pine stands. *Forest Ecology and Management* 205, pp 29 – 41

Williams, D. J. and Kepner, W. G. 2003. Imaging spectroscopy for determining rangeland stressors to western watersheds. U.S. Environmental Protection Agency, Office of Research and Development, Reston, Virginia 20192

Winch, J. E and Major, H. 1981. Predicting Nitrogen and Digestibility of Forage Using Near Infrared Reflectance Photometry. *Canadian Journal of Plant Science* 61, pp 45 – 51

Wise, L. E. and Jahn, E. C. 1952. *Wood Chemistry: 2nd Edition*. Reinhold Publishing Corp, New York. pp 240 – 300

Wolmarans, L. G. and Du Preez, J. W. 1986. *The geology of St Lucia area*. Mineral and Energy Affairs. Pp 34 – 50

Wulder, M. 1998. Optical Remote sensing techniques for the assessment of forest inventory and biophysical parameters. *Progress in Physical Geography* 22 (4), pp 449 – 476

Xavier, A. C. and Vettorazzi, C. A. 2003. Leaf area index of ground covers in a subtropical watershed. *Scientia Agricola* 60 (3), pp 425 – 431

Zarco-Tejada*, P. J.; Miller, J. R.; Harron, J.; Hu, B.; Noland, T. L.; Goel, N.; Mohammed, G. H. and Sampson, P. 2004. Needle chlorophyll content estimation through model inversion using hyperspectral data from boreal conifer forest canopies. *Remote Sensing of Environment* 89, pp 189 – 199

Zarco-Tejada, P. J.; Miller, J. R.; Morales, A.; Berjon, A. and Aguera, B. J. 2004. Hyperspectral indices and model simulation for chlorophyll estimation in open-canopy tree crops. *Remote Sensing of Environment* 90, pp 463 – 476

Zarco-Tejada, P. J.; Berjon, A.; Lopez-Lozano, R.; Miller, J. R.; Martin, P.; Cachorro, V.; Gonzalez, M. R. and de Frutos, A. 2005. Assessing vineyard condition with hyperspectral indices: leaf canopy reflectance simulation in a row-structured discontinuous canopy. *Remote Sensing of Environment* 99, pp 271 – 287

Zhang, q.; Xiao, X. Braswell, B.; Linder, E.; Baret, F. and Moore III, B. 2005. Estimating light absorption by chlorophyll, leaf and canopy in a deciduous broadleaf

forest using MODIS data and radiative transfer model. *Remote Sensing of Environment* 99, pp 357 – 371

Zhao, D. H.; Li, J. L. and Qi, J. G. 2005. Identification of red and NIR spectral regions and vegetation indices for discrimination of cotton nitrogen stress and growth stage. *Computers and Electronics in Agriculture* 48, pp 155 – 169

Zhu, J. H. and Gray, D. G. 1995. Photoyellowing of lignin-rich paper: interacting of excited states with selected additives. *Journal of Photochemistry and Photobiology, A: Chemistry* 87, pp 267 – 273

APPENDICES

APPENDIX 1

Wavelengths of the near infrared spectral region for lignin concentrations predictions using different technologies

Wavelengths used for lignin estimation (nm)	Type of material	R ² of prediction based on their calibration equation	Instrument	Band selection method
1100 – 2498	Dry	0.83 -0.96	NIRS 5000	Partial least square regression
1564, 1680, 2061, 2328,	Dry	Not given	Neotec 51	Multiple linear regression
1500, 1850, 1720, 2100 – 2400	Fresh	Lignin and cellulose together – 0.79	NIRS 6500	ANN algorithm and LIBERTY model
1261, 1297, 2353	Canopy	0.93	AVIRIS	Multiple stepwise linear regression
1730, 2100, 2300	Dry	0.2 -0.71	NIRS 6250	Multiple stepwise linear regression
1438, 1828, 2218, 2386	Fresh-dry	0.24 – 0.50	NIRS 6250	Multiple linear regression
1660, 1740, 1900, 2280	Canopy	0.71 – 0.90	AVIRIS	Multiple linear regression
1438, 1708, 2154, 2320	Dry	0.76 – 0.82	NIRS 50	Multiple stepwise linear regression
1438, 1828, 2218, 2386	Dry	0.77	NIRS 50	Based on biophysical meaning and good statistical fit
1654, 1693, 2076, 2135, 2270, 2327	Dry	0.37	Perkin Elmer 360	Multiple stepwise linear regression
1654, 1693, 2076, 2135, 2270, 2327	Dry	0.71	Neotec 51A	Multiple stepwise linear regression

Foliar and/ or branch material is dried and ground into fine powder (Soukupova *et al.*, 2000).

APPENDIX 2

Image Processing

A number of approaches have been advanced to compensate for the atmospheric contamination of spectra, increase in the volume of data and the relatively poor signal to noise ratios. Two specific techniques, Internal Average Relative Reflectance (IARR) and Log Residuals are implemented in ERDAS IMAGINE. These have the advantage of not requiring auxiliary input information; the correction parameters are scene-derived. The disadvantage is that they produce relative reflectances (they can be compared to reference spectra in a semi-quantitative manner only). As a result the image processing techniques that are used to analyse hyperspectral imagery differ from the norm. In general, image analysis requires more attention to issues of atmospheric correction and relies more heavily on physical and biophysical models rather than on purely statistical techniques such as maximum likelihood classification (Erdas, 1999).

Enhancement of Hyperspectral Images

There are a number of methods that can be employed to improve and enhance hyperspectral images.

A. Normalise

Sensor look angle and local topographic effects affect pixel albedo. For airborne sensors the look angle effect can be large across the scene whereas it is less pronounced for satellite sensors. Most scanners look to both sides of the aircraft and the average scene luminance between the two half-scenes can be large. To help minimise these effects, an equal area normalisation is applied. This calculation shifts each pixel spectrum to the same overall average brightness. This method must be used with a consideration of whether this assumption is valid for the scene. For example, in the image that contains two distinctly different regions, like the ocean and the forest, this method is not exactly useful. Correctly applied, this method helps remove albedo variations and topographic effects (Erdas, 1999).

B. IAR Reflectance (Internal Average Reflectance)

This technique calculates a relative reflectance by dividing each spectrum by the scene average spectrum. The algorithm is based on the assumption that the scene average spectrum is largely composed of the atmospheric contribution and that the atmosphere is uniform across the scene, however these assumptions are not always valid. In fact the average spectrum could easily contain absorption features related to the target material of interest. This method could then overcompensate (remove) these absorbance features. Therefore the average spectrum should be visually inspected to check for this possibility. Properly applied, this technique can remove the majority of atmospheric effects (Erdas, 1999).

C. Log Residuals

The Log Residuals has been modified by the researchers over the years but was originally described by Green and Craig in 1985. This algorithm can be written as:

Output Spectrum = input spectrum – average spectrum – pixel brightness + image brightness.

All parameters in the above equation are in logarithmic space, hence the name. This algorithm corrects the image for atmospheric absorption, systemic instrumental variation and illuminance differences between pixels (Erdas, 1999).

D. Rescaling

Many Hyperspectral scanners record the data in a format larger than 8-bit. In addition, many of the calculations used to correct the data are performed with a floating-point format to preserve precision. At some point it is advantageous to compress the data back to an 8-bit range for effective storage and display. When rescaling data to be used for imaging spectrometry analysis, however, it is necessary to consider all data values within the data cube, not just within the layer of interest. Any bit format can be input but the output image is always 8-bit. When rescaling a data cube, a decision should be made as to which bands to include in the rescaling. A bad band should be excluded. When rescaling data sets it may be appropriate to rescale each electromagnetic region separately (Erdas, 1999).

E. Mean per Pixel

This algorithm outputs a single band, regardless of the number of input bands. By visually inspecting this output information it is possible to if particular pixels are outside the norm. While this does not mean that these pixels are incorrect, they should be evaluated in this concept, for example, the detector could have several sites (pixels) that are dead or have anomalous response, and these would be revealed in the mean-per pixel image. This can be used as a sensor evaluation tool. To help in visualizing this three-dimensional data cube, basic tools have been designed: these are termed profile tools.

- Spectral Profile – a display that plots the reflectance spectrum of a designated pixel,
- Spatial Profile – a display that plots spectral information along a user-defined polyline. The data can be displayed two-dimensionally for a single band (Erdas, 1999).

Processing Sequence

Various processing steps are utilised to convert raw image into a form that is easier to interpret. This interpretation often involves comparing the imagery, either visually or automatically, to laboratory spectra or other known end-member spectra. At present there is no widely accepted standard processing sequence to achieve this, although some have been advanced in scientific literature. Two common processing sequences have been programmed as single automatic enhancements. These are:

- Automatic Relative Reflectance – this implements the following algorithms: *Normalise, IAR and Rescale*
- Automatic Log Residuals – this implements the following: *Normalise, Log Residuals and Rescale.*

A. Signal to Noise

The signal-to-noise (S/N) ratio is commonly used to evaluate the usefulness of a band. In this implementation, signal to noise is defined as Mean/Standard Deviation in a 3x3 moving window. After running this function on a data set, each layer in the output image should be visually inspected to evaluate suitability for inclusion into the analysis. Layers deemed unacceptable can be excluded from the processing by

using the Select Layers option of the various Graphical User Interfaces (GUIs). This can be used as a sensor evaluation tool (Erdas, 1999).

B. Spectrum Average

In some instances it may be desirable to average together several pixels. In preparing reference spectra for classification, or to save in the Spectral Library, an average spectrum may be more representative than a single pixel. In order to implement this function it is necessary to define which pixels to average using the AOI tools. This enables one to average any set of pixels that are defined; the pixels do not necessarily have to be contiguous and there is no limit on the number of pixels averaged. The output from this program is a single pixel with the same number of input bands as the original image (Erdas, 1997).

C. Classification

The advent of data sets with very large numbers of bands has pressed the limits of the traditional classifiers such as Isodata, Maximum likelihood, and Minimum Distance, but has not obviated their usefulness. Much research has been directed towards the use of Artificial Neural Networks (ANN) to more fully utilize the information content of hyperspectral images. To date, however, these advanced techniques have proven to be only marginally better at a considerable cost in complexity and computation. For certain applications, both Maximum Likelihood and Minimum Distance have proven to be appropriate (Erdas, 1999). A second category of classification techniques utilizes the imaging spectroscopy model for approaching hyperspectral data sets. This approach requires a library of possible end-member materials. These can be from laboratory measurements using a scanning spectrometer and reference standards. The JPL and USGS libraries are compiled this way. The reference spectra can also be scene-derived from either the scene under study or another similar scene (Erdas, 1999).

D. Band selection

Unmixing is a popular technique for target detection in hyperspectral imagery. The dimensionality of the hyperspectral data is a challenge to the operational use of the technology, thus, it is important to investigate if unmixing can be achieved using fewer bands. A new procedure based on metric called Target to Clutter Ratio. The

TCR based procedure performs much better than the entropy of based procedure and it has proved to be faster. The preliminary results revealed that a subset approximately 15 bands would suffice to achieve accuracy comparable with the full set of 224 bands. The preliminary results were based on a synthetic image (Shettigara *et al.*, 10th Australian Remote Sensing and Photogrammetry Conference). Spectral unmixing is a popular technique for target detection when using hyperspectral images. A linear mixing model is commonly assumed for unmixing purposes and the observed data is given by the equation:

$$\mathbf{D} = \mathbf{S}\mathbf{f} + \mathbf{e} \quad (1)$$

Where

\mathbf{D} = observed pixel spectra (vector of n elements or bands)

\mathbf{S} = $n \times k$ matrix containing field spectra s_k Of objects of interest in columns

\mathbf{f} = vector of k elements f_i ($i = 1, \dots, k$) denoting areal fractions of k materials in a pixel.

\mathbf{e} = noise in pixel data (vector of n elements or bands)

Target detection through unmixing is achieved by recognising the presence of spectra, i.e. spectra s_i belonging to material i , which covers a minimum area in a pixel. The minimum area needs to be above the noise level. Unmixing is not a simple process and presently there is no known method to guarantee correct and accurate recovery of the unknown fractional coverage f_i . However, the following multiple regression equation provides a reasonably good estimate of f_i :

$$\mathbf{f} = (\mathbf{S}^T\mathbf{S})^{-1} \mathbf{S}^T \mathbf{d} \quad (2)$$

Where \mathbf{f} is an estimate of \mathbf{f} and \mathbf{S}^T is a transpose of \mathbf{S}

Equation (2) does incorporate the stochastic nature of the spectral signatures in \mathbf{S} . This matrix contains mean spectra of materials under consideration and is fixed during the unmixing process whereas ideally the bands should be selected taking into consideration that the spectra in \mathbf{S} are variable. The band selection methods may be grouped into two categories based on properties they use: a) spectral fidelity, b) class separability measure (William and Kepner, 2003).

APPENDIX 3

Table 2.3: Differences in correlations with LAI between traditional indices and optimal indices

Index	R ²		Band centre (nm)	Bandwidth (nm)	Band description (spectral region and possible absorption features)
	SR NIR/R	Optimal			
SR/SVI	0.55	0.78			
			230	NIR-SWIR region, water , protein , lignin, starch and oil absorption	
			1250	180	SWIR region, water , cellulose, starch and lignin absorption
			1648	290	SWIR region, protein , nitrogen , lignin , cellulose , sugar, starch absorption
NDVI	0.55	0.70	4 bands similar to SR's
			1050	100	NIR-SWIR region, protein , lignin, and oil absorption
			1250	190	SWIR region, water , cellulose, starch and lignin absorption
			2100	10	SWIR region, starch, cellulose absorption
SAVI	0.50	0.67	4 bands similar to NDVI's or SR's
NLI	0.50	0.73	821	157	NIR region, cell structure multi-reflected spectra
			1200	578	NIR-SWIR region, water , protein , lignin, cellulose, starch and oil absorption
			1250	191	SWIR region, water , cellulose, starch and lignin absorption
			1640	300	SWIR region, protein , nitrogen , lignin , cellulose , sugar, starch absorption
RDVI	0.45	0.66	810	170	NIR region, cell structure multi-reflected spectra
			1054	10	SWIR region, lignin and oil absorption
			1255	161	SWIR region, water , cellulose, starch and lignin absorption
			1669	10	SWIR region, lignin and starch absorption
			2093	10	SWIR region, starch, cellulose absorption
MSR	0.50	0.70	4 bands similar to NDVI's or SR's
			2285	30	SWIR region, starch, cellulose and protein absorption
MNLI	0.45	0.75	4 bands similar to NDVI's or SR's
NDVI SR *	0.50	0.71	4 bands similar to NDVI's or SR's, but
SAVI SR *	0.50	0.71	1-4 bands similar to SAVI's or SR's
			2083	30	SWIR region, sugar, starch and cellulose absorption
			2153	10	SWIR region, protein absorption

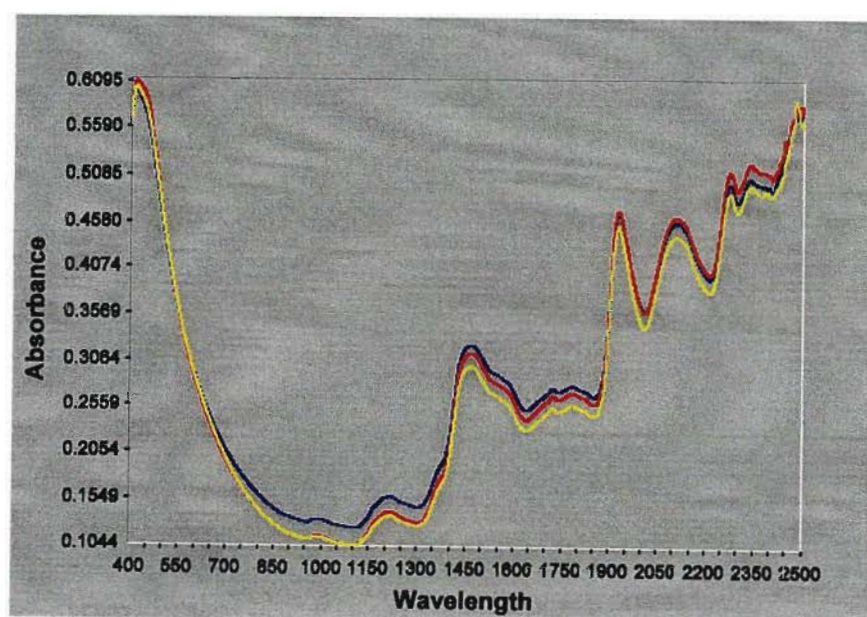
APPENDIX 4

A: Information on the compartments used for the study

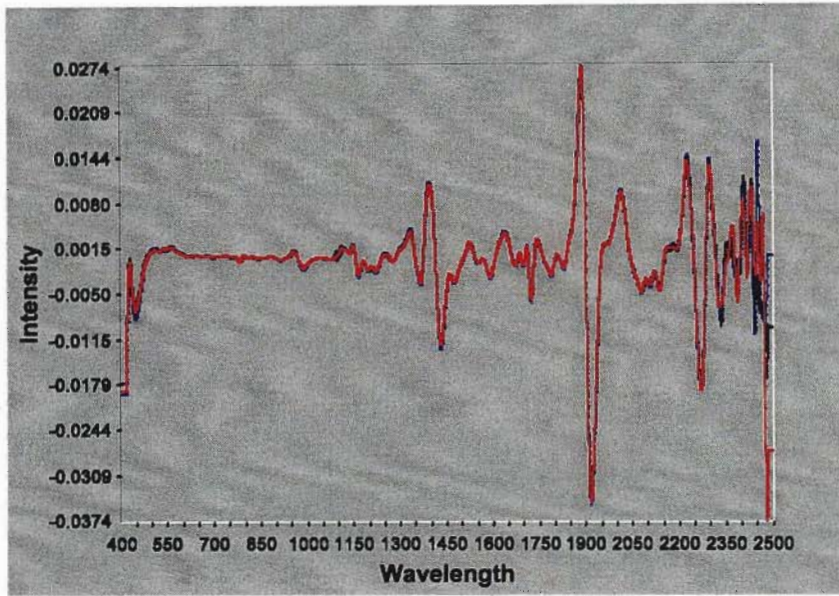
Compartment	Clone Type	Age at Sampling	Tree Spacing	Measured SI	Measured MAI
1	E. urophylla	7.25	3.0 x 3.0	21.29	43.37
2	GU-1	7.25	3.0 x 3.0	22.41	47.62
3	GU-2	6.92	3.0 x 2.7	25.90	68.27
4	GC-1	7.42	2.7 x 2.4	23.81	48.50
5	E. urophylla	7.25	2.7 x 2.7	24.13	56.29
6	GU-1	8.33	3.0 x 2.0	23.07	49.62
7	GU-1	6.33	2.7 x 2.2	22.89	49.11
8	GU-3	6.33	2.7 x 2.2	23.80	47.80
9	GC-2	8.08	3.0 x 2.0	21.96	43.99
10	GU-4	8.00	3.0 x 2.0	17.61	25.86
11	GT	8.75	3.0 x 2.5	27.34	53.00
12	<i>E. gra</i>	8.00	2.7 x 2.4	18.05	21.45

APPENDIX 5

Typical NIRS spectra scan for a *Eucalyptus* clone



Typical second derivative NIRS spectrum



APPENDIX 6

Site index calculation from stand enumeration data

Compartment	Plot radius (m)	Base Age (yrs)	Mean Top Height (m)	Mean thick DBH (cm)	Measured SI
1	15.000	5.000	25.475	24.289	21.291
2	15.000	5.000	26.815	26.816	22.412
3	15.000	5.000	30.325	27.144	25.901
4	15.000	5.000	28.785	21.448	23.808
5	15.000	5.000	28.871	23.095	24.130
6	15.000	5.000	29.412	25.971	23.068
7	15.000	5.000	25.721	21.505	22.893
8	15.000	5.000	26.740	21.565	23.800
9	15.000	5.000	27.617	20.777	21.962
10	15.000	5.000	22.038	18.700	17.608
11	15.000	5.000	35.635	23.929	27.335
12	15.000	5.000	22.595	20.915	18.053

APPENDIX 7

Scene ID : EO11670802004216110PZ
 Ground site ID : SGS
 Acquisition time : 2004 216. 07:34:54
 Acquisition date : 24 August 2004

Instrument : Hyperion
 Processing level : Hyperion Level 1R
 Number of spectral bands : 242
 Scene dimensions : 42 x 7.5 km
 Vertical pixel resolution : 30m
 Horizontal pixel resolution : 30m
 Data format : Hierarchical Data Format
 Projection : UTMS
 Horizontal datum : WGS84
 Resampling method : CC (cubic convolution)
 Image orientation : Map (north up)
 Scene centre coordinates : (-28.53, 32.14)

Table showing the Hyperion sensor pointing angles for different latitudes

Latitude	West Path Sensor pointed East (degrees)	Overhead Path (degrees)	East Path Sensor pointed West (degrees)
80N	0.716 to 2.145	± 0.716	-0.716 to -2.145
60N	3.369 to 10.016	± 3.369	-3.369 to -10.016
45N	4.856 to 14.297	± 4.856	-4.856 to -14.297
30N	5.975 to 19.338	± 5.975	-5.975 to -19.338
15N	6.672 to 19.338	± 6.672	-6.672 to -19.338
0	6.909 to 19.976	± 6.909	-6.909 to -19.976
15S	6.672 to 19.338	± 6.672	-6.672 to -19.338
30S	5.975 to 19.338	± 5.975	-5.975 to -19.338
45S	4.856 to 14.297	± 4.856	-4.856 to -14.297
60S	3.369 to 10.016	± 3.369	-3.369 to -10.016
80S	0.716 to 2.145	± 0.716	-0.716 to -2.145

APPENDIX 8

Bands suitable for calculating different vegetation indices using Hyperion data according to Gong et al, 2003

INDEX	BAND CENTRE	BANDWIDTH
SR	825	140
	1038	230
	1250	180
	1648	290
NDVI	4 bands similar to SR's	Similar to SR's
PVI	814	140
	1050	100
	1250	190
	2100	10
SAVI	4 bands similar to NDVI's or SR's	Similar to NDVI's or SR's
NLI	821	157
	1200	578
	1250	191
	1640	300
RDVI	810	170
	1054	10
	1255	161
	1669	10
	2093	10
MSR	4 bands similar to NDVI's or SR's	Similar to NDVI's or SR's
WDVI	1639	10
	2113	10
	2285	30
MNLI	4 bands similar to NDVI's or SR's	Similar to NDVI's or SR's
NDVI * SR	4 bands similar to NDVI's or SR's	Similar to NDVI's or SR's
SAVI * SR	1-4 bands similar to SAVI's or SR's	Similar to SAVI's or SR's
	2083	30
TSAVI	2153	10
	832	120
	1038	150
	1240	170
	1660	260
2108	20	

APPENDIX 9

Table showing the description of different vegetation indices and their equations according to Gong et al, 2003

Index	Formula	Description
SR	$\frac{\lambda_{\text{NIR}}}{\lambda_{\text{R}}}$	The Simple Ratio index is related to changes in amount of green biomass, pigment content and leaf water stress
NDVI	$\frac{(\lambda_{\text{NIR}} - \lambda_{\text{R}})}{(\lambda_{\text{NIR}} + \lambda_{\text{R}})}$	The Normalized Difference Vegetation Index is related to changes in amount of green biomass, pigment content and leaf water stress
SAVI	$\frac{(\lambda_{\text{NIR}} - \lambda_{\text{R}}) (1 + L)}{(\lambda_{\text{NIR}} + \lambda_{\text{R}} + L)}$ L = Correction Factor	In the Soil Adjusted Vegetation index, the L ranges from 1 (for very high vegetation cover) to 1 (for very low vegetation cover). This index minimizes soil brightness induced variations.
NLI	$\frac{(\lambda_{\text{NIR}}^2 - \lambda_{\text{R}})}{(\lambda_{\text{NIR}}^2 + \lambda_{\text{R}})}$	The Non-Linear Vegetation Index considers the relationship between many VIs and surface biophysical that are often non-linear.
RDVI	$\frac{(\lambda_{\text{NIR}} - \lambda_{\text{R}})}{(\lambda_{\text{NIR}} + \lambda_{\text{R}})^{1/2}}$	Renormalized Vegetation Index also tends to linearize non-linear relationships between VIs and biophysical parameters
MSR	$\frac{(\lambda_{\text{NIR}} / \lambda_{\text{R}} - 1)}{(\lambda_{\text{NIR}} / \lambda_{\text{R}})^{1/2} + 1}$	Modified Simple Ratio was formulated as an upgrade of the RDVI See RDVI
MNLI	$\frac{(\lambda_{\text{NIR}}^2 - \lambda_{\text{R}}) (1 + L)}{(\lambda_{\text{NIR}}^2 + \lambda_{\text{R}} + L)}$ L = Correction Factor	Modified Non-Linear Vegetation Index is an improved NLI while it considers the merits of the SAVI
NDVI*SR	$\frac{(\lambda_{\text{NIR}}^2 - \lambda_{\text{R}})}{(\lambda_{\text{NIR}} + \lambda_{\text{R}}^2)}$	This index was developed by Gong et al. (2003) to combine the merits of the NDVI with that of the SR
SAVI*SR	$\frac{(\lambda_{\text{NIR}}^2 - \lambda_{\text{R}})}{(\lambda_{\text{NIR}} + \lambda_{\text{R}} + L) \lambda_{\text{R}}}$ L = Correction Factor	This index was developed by Gong et al. (2003) to combine the merits of the SAVI with that of SR